NETHERLANDS GEODETIC COMMISSION

PUBLICATIONS ON GEODESY NEW SERIES

NUMBER 32

NAVGRAV
NAVIGATION AND GRAVIMETRIC EXPERIMENT AT THE NORTH SEA

by

R. H. N. HAAGMANS
G. J. HUSTI
P. PLUGERS
J. H. M. SMIT
G. L. STRANG VAN HEES

1988

RIJKSCOMMISSIE VOOR GEODESIE, THIJSSEWEG 11, DELFT, THE NETHERLANDS

PRINTED BY W. D. MEINEMA B.V., DELFT, THE NETHERLANDS

ISBN 90 6132 237 5

PREFACE

Accurate gravity information at sea can serve many important purposes in geodesy, solid earth physics and oceanography. But only since the early twenties of this century, through the pioneering work of Vening Meinesz (1929) or (1948) gravity measurements at sea became possible. The inherent complication, whenever measuring while moving, is the separation of the disturbing effects of the motion from the vertical acceleration due to gravity. Meanwhile sophisticated modern gravity meters exist, see e.g. (Bell and Watts, 1986) that largely eliminate these disturbances. However there remains an effect that cannot be eliminated instrumentally, the Eötvös correction. It can only be determined accurately if very precise navigation is available. With the exception of a few areas, where accurate radiopositioning is available, this causes a problem. With the establishment of the Global Positioning System (GPS) precise navigation anywhere at any time became feasible. Hence around 1984 the idea was born to investigate the potential of GPS for this purpose in the North Sea, where several precise radiopositioning systems are available for comparison. Since such an experiment required GPS as well as sea gravimetry, it was only logical to broaden the scope of the experiment by addressing at the same time other interesting items in the fields of navigation and sea gravimetry. The experiment was named NAVGRAV.

On one hand the test offered the opportunity to take a closer look at the precision, repeatability and resolution of sea gravimetry and its trade-off with satellite altimetry derived gravity. For these purposes two modern sea gravimeters were measuring simultaneously. Several ship tracks of an earlier experiment in 1979 (Strang van Hees, 1983) were repeated, and SEASAT altimetry data were analysed. On the other hand very little experience was present in the area of GPS in the Netherlands around 1984. Thus, the experiment gave opportunity to involve as many future potential users from private companies, government agencies and universities, to gain experience on the capabilities of GPS at sea and to compare it with the established radio positioning systems in a variety of experiments. A preparatory GPS

experiment was carried out on board of Hr.Ms. Tydeman in December 1985 with the support of the Hydrographic Service.

The NAVGRAV experiment has been organized by the Faculty of Geodesy of the Delft University of Technology (DUT). However the experiment would not have been possible without the support of a large number of organizations and individuals. The main support came from the Netherlands Council for Oceanic Research (NRZ). This organization provided cruise time on board of Hr.Ms. Tydeman of the Hydrographic Service of the Royal Netherlands Navy as well as financial support. Additional support came from the Universities of Hamburg (U.H.) and Hannover (U.Han.) and the Technical University Munich (TUM), from the University of Utrecht (U.U.), from the Survey Department of Rijkswaterstaat, Ministry of Transport and Public Works, from the co-operative effort of several private companies (Intersite Surveys, NESA, Osiris Seaway, Netherlands Hydrographic Services, Oretech, Nortech Surveys and Radio Holland) and from Shell Internationale Petroleum Maatschappij. Sincere thanks for their support go to Prof. Dr. R. Sigl (TUM), Prof. Dr. K. Deichl (TUM), Prof. Dr. G. Seeber (U.Han.), Prof. Dr. J. Makris (U.H.) and Ir. J.G. Riemersma (Shell).

The actual experiments have been carried out under supervision of Ir. G.J. Husti, Ir. G.L. Strang van Hees and P.G. Sluiter. About thirty scientists and students have participated: P. van Es (student), P.J. van Ess (student), Ir. G.J. Husti, C.D. de Jong (student), G.M. Lammerts van Bueren (student), Ing. P. Plugers, Ir. M.A. Salzmann, J.H.M. Smit (student), Ir. G.L. Strang van Hees and J.L.M. Visser (student), all participants from the Delft University of Technology (DUT), Ir. L.M. Murre (Rijkswaterstaat), P.W. Hardie (Nortech Surveys), Ir. J. Larthe de Langladure and P.G. Sluiter (both from Shell), Ing. A.M. Jongsma and Drs. A. Lubbes (Intersite Surveys), M.M. Mehta (N.H.S.), Ir. N.J. Belgraver (Radio Holland), Ing. H. v.d. Meer (U.U.), Dipl. ing. F. Heimberg (U.Han.), Dipl. ing. E. Kistler (TUM), T. Liebe (U.H.). Due to their enthusiastic participation the experiment became a success. Many thanks for all their effort. Last but not least we gratefully acknowledge the active support of the Royal

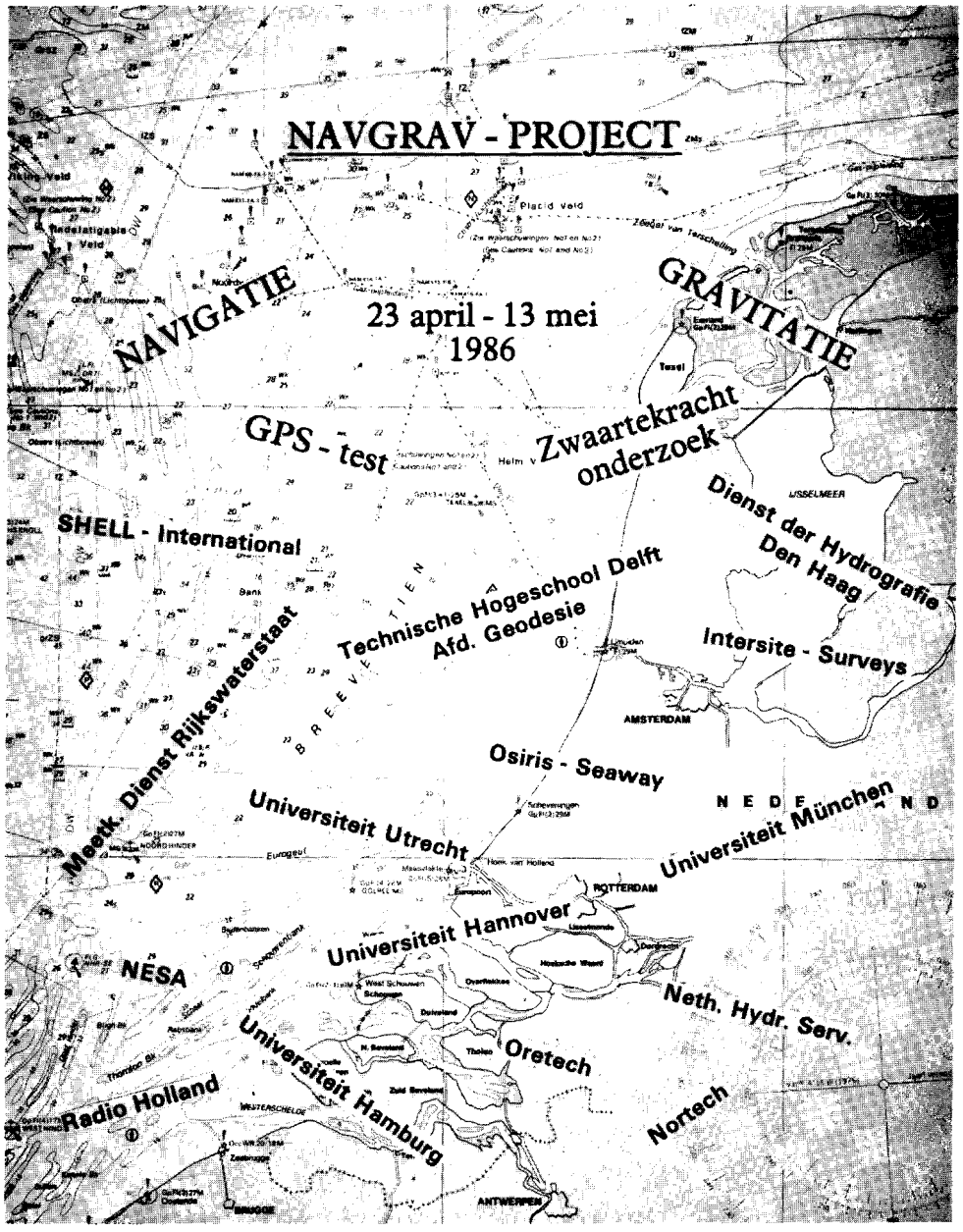
NAVGRAV - PROJECT
NAVIGATIE
23 april - 13 mei
1986
GRAVITATIE
GPS - test
Zwaartekracht
onderzoek
SHELL - International
Dienst der Hydrografie
Den Haag
Technische Hogeschool Delft
Afd. Geodesie
Intersite - Surveys
Meetk. Dienst Rijkswaterstaat
Osiris - Seaway
Universiteit Utrecht
Universiteit München
Universiteit Hannover
NESA
Neth. Hydr. Serv.
Oretech
Universiteit Hamburg
Radio Holland
Nortech
AMSTERDAM
ROTTERDAM
ANTWERPEN
BRUGGE
N E D E R L A N D

Netherlands Navy, the commander of Hr.Ms. Tydeman Kltz. G.R. van Hengel and his officers and crew.

The experiments yielded an enormous amount of navigation and gravity information and a lot of experience. This report gives the results of the NAVGRAV project as they are obtained until now. It is our impression that the available data could still be used for future investigations and for student projects. The data and the required documentation can be made available to any interested group.

Delft, December 1988
Reiner Rummel

References

Bell, R.E., A.B. Watts (1986): Evaluation of the BGM-3 sea gravity meter system on board R/V Conrad. Geophysics, vol. 51, no. 7.

Strang van Hees, G.L. (1983): Gravity Survey of the North Sea. Marine Geodesy, vol. 6, no. 2.

Vening Meinesz, F.A. (1929): Theory and Practice of Pendulum Observations at Sea. Netherlands Geodetic Commission, Technische Boekhandel Waltman, Delft.

Vening Meinesz, F.A. (1948): Gravity Expeditions at Sea 1923-1938. Delftse Uitgevers Maatschappij, Delft.

Contents

SUMMARY

In April 1986 extented test measurements were executed with GPS instruments on board of the Dutch Navy vessel Hr.Ms. Tydeman. The GPS positions were compared with the best available terrestrial radio navigation systems, under variable conditions. The precision of GPS turned out to be 10 to 15 m in absolute position, and better than 3 m in differential mode.

Gravity measurements were carried out with two sea gravimeters. The differences between the instruments were less than 1 mgal for random errors. However systematic errors occured on some lines up to a few mgal, probably due to errors in the cross-coupling corrections. Also a comparison was made with results of a similar project in 1979. Only minor differences are present. Remarkable is the rather irregular shape of the gravity field, although the sea bottom is very flat. A significant gravity anomaly appears at latitude $55^{0}13'$, longitude $5^{0}38'$. This anomaly is caused by a mass disturbance due to mantle material intruded into the crust.

In sea gravimetry the realizable accuracy is limited by Eötvös correction errors. To determine Eötvös corrections better than 0.5 mgal, ship velocity estimation with an accuracy of 5 cm/s or 0.1 knot is necessary. The possibilities of obtaining ship velocity estimates with high accuracy by using GPS pseudorange code measurements and carrier phase measurements are investigated. The comparison of Eötvös corrections computed with ship velocity estimates from GPS pseudoranges, Doppler smoothed pseudoranges, carrier phase measurements and Syledis and Hyperfix positions shows no discrepancies. Best results are obtained from the GPS Doppler smoothed pseudorange method. This justifies the conclusion that the effect of Eötvös correction errors in sea gravimetry can be reduced significantly.

Gravity anomalies as derived from ship measurements were compared with gravity anomalies computed from SEASAT altimetry. Altimetry provides, after correction for various disturbances, accurate sea surface heights. With good approximation one can identify the latter with geoid heights (neglecting those parts of

the sea surface topography for which no models are available). Two alternative methods were applied for the estimation of point gravity anomalies from the altimeter derived geoid heights. One method was least squares collocation, the other a very fast but theoretically less sound technique based on Fourier transformation. In both cases the long wavelength part was dealt with using the GEM10B set of potential coefficients. Collocation yielded better results. The agreement with shipborne point gravity anomalies is on the 7 mgal level with no significant bias. This proves that altimeter derived gravity is well suited for a preliminary inspection of the gravity field structure of an area of interest.

Acknowledgements

The authors wish to thank Mr. M.G.G.J. Jutte for drawing some maps and making the headers of the articles, Mr. A.B. Smits for the photographical reproduction of all graphs, Mrs. W.G. Coops-Luyten and Mrs. W. van Lingen for typing parts of the manuscript.

NAVGRAV

NAVIGATION AND GRAVIMETRIC EXPERIMENT AT THE NORTH SEA

G.L. Strang van Hees
Delft University of Technology
Faculty of Geodesy

1. Introduction

The NAVGRAV project was a combined NAVigation and GRAVimetric experiment at the North Sea. For this project the oceanographic vessel H.M. Tydeman of the Royal Dutch Navy was made available. The expedition took place from April 23 to May 13, 1986. The experiment was divided into two parts. The first week from April 23 to 30 was devoted to a test of the perspectives of modern navigation systems. During the second period from April 30 to May 13 the primary goal was the evaluation of the perspectives of modern sea gravimetry.

2. Navigation

The following terrestrial radio positioning systems were available: Syledis, Hifix and Hyperfix. On the other hand six GPS receivers were on our disposal: three Texas Instruments, two Sercel and one Trimble. Four instruments were placed on board and two on land as reference stations. To compare the precision of the GPS with the terrestrial systems a scheme of lines were steamed, mainly in the area covered by Syledis (see figure 1). Syledis was assumed to be the most accurate terrestrial system. In the same area Hifix was available too, which gave a good insight into the reliability of the terrestrial systems. The third system, Hyperfix, was used as reference system in the northern part of the measuring area (figure 1). However the latter system was only recently installed and still in a testing phase. This caused sometimes lane slips, and a complete one day gap when the system was out of order.

Some special tests were carried out in order to test the reliability of the systems under special conditions.

- steaming around oil platforms in circles with radii of 100m, 500m and 1500m, to check the influence of reflections;
- suddenly increasing and decreasing of the ships velocity, and sudden changes of the ships direction;
- precision of the radio systems in case of a long landpath of the radio waves.

However all these experiments caused no measurable deviations.

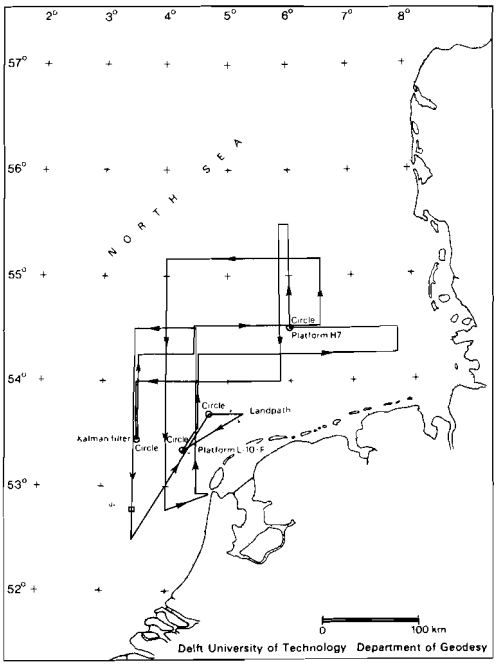

Figure 1:
Navigation experiment NAVGRAV

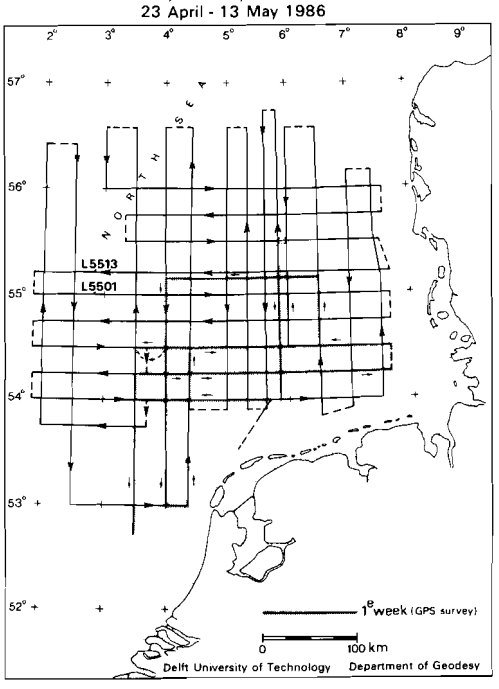

Figure 2:
Gravity survey NAVGRAV

The GPS tests were aimed at:

- absolute precision compared with terrestrial systems;
- relative precision between ship and land receivers;
- relative precision between different receivers on board;
- relative precision between ship and launch, and
- velocity determination with GPS.

All data were registrated at 3 seconds intervals.

3. Gravity

During the second period a rectangular pattern of lines was steamed (see figure 2). As the available navigation systems were out of range in the northern North Sea, another radio positioning system was chosen, Pulse 8. The precision of this system was 20 m, which is sufficient for gravity survey needs.

The purpose of the sea gravity measurements was to determine the precision of modern sea gravimeters. Two gravimeter systems were installed next to each other, the sea gravimeters Bodensee Kss 5 of the Delft University of Technology and the Bodensee Kss 30 of the University of Hamburg. The difference between the measured gravity of both instruments gives an insight into the internal precision and bias of the gravimeters. External errors like navigation errors and the Eötvös correction were eliminated.

Part of the region has already been surveyed in 1979 (Strang van Hees, 1983). Some of these lines were remeasured in order to determine the external precision of gravity measurements. Additional lines were put in between the previous measured lines. This gives the possiblity to investigate the precision of the interpolation of gravity anomalies in cross line direction. The lines are about 25 km apart, which is chosen in correspondence with the estimated roughness of the gravity field.

Nearly all measurements were carried out under excellent weather conditions. Therefore the quality of the measurements is very good.

The good cooperation on board between the scientists and the Royal Netherlands Navy is very much appreciated. Commander Kltz. G.R. van Hengel of the H.M. Tydeman and his officers and crew gave all support to make this expedition succesful.

4. List of participating institutes and firms

- Delft University of Technology, Faculty of Geodesy
- University of Hannover, Institute of Geodesy
- Technical University Munich, Institute of Astronomical and Physical Geodesy
- University of Hamburg, Institute of Geophysics

- University of Utrecht, Faculty of Geophysics
- Hydrographic Service of the Royal Netherlands Navy
- Survey Department of Rijkswaterstaat
- Shell Internationale Pretroleum Maatschappij
- Osiris Seaway
- Intersite Surveys
- Radio Holland
- NESA
- Netherlands Hydrographic Services
- Oretech
- Nortech Surveys

5. References

Rummel, R., G.L. Strang van Hees and H. Versluijs (1983): Gravity Field Investigation in the North Sea. In: Satellite Microwave Sensing (ed. T.D. Allen), John Wiley & Sons, New York.

Salzmann, M.A., G.J. Husti, G.L. Strang van Hees, P.J.G. Teunissen (1987): NAVGRAV, a comprehensive combined navigation and gravimetry experiment on the North Sea; objectives and first experiences. Proceedings International Symposium on Marine Positioning, Reston, October 14-17, 1986.

Strang van Hees, G.L. (1983): Gravity Survey of the North Sea. Marine Geodesy, vol. 6, no. 2.

GPS AND TERRESTRIAL RADIOPOSITIONING SYSTEMS

G.J. Husti
P. Plugers
Delft University of Technology
Faculty of Geodesy

1. Introduction

One of the objectives of the NAVGRAV project was to investigate the suitability of the Global Positioning System for position and velocity determination at sea. GPS will obviously play an important role in gravimetric surveying in the near future, where the desired accuracy is about 20 meter in position and 5 cm/sec in velocity. Such an accuracy is now quite possible with GPS, but could not be achieved during the 24 hour non-stop gravimetric survey, because of the limited number of satellites available in 1986. Each day two observation windows were available (figure 1):

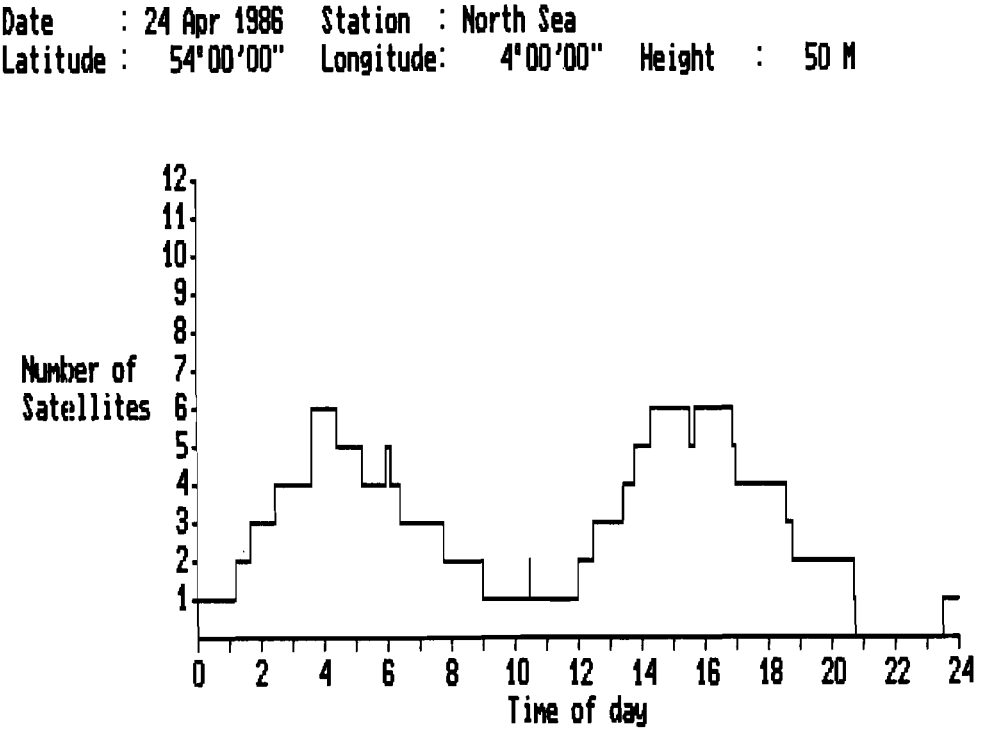

Figure 1. GPS windows in April 24, 1986 ($\phi = 54^{o}$, $\lambda = 4^{o}$)

first period 2:00 - 8:00 hours
second period 13:00 - 18:00 hours

For this reason GPS was used during the NAVGRAV project only for various experimental purposes. For the gravimetric survey traditional radio positioning systems were deployed.

2. Equipment

Several positioning systems were on board during both periods of surveying, as shown below:

1st period: April 23 - 29	*2nd period: April 30 - May 13*
GPS receivers	*GPS receivers*
Trimble 4000A (Radio Holland)	Trimble 4000A (Radio Holland)
Sercel TR5S (Rijkswaterstaat*)	Rubidium clock (T.U. Munich)
TI-4100 (University of Hannover)	
TI-4100 (Technical University Munich)	
Cesium clock (Nortech Surveys)	
Rubidium clock (Technical University Munich)	
Radio positioning systems	*Radio positioning systems*
Syledis (Osiris Seaway)	Pulse 8
Hifix (Hr.Ms. Tydeman)	Hyperfix (Hr.Ms. Tydeman)
Hyperfix (Hr.Ms. Tydeman)	Oceanlog (Hr.Ms. Tydeman)
Loran C (Rijkswaterstaat*)	
Oceanlog (Hr.Ms. Tydeman)	

* Survey Department of the Ministry of Transport and Public Works

During the first period an additional TI-4100 receiver (Nortech Surveys) was set up at an on-shore station. First at Haarlem (April 21 - 25), and after that at Delft (April 25 - 28), in order to be able to post-process the data in translocation, i.e. differential, mode. For this reason, all GPS receivers were scheduled to operate in the same mode (P or S code) and to track the same satellites.

In addition, GPS measurements carried out at a second

on-shore station (Stavanger, Norway) were kindly provided by the Norwegian Hydrographic Service, for translocation purposes over a greater distance. Unfortunately, these data could not be used, because of a different satellite observation scheme at Stavanger.

A complete overview of the equipment is shown in appendices 1 and 2. The instruments were set up on board at two locations: in the chartroom and in lab-1, where the observers kept contact by telephone. In the chartroom the INTERPLOT-200 software of Intersite Surveys was running on a HP9920 computer for real-time navigation. A very important subject was the time synchronisation of all the positioning systems. This problem was solved by synchronizing the clock of the Hewlett Packard computer with GPS time using the one pulse per second output from the TI-4100 receivers.

During the second period of the project from April 30 to May 13 only one Trimble GPS receiver remained on board and the Pulse 8 positioning system was used as primary positioning system for the gravimetric survey. Both positioning systems yielded satisfactory results during the entire period.

3. Antenna offset

The intersection point of the main mast and the horizontal beam was adopted as the reference point for all positioning systems. The antenna offsets, as determined in a three dimensional coordinate system, are given in table 1.

GPS receiver	X(m)	Y(m)	ΔH(m)	remark
TI-4100 (Munich)	-0.25	+38.8	-5.0	until Apr.27, 15h
TI-4100 (Hannover)	-3.0	+ 0.1	+0.5	until Apr.27, 15h
TI-4100 (Hannover)	-0.25	+38.8	-5.0	from Apr.27, 15h
Trimble 4000A	+2.6	+ 0.1	+0.8	until Apr.27, 12h
Trimble 4000A	+0.4	- 2.3	+3.8	from Apr.27, 12h
Sercel	+0.25	+38.8	-5.0	

Y = heading direction
X = starboard direction
ΔH = vertical height difference (up = positive)

Table 1. Antenna offsets

The antenna offset to the reference point was computed as follows:

$$\Delta\varphi^0 = (X \sin\alpha - Y \cos\alpha) \frac{\rho}{R}$$

$$\Delta\lambda^0 = - (X \cos\alpha + Y \sin\alpha) \frac{\rho}{R \cos\varphi} \qquad (1\ a,b,c)$$

$$H_c = H - \Delta H$$

where:

$\rho = 180^0/\pi$

R = 6378388 metre

α = ship course

4. Real-time navigation

The real-time navigation data was handled by the HP9920 computer using the INTERPLOT-200 software, by which the Syledis, Hifix and Hyperfix positions were recorded. The raw data and the computed positions were simultaneously stored on 3.5" diskettes. The currently most reliable terrestrial radio position was selected as primary position and used for the gravimetric survey. This primary position was also monitored on the bridge for controlling the desired sailing route for the gravimetric survey.

Moreover, the following GPS positions were computed in real-time and recorded on 3.5" diskettes or 4 track tape:

1. TI-4100 (Munich), after April 27 the TI-4100 (Hannover) using the Nortech real-time navigation software
2. Trimble, using the receiver software
3. Sercel, using the receiver software (not involved here).

5. GPSFIX program

In order to post-process the TI-4100 raw data new software was developed at the Faculty of Geodesy on the VAX 750 computer. Various subroutines, which had been developed before (cf. de Jong, 1985 and Visser, 1988) were utilized here. However, these subroutines had to be converted from HP Basic 3.0 to Fortran 77. This conversion was necessary, because the HP computer could not

handle such large amounts of data within a reasonable period of time.

Since the structure of such a navigation program is generally known, only some main features are presented here. The navigation program GPSFIX has the following steps:

1. read TI-4100 raw data (8 bit numbers) in "Hannover" or "Shell" format
2. decode the datablocks ("ephemeris" or "measurements")
3. compute satellite coordinates from Broadcast Ephemeris
4. compute pseudoranges or Doppler aided pseudoranges, using either P or S code and apply ionospheric correction and tropospheric correction for a standard atmosphere
5. compute position and velocity (either from 4 satellites or from 3 satellites with fixed height or from two satellites with fixed height and fixed clock offset)

The menu options of the GPSFIX program are presented below in table 2.

```
$RUN GPSFIX
enter receiver type  (ti or trimble)        [          ti] =>
shell or hannover data  (1 or 2)            [           2] =>
enter input dataset name                                   =>
enter output dataset name                                  =>
unformatted output  (y or n)                [           n] =>
store usersolution  (y or n)                [           n] =>
enter itest  (notest=0,  level=1,2,3,4)     [           0] =>
enter latitude   ( dd,mm,ss)                               =>
enter longitude  (ddd,mm,ss)                               =>
enter height (m)                                           =>
enter a priori s.d. of latitude  (m)        [     1000.00] =>
enter a priori s.d. of longitude (m)        [     1000.00] =>
enter a priori s.d. of height    (m)        [        5.00] =>
enter a priori s.d. of bias      (m)        [100000000.00] =>
enter a priori s.d. of pseudoranges (m)     [        4.00] =>
enter minimum elevation (degr)              [        5.00] =>
enter dry temperature (c)                   [       15.00] =>
enter wet temperature (c)                   [       12.00] =>
enter pressure (mbar)                       [     1012.00] =>
doppleraid or normal (doppler or normal)    [     doppler] =>
s.d. of phase measurements (cycles)         [        0.02] =>
```

Table 2. Menu of the GPSFIX program

The unknowns are estimated from the following equation:

$$dX = (P_X + A^T P_L A)^{-1} A^T P_L dL \qquad (2)$$

where:

dX = vector of corrections $(\Delta\varphi \quad \Delta\lambda \quad \Delta h \quad \Delta T)^T$

dL = vector of observed minus computed pseudoranges

A = design matrix

P_L = weight matrix of the observations

P_X = weight matrix of the unknowns (for fixing the height or fixing the height and the clock offset)

The clock drift $\Delta\dot{T}$ can be determined from the previous clock offsets ΔT by means of a regression line. This clock drift is used for the prediction of the "fixed" clock offset, when only two satellites are available for positioning.

The velocity can be estimated in a similar way using the same design matrix (cf. Smit, this issue).

An example of the output data is shown in appendix 3. Each record of position fix contains the following data:

-date [yymmdd] and time [s]
-latitude [deg], longitude [deg], height [m],clock offset [m]
-clock drift with its standard deviation [m/s]
-speed [m/s] and heading [deg]
-number of satellites used for the position fix
-estimated standard deviations of the unknowns [m]
-tracked satellites (satellite PRN numbers) and GDOP

6. Transformation between WGS72 and ED50

Transformation between WGS72 and ED50 was carried out in a local system using seven transformation parameters according to:

$$X_{ED50} = X_T + S\ R\ (\ X_{WGS72} - X_0\ ) + X_0 \qquad (3)$$

where:

X_{WGS72} = vector of GPS coordinates in WGS72 $(X \quad Y \quad Z)^T$

X_{ED50} = vector of terrestrial ED50 coordinates $(X' \quad Y' \quad Z')^T$

X_0 = centre of the shifted local system

X_T = vector of translation parameters $(X_T \quad Y_T \quad Z_T)^T$

S = scale factor

R = differential rotation matrix as follows:

$$R = \begin{bmatrix} 1 & -\varepsilon_z & \varepsilon_y \\ \varepsilon_z & 1 & -\varepsilon_x \\ -\varepsilon_y & \varepsilon_x & 1 \end{bmatrix} \qquad (4)$$

The following values obtained from the NEDOC-project (Husti, 1983) are used for the transformation parameters:

X_T = 82.28 m

Y_T = 111.86 m

Z_T = 114.23 m

S = 0.9999989034

ε_x = -0.500"

ε_y = 0.492"

ε_z = 1.443"

The centre of the local system is given by the mean values of the Doppler coordinates of the NEDOC stations (Leeuwarden, Kootwijk, Herikerberg, Tongeren, Delft, Axel, Herstmonceau and Kessingland), which were used for the determination of the above transformation parameters:

X_0 = 3933097.25 m

Y_0 = 290642.89 m

Z_0 = 4993265.56 m

The inverse transformation can be derived from equation (3) and is given by:

$$X_{WGS72} = \frac{1}{S} R^T (X_{ED50} - X_0 - X_T) + X_0 \qquad (5)$$

The precision of this transformation is estimated to be better than 1 metre. The small differences between Transit WGS72 and GPS WGS72 are neglected.

7. Post-processing

The post-processing was carried out on the VAX 750 at the Faculty of Geodesy. The following preparations had to be done first:

a. the 3.5" diskettes containing real-time positions and raw data were transferred from HP217 to VAX using a HP conversion program
b. the GPS raw data (data blocks with 8 bit numbers) were copied to 9 track tape by Shell and the Hannover University
c. development of various software, in order to carry out transformations, file selection, translocation and comparison of different types of positioning systems.

The following software was developed in Fortran 77:

GPSFIX : GPS navigation program

TRANS : transformation between WGS72 and ED50 in three steps
1. φ,λ,h (WGS72) -> X,Y,Z (WGS72)
2. X,Y,Z (WGS72) -> X,Y,Z (ED50)
3. X,Y,Z (ED50) -> $\varphi,\lambda,(h)$ (ED50)

SELECT : reads various position files, checks, selects and writes to a binary position file (BPF), which can be read by all the following programs

READBF : reads the binary position files (BPF) and converts them to ASCII files

TRANSLOC: prepares differential GPS computation:
1. reads two simultaneous binary position files for the reference and the moving station
2. finds the corresponding records and checks whether for instance the observed satellites and the used ephemeris data are identical
3. computes a position correction per fix at the reference station and applies this correction to the moving station

4. output: corrected binary position file of the moving station

COMPARE : 1. reads two binary position files (BPF) which are to be compared, and finds the corresponding positions (if necessary by interpolation)
2. corrects the GPS position for antenna offset and transforms from WGS72 to ED50
3. computes the position differences and standard deviations
4. output: a. precision/accuracy analysis
b. plotfile

A flow chart of the post-processing is presented in appendix 4. The left hand side shows the processing of the real-time GPS positions and the various radio positioning systems, such as Syledis, Hifix and Hyperfix. The right hand side shows the post-processing using the program GPSFIX.

The position files obtained for the various systems can be compared and analysed by the program COMPARE. The subjects below will be treated in the sequel:

- zero base line test in Haarlem
- reference stations Haarlem/Delft
- comparison of positions from Hifix and Syledis
- comparison of real-time positions from Trimble and Syledis
- comparison of positions from TI-4100 to Syledis (including translocation)
- translocation between two GPS receivers on board of Hr.Ms. Tydeman.
- launch experiment (including translocation)

Some parts of the navigation data have already been investigated (cf. Smit, 1988 or Visser, 1988).

8. Zero base line test in Haarlem

On April 21 two TI-4100 receivers of the Munich University of Technology and Nortech Surveys were set up at Haarlem and

connected to the same antenna using a beam splitter. The observations were recorded from 14:00 to 18:15 UTC.

The position differences between two receivers, obtained from separate computations using the program GPSFIX with P code non smoothed pseudoranges are presented in appendix 5. During the first hour, where exactly the same satellites and ephemeris were used for both computations, there is good agreement: the noise level is approximately 1.2 meter. In the next part, when only two satellites were available and no atomic clock was used, there is a remarkable clock drift effect. Since each receiver uses its own internal quartz clock, such a clock drift can be expected.

9. Reference stations Haarlem and Delft

During the first week of the NAVGRAV project one on-shore TI-4100 receiver (Nortech Surveys) was observing simultaneously with the GPS receivers on board of the Hr.Ms. Tydeman, first at Haarlem (April 21-25) and then at Delft (April 25-28), in order to be able to process in translocation mode. The single point results are discussed here separately, while the translocation results using these reference positions will be discussed in section 12.

The known terrestrial coordinates and the computed mean value of the GPS positions are shown in table 3. The transformed WGS72 coordinates are obtained from ED50 coordinates (cf. equation (3)).

station:		Haarlem	Delft
ED50 (terrestrial)	φ	$52^{0}23'13.''226$	$51^{0}59'12.''848$
	λ	4 37 05.666	4 23 19.847
	h	17.00 m	27.17 m
WGS72 (transformed)	φ	$52^{0}23'10.''44$	$51^{0}59'10.''00$
	λ	4 37 00.13	4 23 14.33
	h	66.59 m	77.75 m
WGS72 (by GPS)	φ	$52^{0}23'10.''36$	$51\ 59^{0}09'.''67$
	λ	4 37 00.61	4 23 14.16
	h	66.78 m	67.45 m

Table 3. Coordinates of the reference stations

Differences between stationairy 3-D positions and their mean values are plotted for the stations Haarlem and Delft:

Appendix 6: Station Haarlem: P code / non-smoothed pseudorange
Appendix 7: Station Delft : P code / non-smoothed pseudorange
Appendix 8: Station Delft : P code / Doppler-aided pseudorange
Appendix 9: Station Delft : S code / non-smoothed pseudorange

The single point positioning with P code yields generally excellent results. The obtained differences with the known values are within 10 m (appendices 6 and 7). Computation with Doppler aided pseudorange gives a lower noise level, but no improvement in accuracy (appendix 8). The positioning using S code gives a much higher noise level and in this case small systematic errors (appendix 9).

10. Comparison of positions from Hifix and Syledis

The precision of Hifix and Syledis distance or distance difference measurements is estimated to be 1 - 2 metres. However, both systems may have much larger systematic position errors due different reference systems, to calibration errors and to the influence of the geometric intersection. Therefore it is common practice to carry out a local "re-calibration" by applying local corrections, in order to remove the systematic errors and to improve the external accuracy.

A comparison between the two systems, without any "re-calibration", measured in an area of good coverage, is shown in appendix 10. Obviously there always exists a certain systematic error between the two positioning systems, in this special case an average of 6.6 m in latitude and 3.8 m in longitude. The error distribution in figure 2 shows the same systematic errors. The standard deviations of the differences after elimination of these systematic errors are:

$$\sigma_{\varphi} = 3.3 \text{ m}$$
$$\sigma_{\lambda} = 3.1 \text{ m}$$

In these standard deviations the influence of both Syledis and Hifix position errors are involved. Thus the precision of each system may be about 2 metre (in position), which seems reasonable.

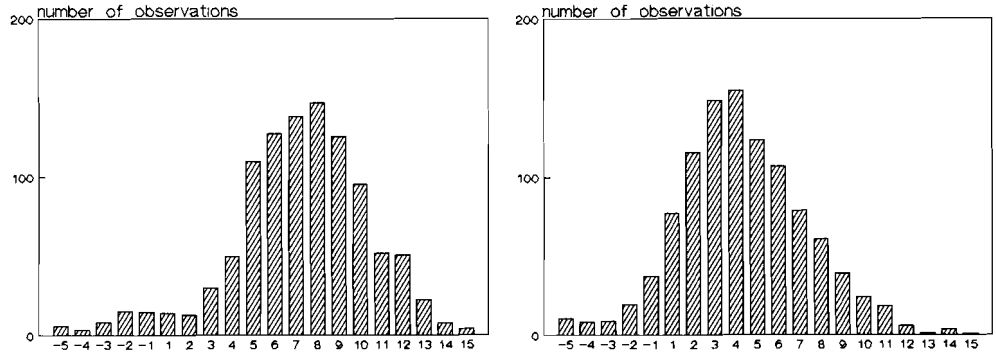

Figure 2. Latitude and longitude differences. Hifix - Syledis (m)

However, the systematic position errors, which are expected to be at a 3-5 metres level are difficult to determine. It should be pointed out that this position accuracy does not allow to evaluate GPS positions better than this level.

11. Comparison of positions from Trimble and Syledis

The Trimble 4000A receiver yielded very satisfactory results throughout the whole period and provided reliable positions at 15 seconds intervals. An example of these real-time positions compared to Syledis is shown in appendix 11. From the differences (including systematic errors) the following standard deviations are obtained:

$$\sigma_{\varphi} = 6.9 \text{ m}$$
$$\sigma_{\lambda} = 13.4 \text{ m}$$

This result, obtained from 911 position fixes at intervals of 15 seconds, is quite good for a single frequency receiver. The error distributions of these differences are shown in figure 3.

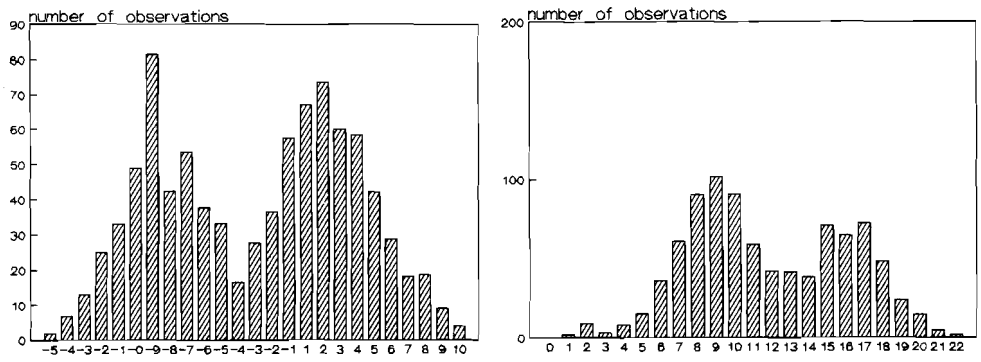

Figure 3. Latitude and longitude differences. Trimble-Syledis (m)

12. Comparison of positions from two TI-4100 receivers and Syledis

A number of TI-4100 positions obtained on board of the Hr.Ms. Tydeman were post-processed with the GPSFIX program. The single positions obtained by the Munich and Hannover receivers on April 25, in the same observation period (using P code) are compared to Syledis, after reduction of both GPS antenna positions to the same reference point. The differences are plotted in appendices 12 and 13 respectively, showing a precision of about 10 metres.

If we compare the position differences of the two GPS receivers on board (cf. appendix 14) we may conclude that there is no significant discrepancy.

In addition, the observations collected by the Hannover receiver on April 25 are also processed as Doppler aided pseudoranges, compared with Syledis and plotted in appendix 15. This gives some improvement in precision and accuracy. Compared with the stationary measurement shown in appendix 8, it has a higher noise level possibly caused by Syledis.

The Hannover receiver observations of April 25 were also processed in translocation mode relative to the station Delft. The differences with the Syledis positions are plotted in appendix 16. If these results are compared with those of appendix 13, it appears that some improvement of the accuracy is obtained in

translocation mode since the slopes are removed. The noise level (including Syledis) is now below 3 m. The gaps in the plot in appendix 16 are caused by the fact that not always the same satellite configuration was observed by both receivers. In case of different satellite configurations or ephemeris of different ages, the position fixes are ignored by program TRANSLOC.

13. Launch experiment

On April 24 a launch experiment was carried out. A TI-4100 receiver and a Hifix receiver were installed in the launch, which was sailing near the Hr.Ms. Tydeman at distances of up to 4 km. It was intended to investigate the accuracy of differential GPS between two moving vessels at short distance. Thus, we have a GPS position difference and a corresponding Hifix position difference between the Hr.Ms. Tydeman and the launch, which can be compared. This experiment was, however, not successful, because the TI-4100 receiver on board of the Hr.Ms. Tydeman was set to S code (operator mistake), while the TI-4100 receiver on the launch set to P code. The results of the computations were very poor.

The launch positions obtained from the TI-4100 data were compared in the following way:

a. The single GPS positions are compared to the Hifix positions, both measured on board of the launch. The results shown in appendix 17 are very satisfactory since a precision in latitude and longitude of about 2 metre and systematic errors of 4.1 m and 13.6 m respectively are achieved. These systematic errors are of course caused by both Hifix and GPS.
b. Next the GPS positions are improved by translocation relative to the station Haarlem and compared to Hifix positions. The results presented in appendix 18 show no significant improvement.

14. Conclusions

The Syledis and Hifix positioning systems, used as a reference during the project, yield a precision of about 2 m in latitude and longitude. However, the systematic error may be 3 - 5

metres. Thus the GPS positions can only be evaluated with the same accuracy level.

The Trimble 4000A internal software provided real-time reliable positions with a standard deviation of 10 - 20 m by S code (contribution of Hyfix/Syledis is included).

The TI-4100 receivers provided good results after post-processing. The standard deviation for a position without translocation is estimated to 10 m using P code, and 10 - 20 m using S code (contribution of Hyfix/Syledis is included). The translocation mode yields a standard deviation of about 3 m including Syledis noise.

15. Literature

Hatch, R.R. (1986): Dynamic differential GPS at the centimeter level. Proceedings of the Fourth International Geodetic Symposium on Satellite Positioning, Austin, Texas.

Jong, C.D. de (1985): Practical Work on GPS. Trainee Report, Delft University of Technology, Faculty of Geodesy.

Lachapelle, G. and N. Beck (1982): NAVSTAR / GPS Single Point Positioning at Sheltech Canada - Preliminary Results. The Canadian Surveyor, vol. 36, no. 1.

Lachapelle, G., W. Falkenberg, M. Casey (1987): Use of Phase Data for Accurate Differential GPS Kinematic Positioning. Bulletin Géodésique, vol. 61, no. 4.

Sluiter, P.G. and G.J. Husti (1987): Evaluation of the TI-user solution in dynamic mode. Marine Geodesy, vol. 11, no. 1.

Smit, J.H.M. (1988): Sea gravimetry and Eötvös correction. Graduate thesis, Delft University of Technology, Faculty of Geodesy.

Visser, J.L.M. (1988): GPS plaatsbepaling op zee. Graduate thesis, Delft University of Technology, Faculty of Geodesy.

APPENDIX

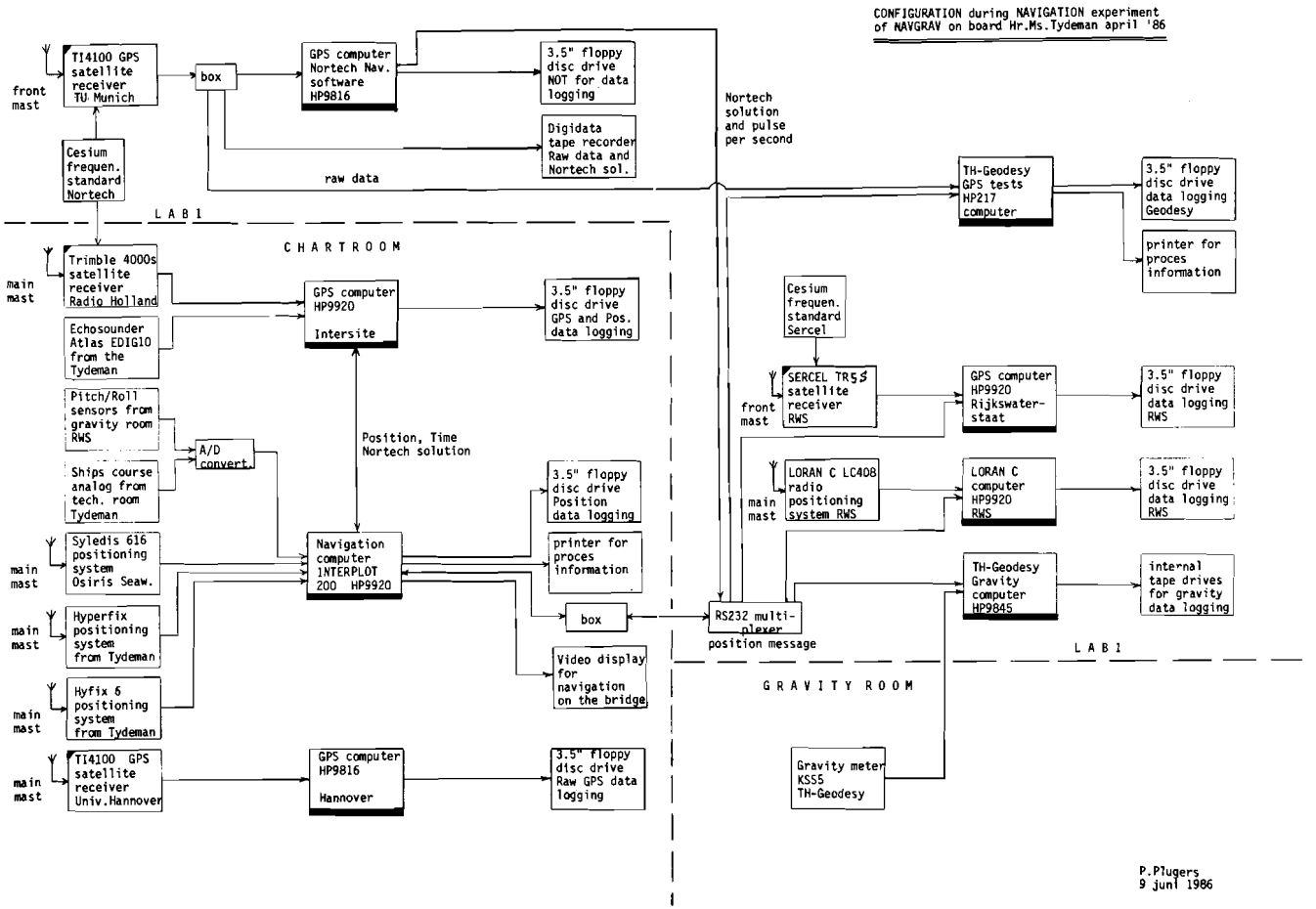

Appendix 1
Equipment in the period April 23-29

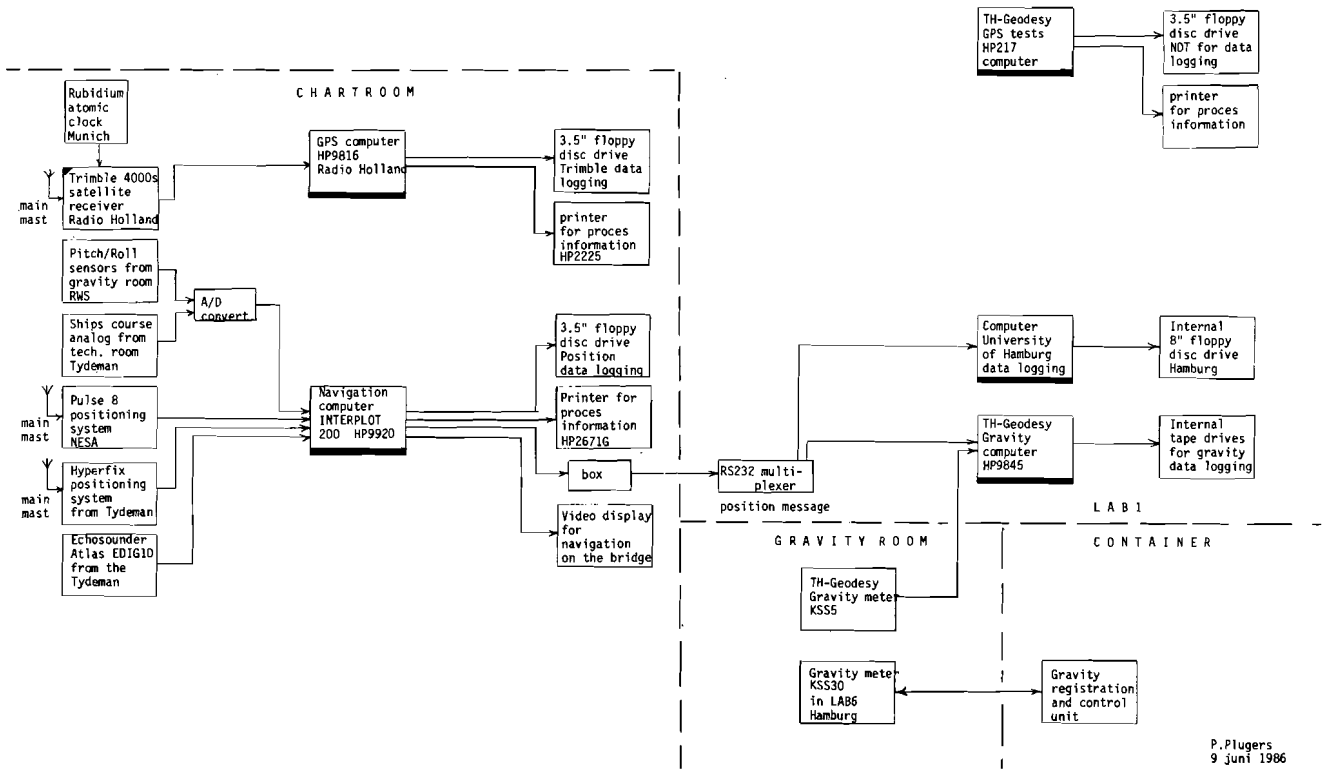

Appendix 2
Equipment in the period May 1-13

```
*** GPSFIX_BATCH ***

receiver: ti    dataset: cemetary    mode: doppler
lat lon height:   53.00 24.00   0.00    4.00 18.00   0.00   65.00
sd unknowns:   10000.0 10000.0    5.0    100000000.0
sd ranges:    4.0    sd phase :   0.02
dryt wett press:   15.0 12.0 1012.0    min elevation:    5.
```

*yymmdd gps_utc	latitude	longitude	height	bias	drift	sd_dr	speed	hdg	nsat	varla	varlo	varh	varb	sv_tracked	sv_health	gdop
860425 54512.0	53.391004	4.315097	66.01	132470.	0.00	0.000	4.66	60.9	4	43.6	10.9	19.5	11.8	8 9 12 11	P 0 0 0 0	3.4
860425 54515.0	53.391070	4.315292	67.08	132485.	0.00	0.000	4.67	62.2	4	21.9	5.7	16.0	8.1	8 9 12 11	P 0 0 0 0	3.8
860425 54518.0	53.391117	4.315478	66.65	132498.	4.96	0.000	4.69	61.1	4	14.6	3.9	13.6	6.4	8 9 12 11	P 0 0 0 0	3.9
860425 54521.0	53.391176	4.315672	67.11	132512.	4.96	0.000	4.71	60.8	4	11.0	3.0	11.8	5.4	8 9 12 11	P 0 0 0 0	3.9
860425 54524.0	53.391235	4.315859	66.98	132525.	4.85	0.103	4.75	62.7	4	8.8	2.4	10.4	4.6	8 9 12 11	P 0 0 0 0	3.9
860425 54527.0	53.391298	4.316044	67.42	132539.	4.85	0.103	4.60	62.2	4	7.3	2.0	9.3	4.1	8 9 12 11	P 0 0 0 0	3.9
860425 54530.0	53.391363	4.316223	66.91	132551.	4.74	0.125	4.72	62.4	4	6.3	1.7	8.4	3.7	8 9 12 11	P 0 0 0 0	3.9
860425 54533.0	53.391417	4.316410	67.01	132565.	4.74	0.125	4.66	62.9	4	5.5	1.5	7.7	3.3	8 9 12 11	P 0 0 0 0	3.9
860425 54536.0	53.391477	4.316594	66.38	132578.	4.67	0.116	4.63	60.0	4	4.9	1.4	7.1	3.0	8 9 12 11	P 0 0 0 0	3.9
860425 54539.0	53.391535	4.316777	65.79	132591.	4.67	0.116	4.77	61.6	4	4.4	1.2	6.6	2.8	8 9 12 11	P 0 0 0 0	3.9
860425 54542.0	53.391589	4.316964	65.62	132604.	4.59	0.116	4.72	63.0	4	4.0	1.1	6.1	2.6	8 9 12 11	P 0 0 0 0	3.9
860425 54545.0	53.391650	4.317153	65.96	132618.	4.59	0.116	4.70	60.8	4	3.7	1.0	5.7	2.4	8 9 12 11	P 0 0 0 0	3.9
860425 54548.0	53.391711	4.317338	66.25	132631.	4.60	0.095	4.72	62.1	4	3.4	1.0	5.4	2.3	8 9 12 11	P 0 0 0 0	3.9
860425 54551.0	53.391769	4.317525	66.21	132644.	4.60	0.095	4.73	61.2	4	3.2	0.9	5.1	2.2	8 9 12 11	P 0 0 0 0	3.9
860425 54554.0	53.391833	4.317710	66.11	132658.	4.57	0.084	4.76	59.9	4	2.9	0.8	4.8	2.0	8 9 12 11	P 0 0 0 0	3.9
860425 54557.0	53.391890	4.317896	65.99	132671.	4.57	0.084	4.73	62.1	4	2.8	0.8	4.6	1.9	8 9 12 11	P 0 0 0 0	3.9
860425 54560.0	53.391948	4.318086	66.21	132684.	4.55	0.076	4.70	61.2	4	2.6	0.7	4.4	1.8	8 9 12 11	P 0 0 0 0	3.9
860425 54563.0	53.392009	4.318272	65.90	132696.	4.55	0.076	4.73	60.9	4	2.5	0.7	4.2	1.7	8 9 12 11	P 0 0 0 0	3.9
860425 54566.0	53.392070	4.318460	66.02	132711.	4.53	0.069	4.70	62.4	4	2.3	0.7	4.0	1.7	8 9 12 11	P 0 0 0 0	3.9
860425 54569.0	53.392126	4.318650	65.72	132724.	4.53	0.069	4.75	62.7	4	2.2	0.6	3.8	1.6	8 9 12 11	P 0 0 0 0	3.9
860425 54572.0	53.392186	4.318838	65.88	132738.	4.52	0.063	4.72	60.3	4	2.1	0.6	3.7	1.5	8 9 12 11	P 0 0 0 0	3.9
860425 54575.0	53.392244	4.319029	65.78	132751.	4.52	0.063	4.70	62.4	4	2.0	0.6	3.5	1.5	8 9 12 11	P 0 0 0 0	3.9
860425 54578.0	53.392304	4.319217	65.93	132765.	4.51	0.058	4.71	61.6	4	1.9	0.6	3.4	1.4	8 9 12 11	P 0 0 0 0	3.9
860425 54581.0	53.392362	4.319405	65.99	132778.	4.51	0.058	4.71	62.2	4	1.8	0.5	3.3	1.4	8 9 12 11	P 0 0 0 0	3.9
860425 54584.0	53.392421	4.319594	65.85	132791.	4.50	0.053	4.73	60.7	4	1.8	0.5	3.1	1.3	8 9 12 11	P 0 0 0 0	3.9
860425 54587.0	53.392487	4.319780	65.57	132805.	4.50	0.053	4.70	60.0	4	1.7	0.5	3.0	1.3	8 9 12 11	P 0 0 0 0	3.9
860425 54590.0	53.392546	4.319967	65.34	132818.	4.50	0.049	4.82	63.1	4	1.6	0.5	2.9	1.2	8 9 12 11	P 0 0 0 0	3.9
860425 54593.0	53.392605	4.320154	64.89	132831.	4.50	0.049	4.71	63.7	4	1.6	0.5	2.9	1.2	8 9 12 11	P 0 0 0 0	3.9
860425 54596.0	53.392658	4.320348	65.21	132844.	4.49	0.047	4.70	65.6	4	1.5	0.4	2.8	1.2	8 9 12 11	P 0 0 0 0	3.9
860425 54599.0	53.392711	4.320539	65.17	132858.	4.49	0.047	4.73	64.3	4	1.5	0.4	2.7	1.1	8 9 12 11	P 0 0 0 0	3.9
860425 54602.0	53.392766	4.320731	65.26	132871.	4.48	0.043	4.68	64.0	4	1.4	0.4	2.6	1.1	8 9 12 11	P 0 0 0 0	3.9
860425 54605.0	53.392822	4.320921	64.83	132884.	4.48	0.043	4.75	64.5	4	1.4	0.4	2.5	1.1	8 9 12 11	P 0 0 0 0	3.9
860425 54608.0	53.392873	4.321115	64.71	132898.	4.48	0.041	4.66	67.7	4	1.3	0.4	2.5	1.0	8 9 12 11	P 0 0 0 0	3.9
860425 54611.0	53.392921	4.321311	64.60	132911.	4.48	0.041	4.73	66.2	4	1.3	0.4	2.4	1.0	8 9 12 11	P 0 0 0 0	3.9
860425 54614.0	53.392973	4.321504	64.62	132924.	4.48	0.039	4.67	65.5	4	1.3	0.4	2.3	1.0	8 9 12 11	P 0 0 0 0	3.9
860425 54617.0	53.393023	4.321699	64.61	132938.	4.48	0.039	4.73	66.0	4	1.2	0.4	2.3	1.0	8 9 12 11	P 0 0 0 0	3.9
860425 54620.0	53.393073	4.321893	64.64	132951.	4.48	0.037	4.72	66.1	4	1.2	0.4	2.2	0.9	8 9 12 11	P 0 0 0 0	3.9
860425 54623.0	53.393122	4.322090	64.64	132965.	4.48	0.037	4.69	68.8	4	1.2	0.3	2.2	0.9	8 9 12 11	P 0 0 0 0	3.9
860425 54626.0	53.393168	4.322287	64.71	132978.	4.48	0.035	4.75	67.4	4	1.1	0.3	2.1	0.9	8 9 12 11	P 0 0 0 0	3.9
860425 54629.0	53.393218	4.322483	64.77	132991.	4.48	0.035	4.67	66.4	4	1.1	0.3	2.1	0.9	8 9 12 11	P 0 0 0 0	3.9
860425 54632.0	53.393269	4.322677	64.71	133005.	4.48	0.033	4.75	66.0	4	1.1	0.3	2.0	0.9	8 9 12 11	P 0 0 0 0	3.9
860425 54635.0	53.393321	4.322871	64.68	133018.	4.48	0.033	4.68	65.4	4	1.1	0.3	2.0	0.8	8 9 12 11	P 0 0 0 0	3.9
860425 54638.0	53.393371	4.323067	64.59	133032.	4.48	0.031	4.70	66.9	4	1.0	0.3	1.9	0.8	8 9 12 11	P 0 0 0 0	3.9
860425 54641.0	53.393418	4.323262	64.70	133045.	4.48	0.031	4.76	67.9	4	1.0	0.3	1.9	0.8	8 9 12 11	P 0 0 0 0	3.9
860425 54644.0	53.393467	4.323458	64.47	133058.	4.48	0.030	4.69	66.7	4	1.0	0.3	1.9	0.8	8 9 12 11	P 0 0 0 0	3.9
860425 54647.0	53.393515	4.323654	64.56	133072.	4.48	0.030	4.80	67.0	4	1.0	0.3	1.8	0.8	8 9 12 11	P 0 0 0 0	3.9
860425 54650.0	53.393564	4.323850	64.49	133085.	4.48	0.028	4.69	67.8	4	1.0	0.3	1.8	0.8	8 9 12 11	P 0 0 0 0	3.9
860425 54653.0	53.393614	4.324047	64.43	133099.	4.48	0.028	4.69	67.0	4	0.9	0.3	1.8	0.7	8 9 12 11	P 0 0 0 0	3.9
860425 54656.0	53.393660	4.324244	64.67	133112.	4.48	0.027	4.72	68.0	4	0.9	0.3	1.7	0.7	8 9 12 11	P 0 0 0 0	3.9
860425 54659.0	53.393708	4.324441	64.68	133126.	4.48	0.027	4.69	64.9	4	0.9	0.3	1.7	0.7	8 9 12 11	P 0 0 0 0	3.9

Appendix 3
Output data of the GPSFIX program

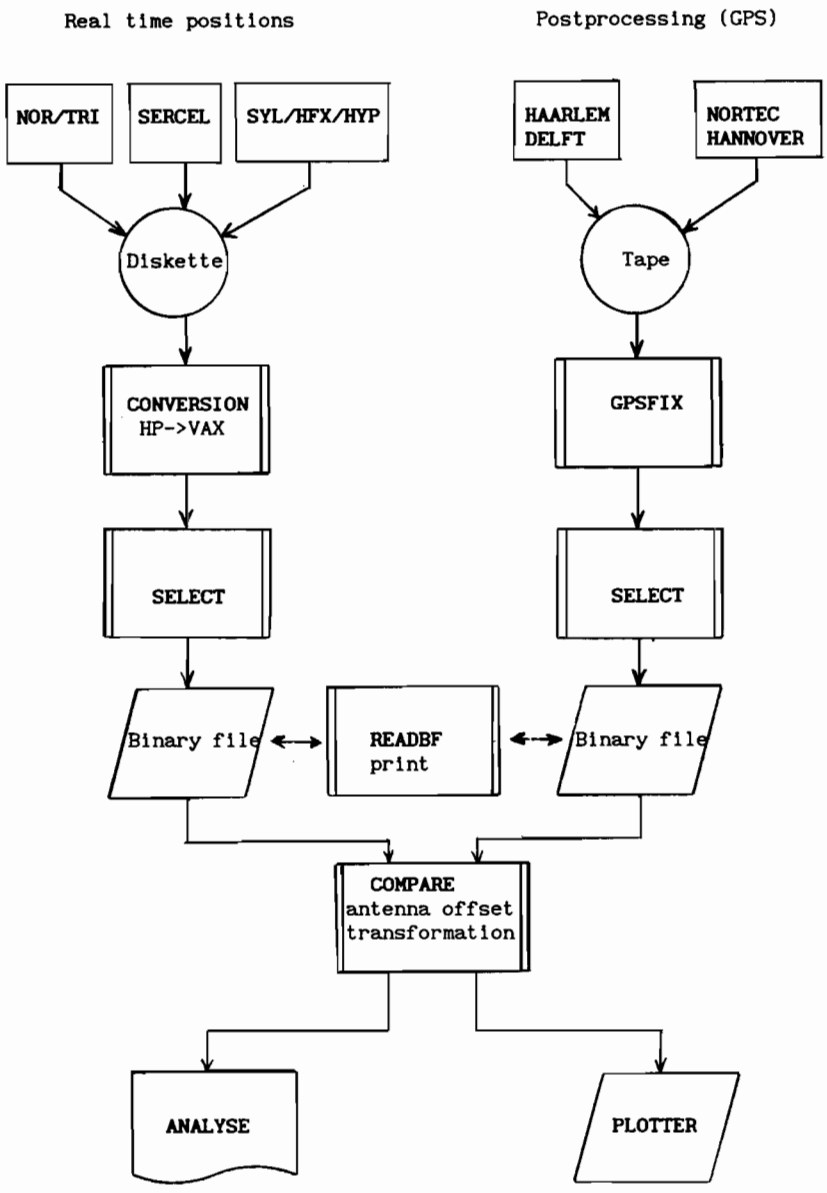

Appendix 4
Flow diagram of the postprocessing

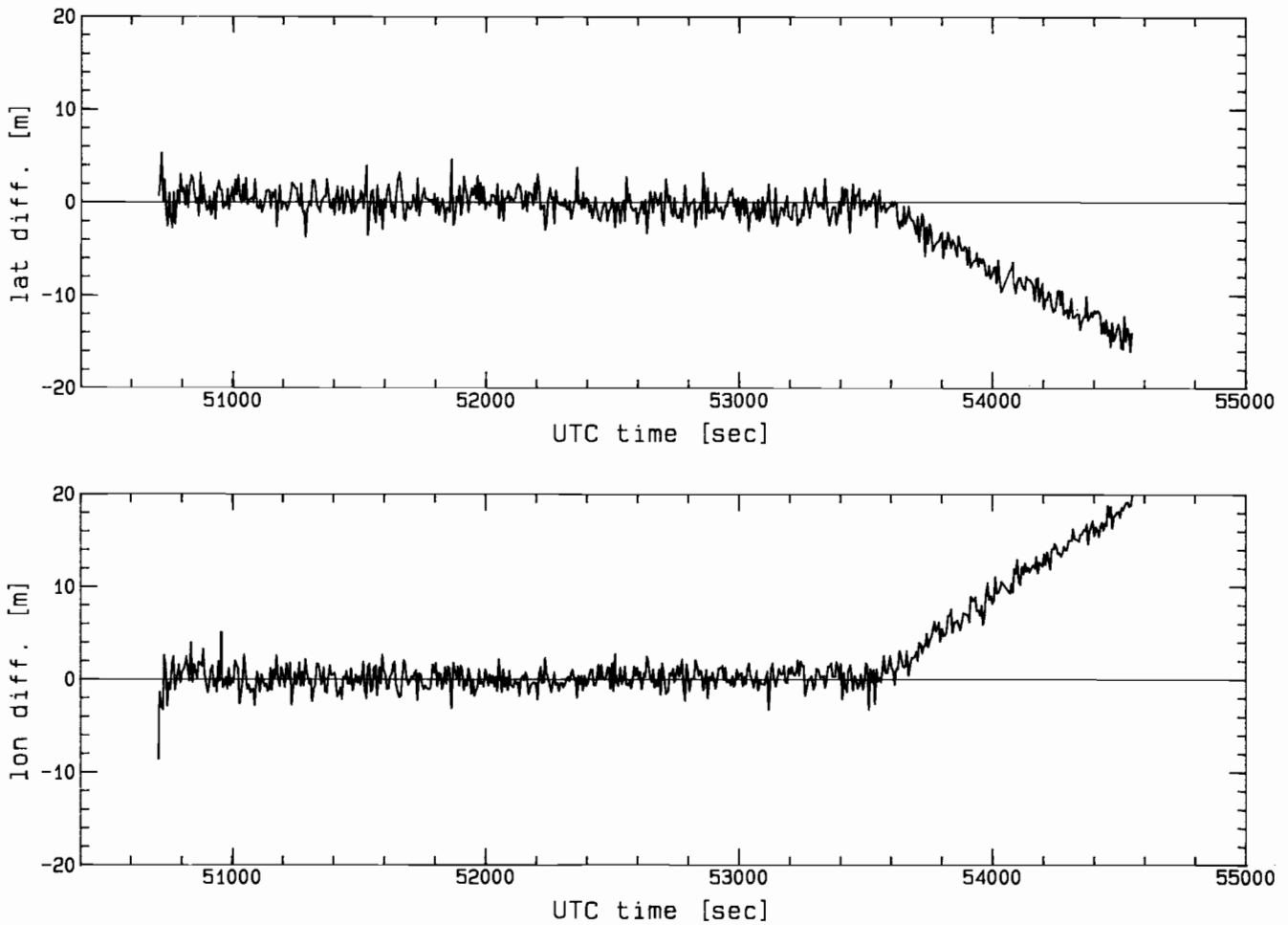

Appendix 5
Zero baseline test in Haarlem (April 21)

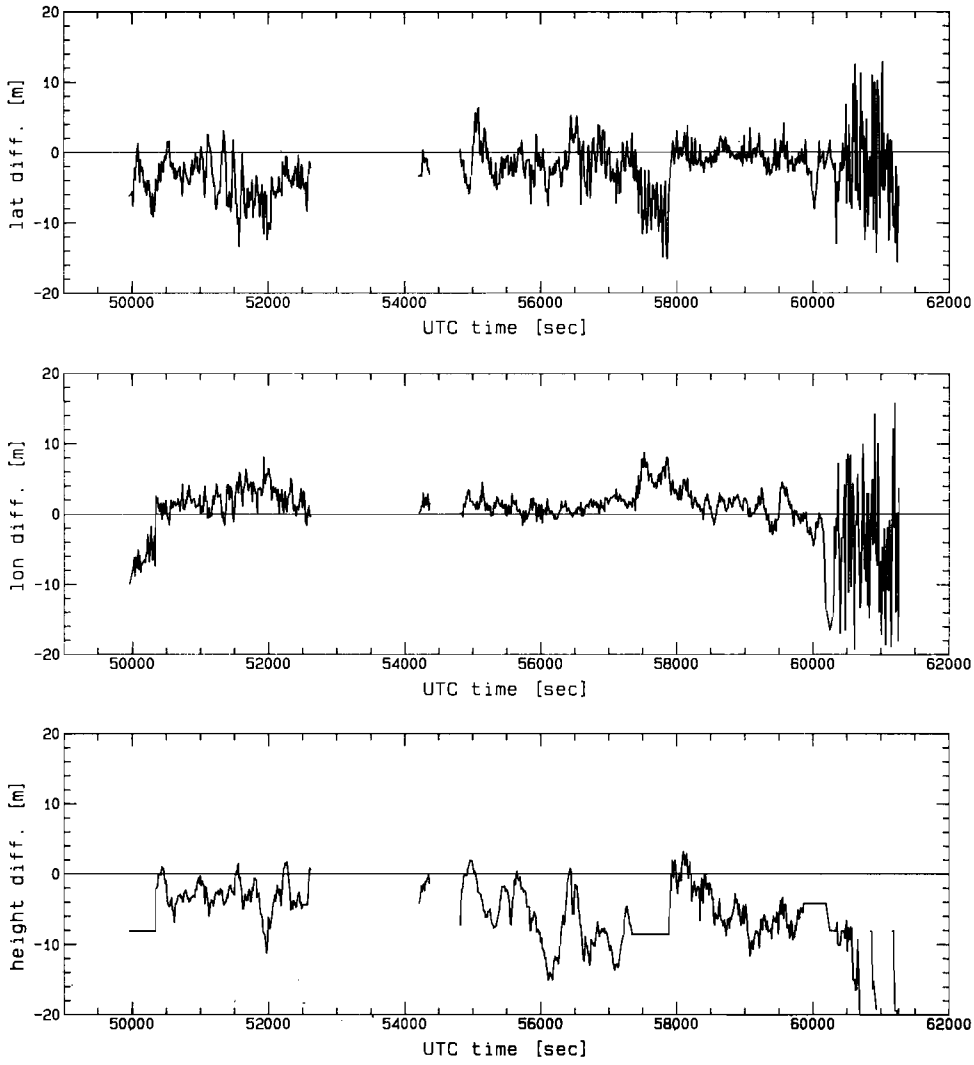

Appendix 6
Reference station Haarlem (April 24)

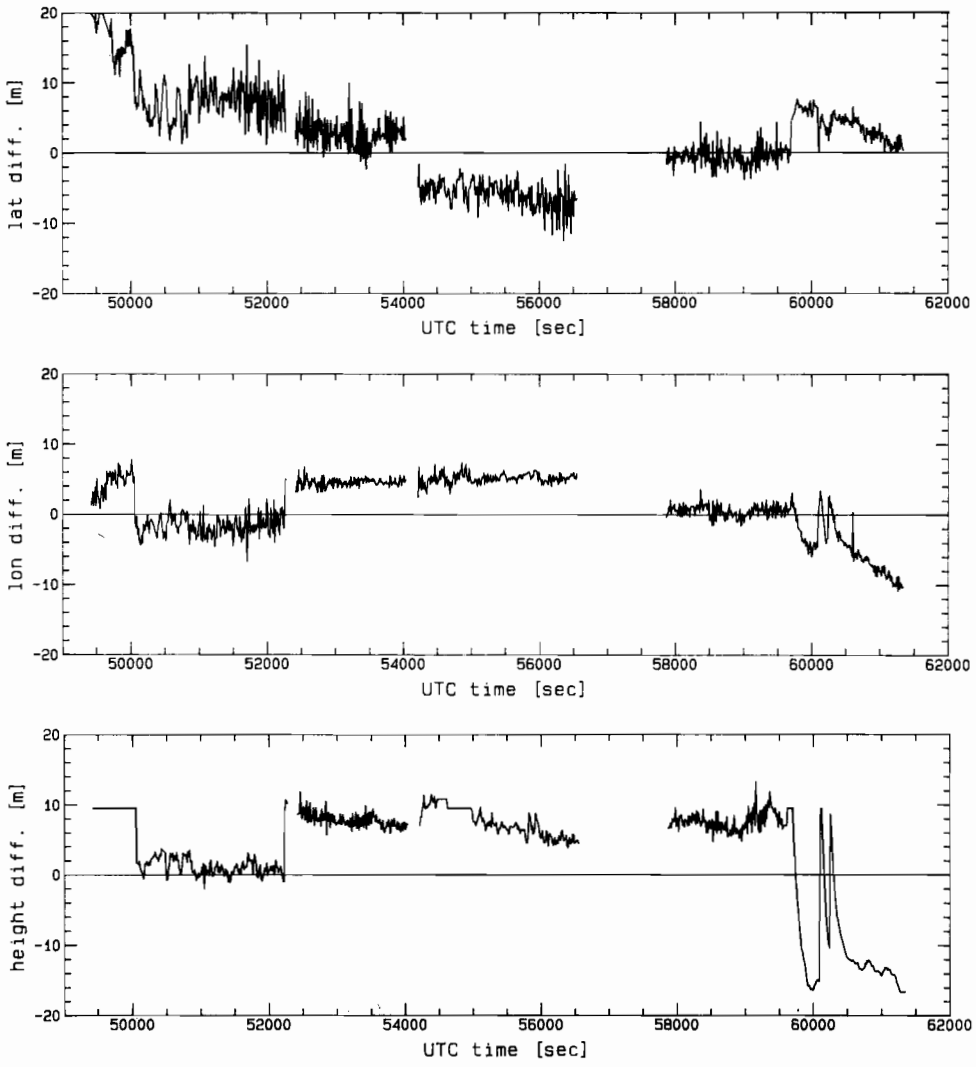

Appendix 7
Reference station Delft (April 25)

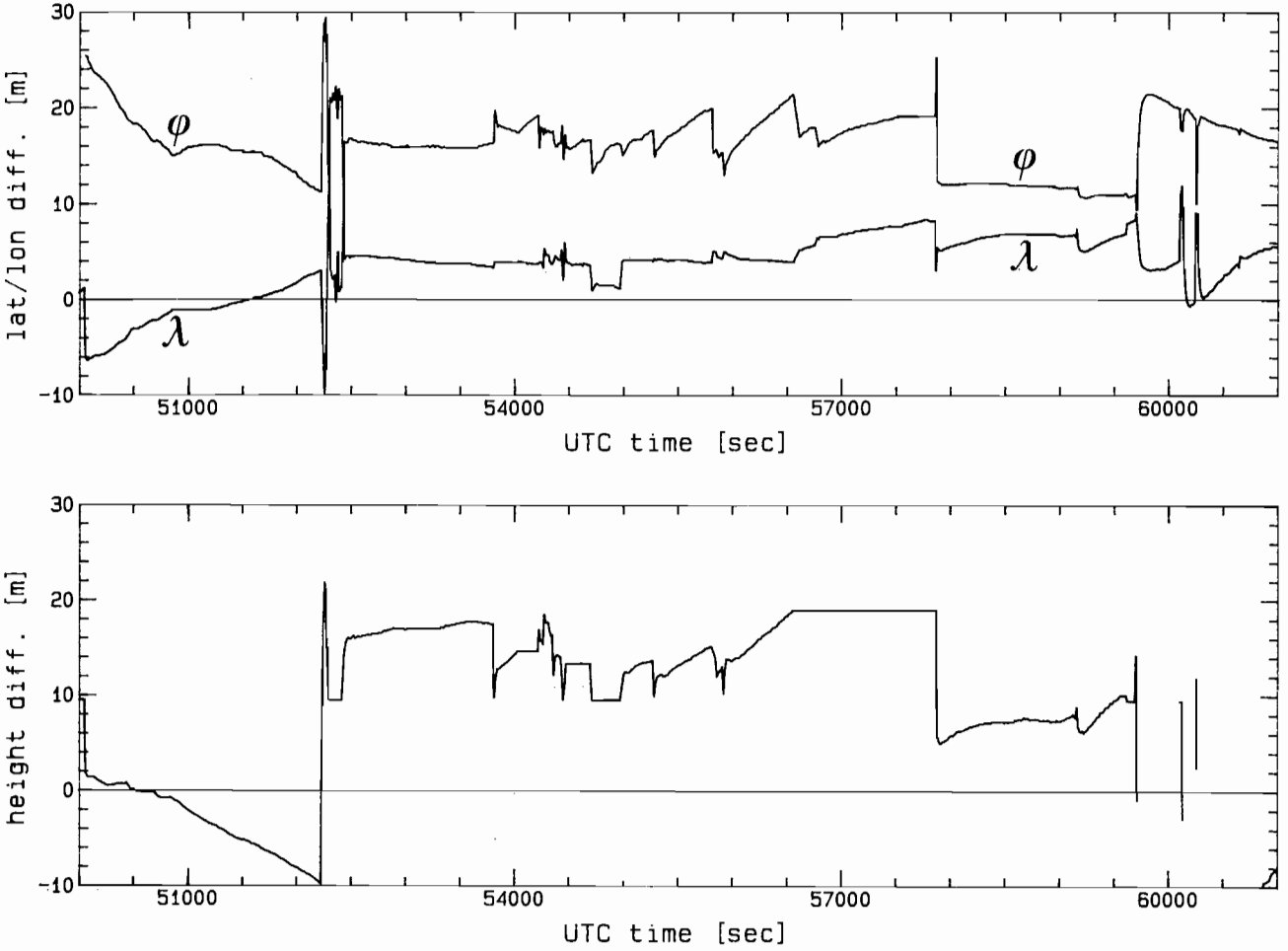

Appendix 8
Reference station Delft ['Doppler aided'] (April 25)

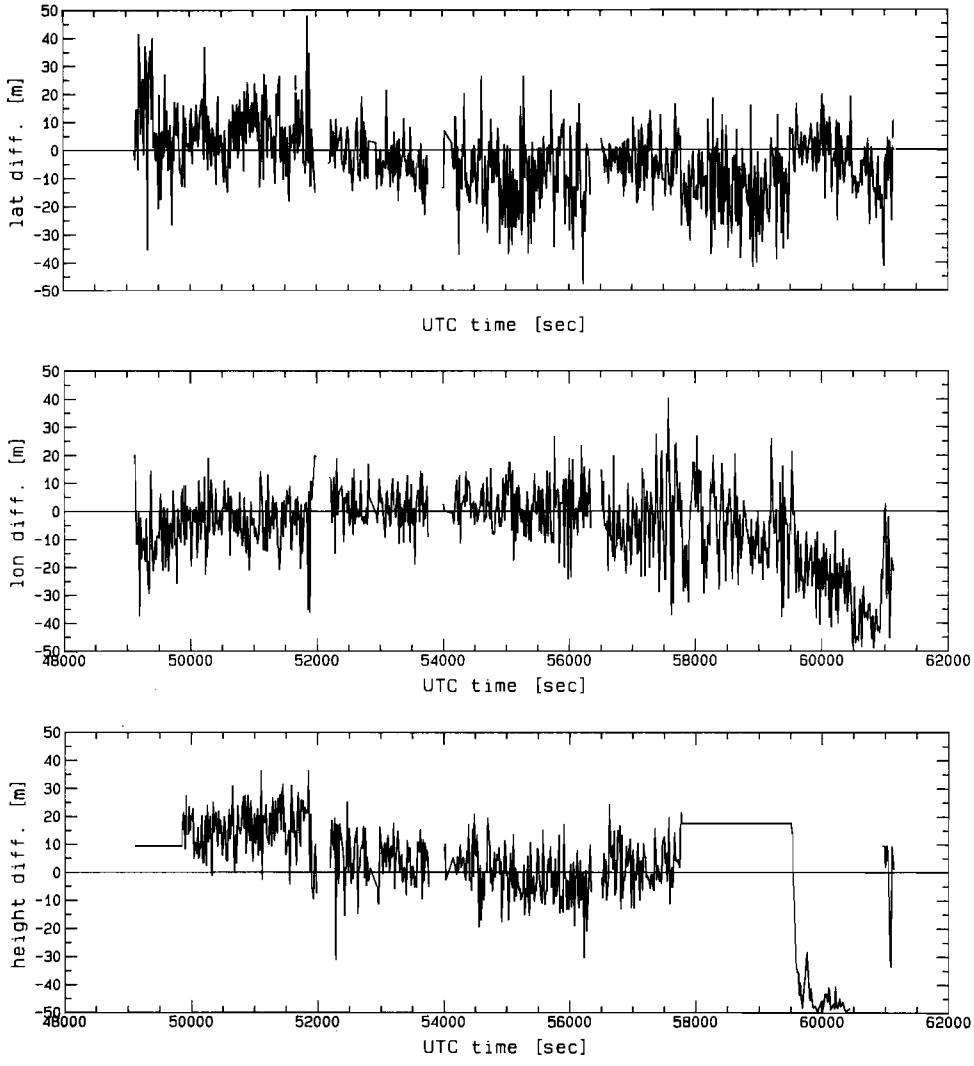

Appendix 9
Reference station Delft ['S-code'] (April 26)

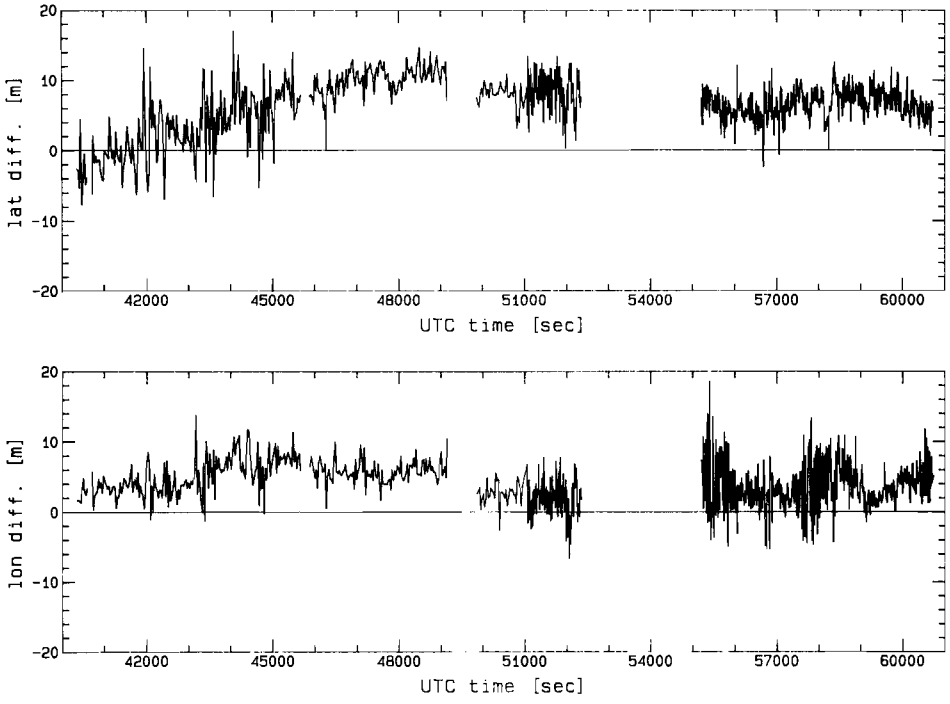

Appendix 10
Comparison Hifix to Syledis (April 24)

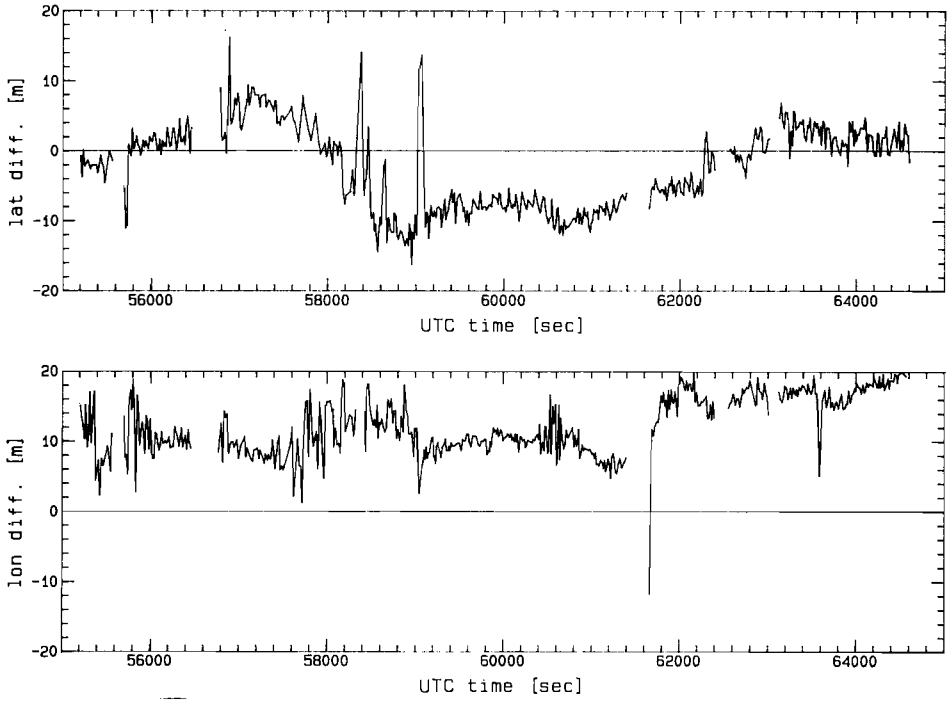

Appendix 11
Comparison Trimble to Syledis (April 24)

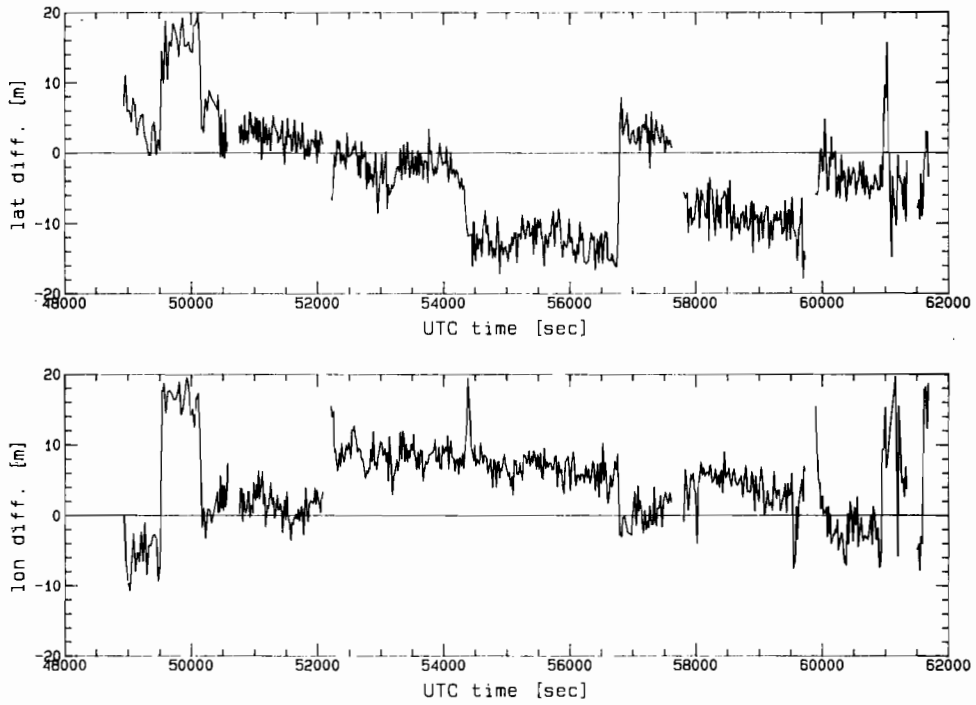

Appendix 12
Tydeman: GPS (TI/ M) - Syledis (April 25)

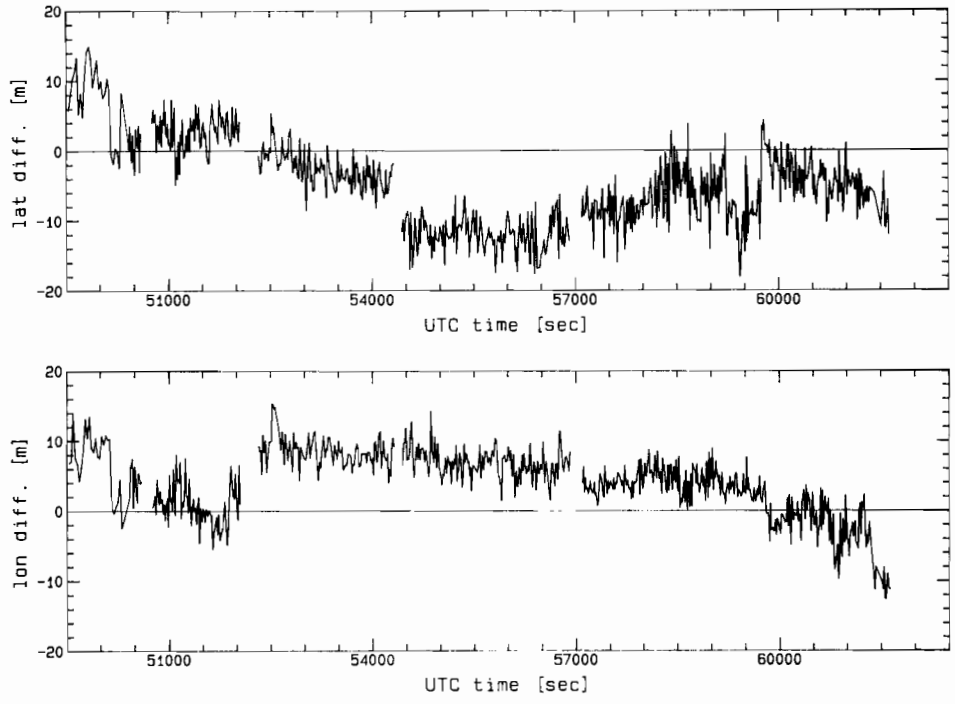

Appendix 13
Tydeman: GPS (TI/ H) - Syledis (April 25)

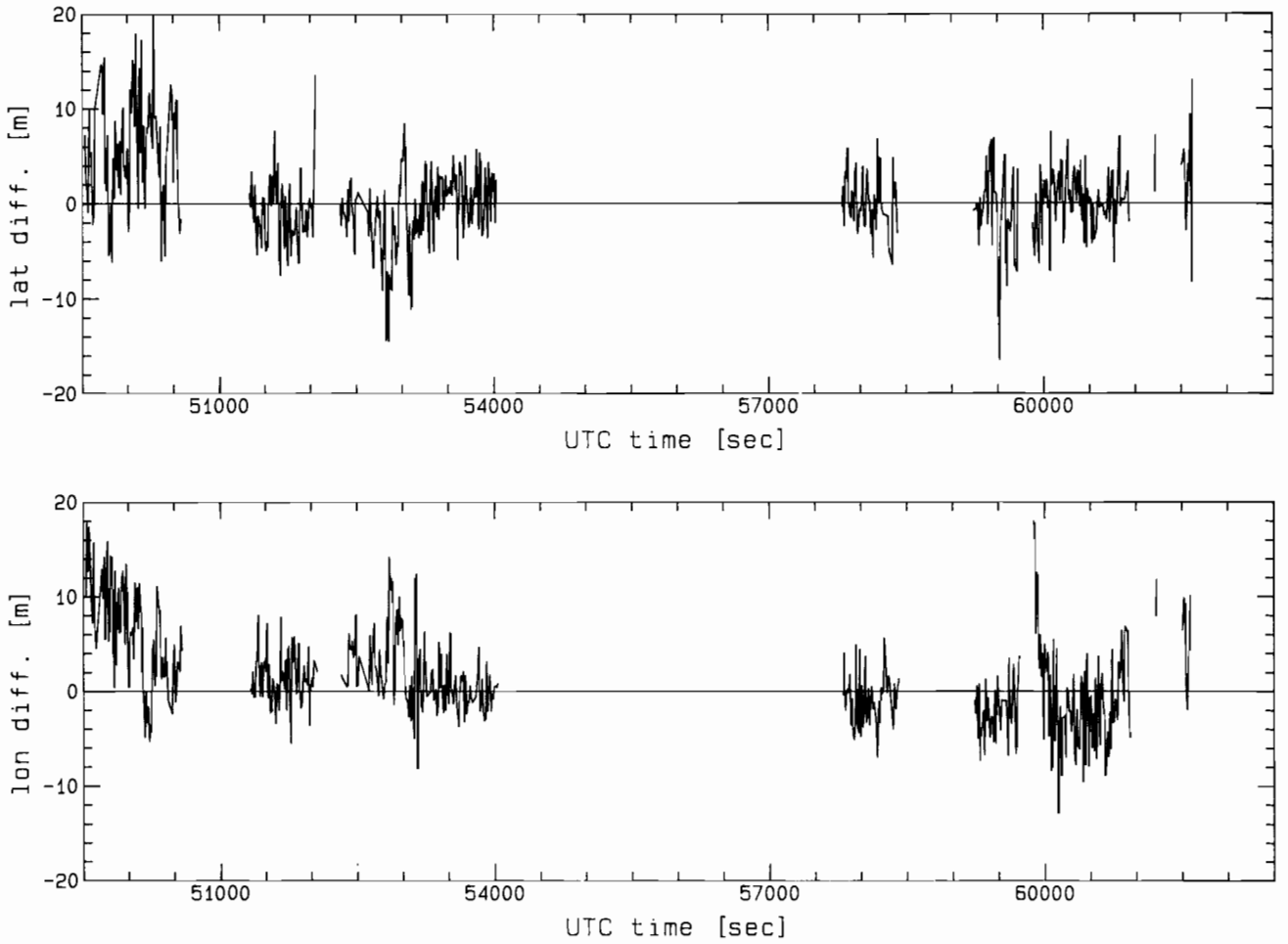

Appendix 14
Tydeman: GPS (TI/ M) - GPS(TI/ H) (April 25

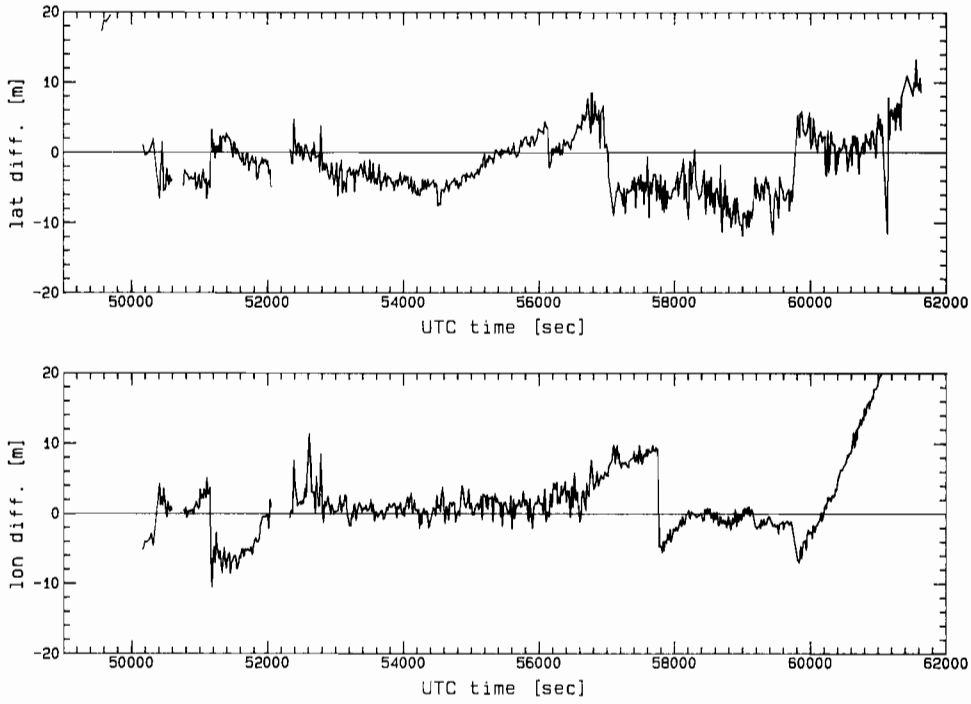

Appendix 15
Tydeman: GPS (TI/ H/ Doppler aided) - Syledis (April 25)

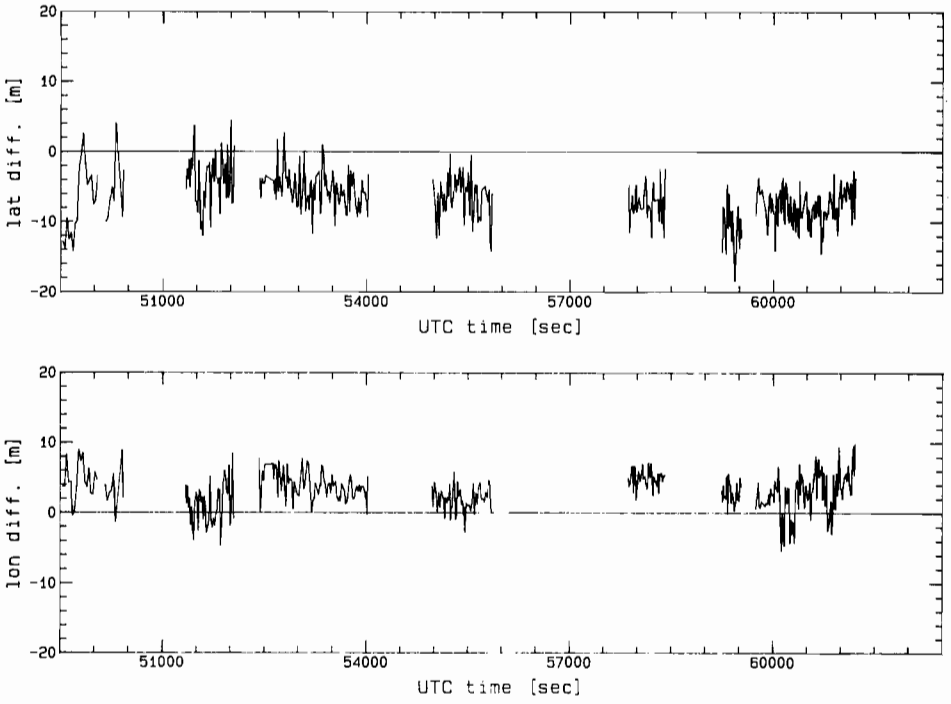

Appendix 16
Tydeman: GPS (TI/ H/ transloc) - Syledis (April 25)

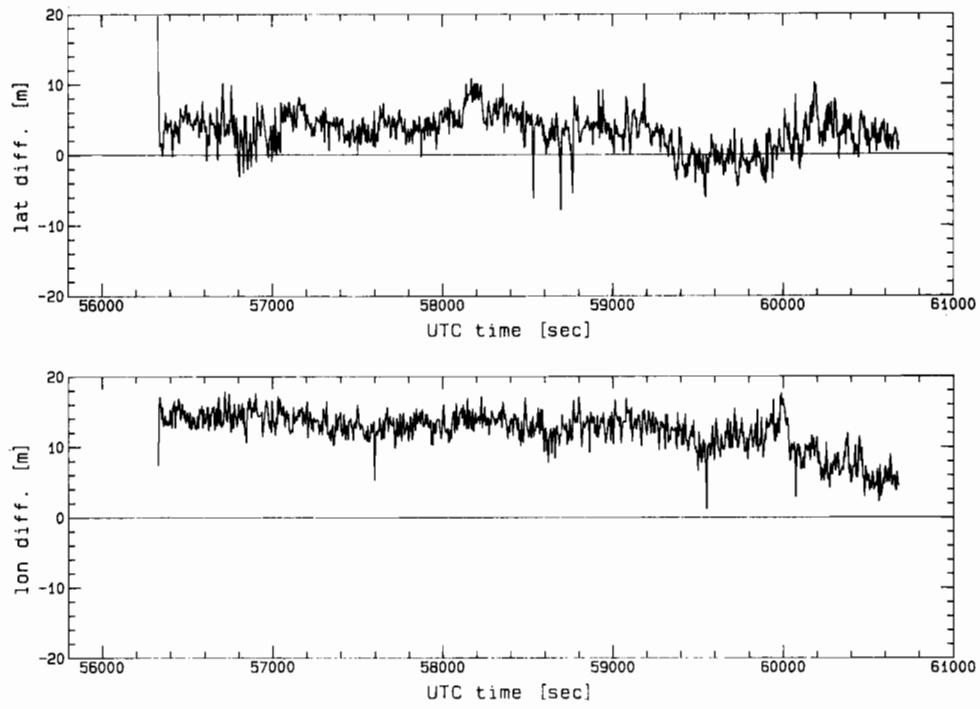

Appendix 17
Launch: GPS (TI/H) - Hifix

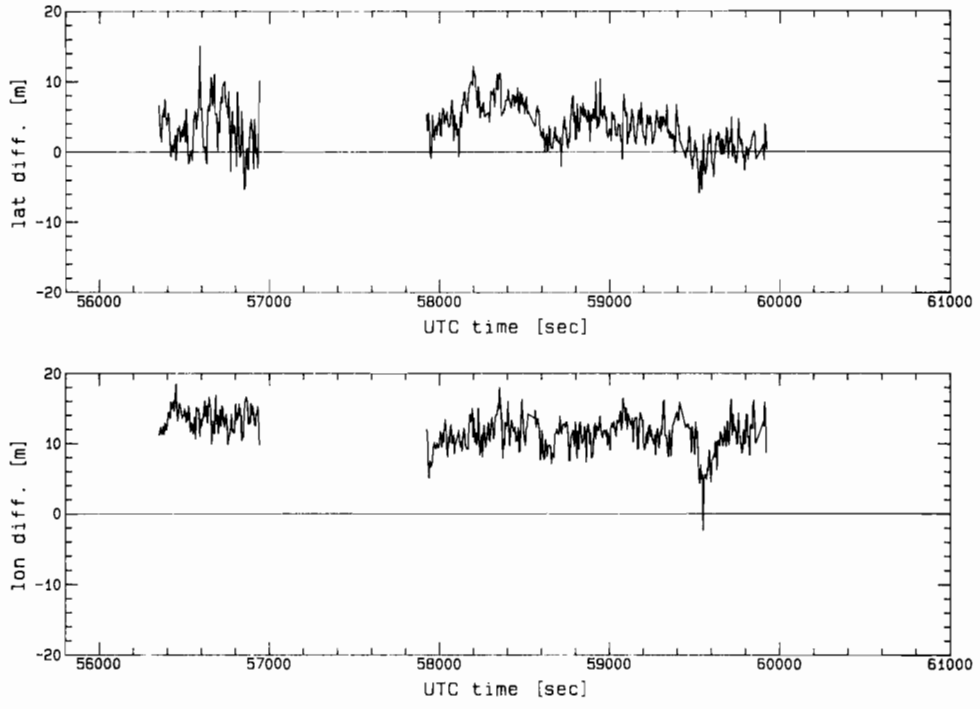

Appendix 18
Launch: GPS (TI/H/transloc) - Hifix

GRAVITY MEASUREMENTS AT THE NORTH SEA

G.L. Strang van Hees
P. Plugers
Delft University of Technology
Faculty of Geodesy
T. Liebe
University Hamburg

1. Introduction

The gravimeter which was used during the survey is the Askania-Bodensee gravimeter Kss-5, owned by the Delft University of Technology, The Netherlands. This instrument was renewed and improved in the Bodenseewerke in Germany in 1978 and 1984. Its sensor has a horizontal beam which means that it is affected by the cross-coupling effect. This effect is dependent on the weather conditions. Most of the time the weather was excellent during the cruise, so this effect was negligible.

The instrument is equipped with a cross-coupling computer which computes the cross-coupling effect on hand of the measured horizontal accelerations and the motion of the beam. This tool reduces the errors due to the cross-coupling effect. However inspection of the cross-over residuals showed a systematic error of a few milligal in bad weather conditions.

During the second period from March 30 to April 13, 1986 a second gravimeter Kss-30 from the Geophysical Institute of the University of Hamburg in Germany was installed on board. This gravimeter is based on a vertical moving mass and is not sensitive to the cross-coupling effect.

One of the main objectives of the gravity survey was to investigate the difference between the two gravimeters under different weather conditions. This way the precision of both instruments can be determined.

2. Navigation

The precision of gravity measurements at sea is mainly depending on the precision of the ship speed and course estimates. The east-west ship velocity component causes a vertical component of the Coriolis acceleration, which can be taken into account by

applying the so-called Eötvös correction. Usually this correction is the limiting factor of the precision of gravity measurements at sea. To obtain a 1 mgal precision in gravity the speed of the ship should be determined with a precision of 0.2 knots = 0.1 m/s. This can only be obtained by very good navigation systems like Syledis, Hifix, Hyperfix, Pulse 8 or by satellite systems like GPS.

As the GPS system was only available during a few hours a day, we navigated most of the time on terrestrial systems. The systems Syledis and Hifix are only reliable within a range of about 100 km from the coast. Hyperfix being just installed turned out to be unreliable and was even out of order during several days. For this reason the decision was made to rent a Pulse 8 receiver during the second period. The Pulse 8 system was used as primary navigation system which led to satisfactory results most of the time.

During the first period we navigated on Syledis and Hifix. Problems arose because of many lane slips and sometimes bad reception of the signal. The position was recorded every 3 seconds resulting in several thousand recordings which had to be inspected afterwards. Very carefully checking and filtering of the data made it possible to create a dataset with the best possible positions during the whole period.

The filtering of the data was executed in the following steps. First, all data were inspected to find the most reliable positioning system for each time. Secondly, this dataset was filtered and tested with a Kalman filter. The Kalman filter has the advantage that every successive observation is tested immediately. A jump due to a lane slip is rejected and will therefore not disturb the following positions. This way the blunders are removed. Thirdly, it was necessary to filter the dataset again to smooth the positions. Noise should be filtered out because it has a strong influence on the computed speed. Small errors in position cause large errors in speed.

The smoothing of the positions is performed with a smoothing spline program. The degree of smoothing can be regulated by a special parameter. After several trials an optimal smoothing parameter is adapted to filter out the irregular changes in position, meanwhile maintaining the regular and probably realistic

changes of speed and course of the ship. The smoothing spline program has the advantage that it computes automatically the derivative of a function which is in this case the required speed of the ship in north and east direction.

The gravimeter has a strong magnetic and electronical damping in order to reduce the influence of the vertical accelerations of the ship. However, this damping causes a slow reaction on course and speed changes. After a change it takes about 15 minutes before the gravimeter is stabilized again. The course and speed changes are obtained from the smoothed position dataset. All periods with changes are removed from the dataset, resulting in a clean dataset with only straight line tracks.

It should be emphasized that filtering and cleaning the position dataset was a time consuming and precise job. All irregularities were inspected and analyzed individually. It was the most important part of the whole computation, because undetected irregular movements of the ship result in large errors in the gravity anomalies, which can possibly lead to false geophysical interpretations.

3. Gravimeter registration

The gravimeter output of the Kss-5 gravimeter (Delft) was recorded on a HP9845 computer, together with the positions and time. Every 10 seconds the gravimeter observation was read by the computer and the mean value over one minute (6 readings) was recorded on magnetic tape. This gave the possibility to immediately detect and eliminate gross errors in the readings, since the 6 readings should be close together. The same technique was used for the positions and time. The time as received from the main clock on board was compared with the internal computer clock. If the difference was too big the error was usually caused by the data transmission and could be corrected for.

The gravity readings were also slightly smoothed by the smoothing spline program. The program is used mainly to test on errors in the gravity registration. This way errors could be corrected for.

The Hamburg gravimeter Kss-30 data was processed

independently. The output was recorded on magnetic tape, together with the ship's gyro and log. The preliminary gravity anomalies were computed at once.

4. Computation of the gravity anomalies

The gravity values (in mgal) are computed with the following formula:

$$g = S \cdot (R + \frac{\partial R}{\partial t} \cdot \tau) + \Delta g_E + D \cdot t + C + H \qquad (1)$$

where:

- g = gravity
- S = calibration constant of the gravimeter = 1.060
- R = reading of the gravimeter
- $\frac{\partial R}{\partial t}$ = change of reading per time unit, computed from the spline program
- τ = time-constant of the gravimeter, 200 seconds
- Δg_E = Eötvös correction
- D = drift of the gravimeter , computed from a harbour connection before and after the measurements
- t = time since beginning of the cruise
- C = cross-coupling correction computed from measured horizontal accelerations and beam motion
- H = harbour connection.

H is computed from the gravity value in the harbour, the gravimeter reading in the harbour and the height difference between the harbour gravity station and the water level. This correction reduces the computed gravity values to the height of the water level.

Strictly speaking the gravity values should also be reduced for tides, however this correction is usually smaller than 1 mgal and is neglected.

The harbour connection in Den Helder can be computed with equation (2) using the g_0 and R_0 values as presented in table 1.

Date and time	:	23 April 1986, 11.00 h.
Gravity value on the jetty:		981323.93 mgal
Corrections to waterlevel	:	0.86 mgal
Gravity on waterlevel	:	981324.79 mgal = g_0
Gravimeter reading	:	4328.5 = R_0

Table 1.

$$H = g_0 - S \cdot R_0 = 981324.79 - 1.060 \cdot 4328.5 = 976736.58 \text{ mgal} \quad (2)$$

On return after the first period on 29 April 1986, 12.00 h. the gravimeter reading was 4329.0.
The drift is 4329.0 - 4328.5 = 0.5 mgal in 6 days. Before start of the second period, 30 April, 17.00 h., the reading was 4329.0 and after return on 13 May, 11.00 h.: 4328.8, thus a drift of 0.2 mgal in 14 days. For both periods the drift may be neglected, so D was set to zero during the whole period.

The Eötvös correction is computed by:

$$\Delta g_E = 2\,\omega\, v \sin\alpha \cos\varphi + \frac{v^2}{R_e} = 2\,\omega\, v_{east} \cos\varphi + \frac{v^2}{R_e} \quad (3)$$

where:

Δg_E = Eötvös correction
ω = earth's angular velocity
v = ship velocity
α = ship course
φ = latitude
R_e = earth radius

The velocity v_{east} is obtained directly from the spline program.

The *free-air anomalies* Δg_{FA} were computed by subtracting the normal gravity from the computed gravity. The Geodetic Reference System 1967 is used for the reduction, in which the normal gravity γ is defined as:

$$\gamma = 978\,031.85 + 5185.88 \sin^2 \varphi - 5.74 \sin^2 2\varphi \text{ mgal} \quad (4)$$

and a free air gravity anomaly as:

$$\Delta g_{FA} = g - \gamma \qquad (5)$$

The *Bouguer anomalies* are computed by the simple Bouguer plate reduction. The Bouguer plate is an infinite flat plate with a thickness of the local depth and a density equal to the difference in density between the crust (2670 kg/m^3) and the seawater (1030 kg/m^3), so ρ = 1640 kg/m^3. The Bouguer anomalies are:

$$\Delta g_{Bou} = \Delta g_{FA} + 2\pi G\rho d = \Delta g_{FA} + 0.0687 \cdot d \text{ mgal} \qquad (6)$$

where d is the depth in meters.

As the bottom of the North Sea is very smooth and the depth varies between about 30 m and 60 m, it is not necessary to compute topographic corrections.

5. Computation of the cross-over points

An independent check on the precision of the measurements is obtained at the cross-over points and on some repeated lines. The NAVGRAV project contained 350 cross-over points. A problem was to develop an efficient method to find the cross-over points. This is solved as follows.

The whole area was devided into 1 x 1 km^2 blocks and each block was uniquely numbered. First, the whole area is divided into 9 blocks, numbered 1 to 9 (see figure 1). Each block is subdivided again into 9 blocks and so on. The smallest block is 1 x 1 km^2. The advantage of this method is that the same numbering can be used to compute mean block anomalies for blocks with different side lengths, increasing with a factor 3 each time, so 1 km, 3 km, 9 km, 27 km, 81 km and 243 km.

The block numbers consist of six digits, e.g. 254268 is a block of 1 x 1 km. The first 5 digits: 25426 is the 3 x 3 km block and 2542 is the 9 x 9 km block in which the point is situated.

Every gravity observation is labelled with a specific block number.

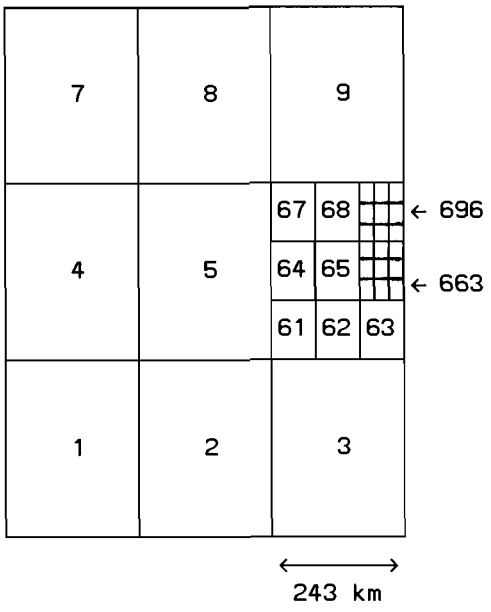

Figure 1. Block numbering

With a very fast sorting routine all measurements (together with their line numbers) are sorted in sequence of the blocknumber. The blocks containing measurements from different lines were considered as cross-over points. The observation interval along a line is about 300 m, so usually 3 points of a line are situated inside one block of 1 x 1 $km.^2$

The mean value of these three points was compared with the mean value of the three points of the other line. The difference is the cross-over point difference and gives an impression of the precision of the measurements.

The NAVGRAV project contained 350 cross-over points. The root mean square of the differences was **1.08 mgal** which is very satisfying. A histogram of these differences is given in figure 2.

59% of the observed differences is less than 1 milligal which is better than expected on beforehand. As the standard deviation of a difference is $\sqrt{2}$ times the standard deviation of the gravity measurements the *standard deviation of a single gravity cross-over point is* $1.08/\sqrt{2}$ = **0.76 mgal**.

As these cross-over point differences are caused by random noise it is not necessary to correct the gravity values between the cross-over points. The same method is used to compute the

cross-over points for the measurements from a similar project in 1979. The cross-over differences of 1979 are presented in the histogram of figure 3. It contains 188 cross-over points with a standard deviation of 1.57 mgal.

Next the NAVGRAV measurements are compared with the gravity measurements observed in 1979 in the same area. One objective of the whole project was to study the repeatability and the external accuracy of the gravity measurements. Therefore some lines, which were measured in 1979, have been repeated in 1986 resulting in 1453 check points both along track and cross-over points.

Figure 4 shows the histogram of all cross-over points of 1979 and 1986. 54% of the measurements show differences of less than 1 mgal and the standard deviation is 1.47 mgal. This value can still be reduced if systematic errors in some lines are removed. The remaining standard deviation becomes 1.20 mgal. As this value is the result of the difference in two observations, each observation has a r.m.s. of $\frac{1}{\sqrt{2}} \cdot 1.20 = 0.85$ mgal.

6. Comparison of the two gravimeters Kss-5 and Kss-30

In order to check the precision of the gravimeters, apart from external influences as errors in the position, speed and course of the ship, both gravimeters were set up next to each other. One Bodensee Kss-5 gravimeter, belonging to the Delft University of Technology and one Bodensee Kss-30 of the University of Hamburg. The comparison is made on 8908 measured gravity points. Figure 5 shows a histogram of the differences.

Curiously there is a systematic difference of 1 mgal between both instruments, probably caused by a difference in the connection to the harbour point. The standard deviation of all differences is **1.12 mgal**.

Apart from this some lines show a systematic difference, caused by inaccuracy of the cross-coupling effect as a result of bad weather conditions. If these systematic errors are corrected for, the remaining standard deviation of the differences is only **0.61 mgal**. This means that both gravimeters correspond incredibly well. Figure 6 shows the differences after correcting for systematic errors.

7. The gravity anomalies

The free air gravity anomalies are computed with the international gravity formula 1967. Iso-anomaly maps have been drawn of the 1979 measurements (figure 7) and the 1986 measurements (figure 8). As these maps are based on completely independent data they give a good impression of the reliability of the results.

Comparison of the two maps shows that all main features of the gravity field are the same in both maps. Only minor differences are present. Remarkable is the rather irregular shape of the gravity field, although the bottom of the North Sea is very flat. The irregularities are caused by structures inside the earth crust beneath the sediment layer. The North Sea Graben running from North-West to South-East can clearly be identified.

The gravity map of the North Sea shows a very detailed picture. It provides valuable information for geophysical interpretation, for oil and gas exploration and for scientific research.

The most remarkable gravity anomaly is situated at latitude $55^{0}13'$, longitude $5^{0}38'$ (figure 9). This anomaly is very sharp. Gravity changes 50 milligal within 20 km distance. The total mass disturbance corresponding to this anomaly is equivalent with a cube with side length of 10 km and an anomalous density of 500 kg/m^{3}. On geological maps a mass intrusion is indicated on this place. Mantle material has ascended into the crust up to a depth of 10 to 15 km. However the size of the intrusion is, according to the measurements, probably bigger than indicated in the map.

Besides the contour representation gravity profiles have been plotted showing the free air and Bouguer anomalies. The profiles reflect the detailed structure of the gravity field and are suited for small scale studies (cf. appendix A).

7.1. Mean block anomalies

In the dataset all point anomalies are stored together with the coordinates and block numbers, which are described in section 5. If the dataset is sorted , for instance on the first of 4 digits of the blocknumbers, we get all the measurements inside

each 9 x 9 km^2 block. The mean value of the measurement inside each block is the mean block anomaly. In the same way it is easy to obtain mean block anomalies of block sizes, which are a multiple of 3 times the unit blocksize. For other blocksizes the block numbers should be recomputed which is an easy job with the existing computer programs.

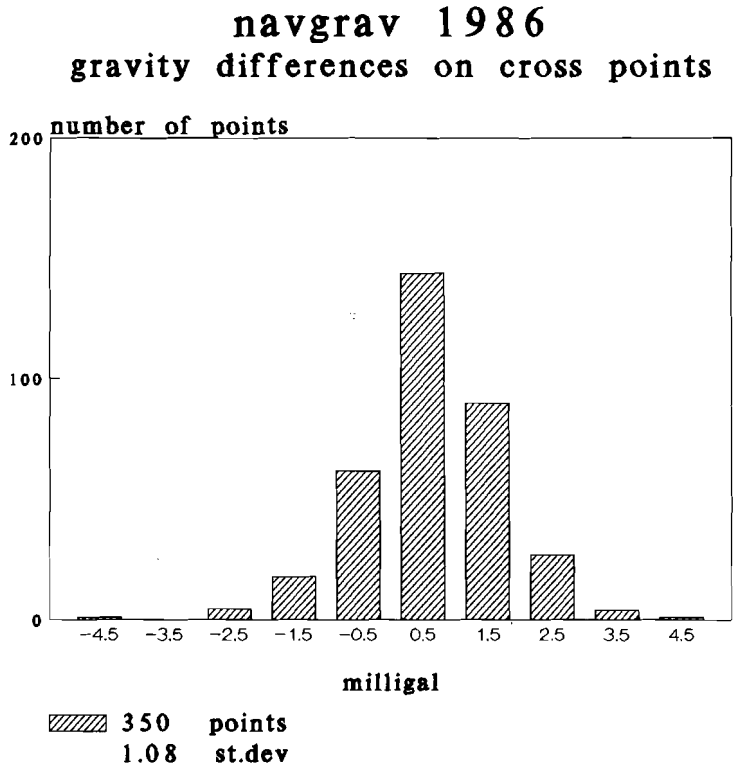

Figure 2

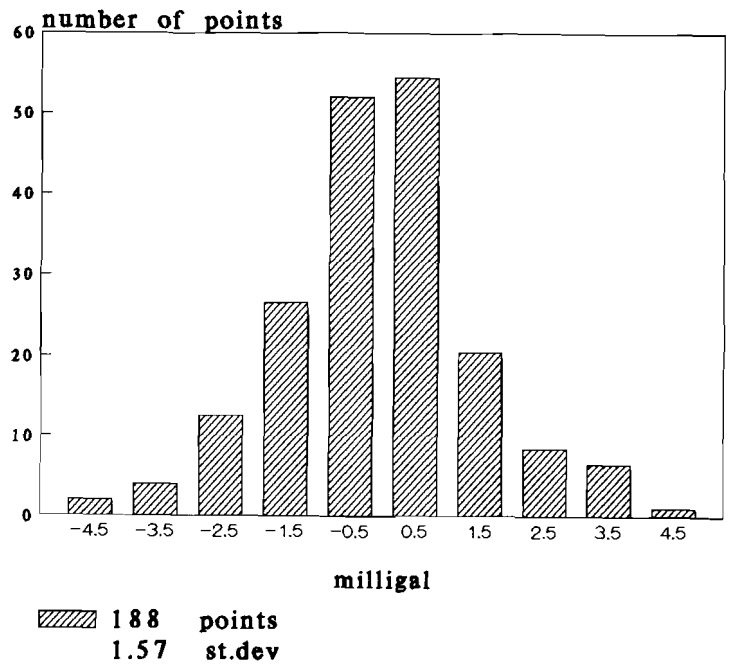

Figure 3

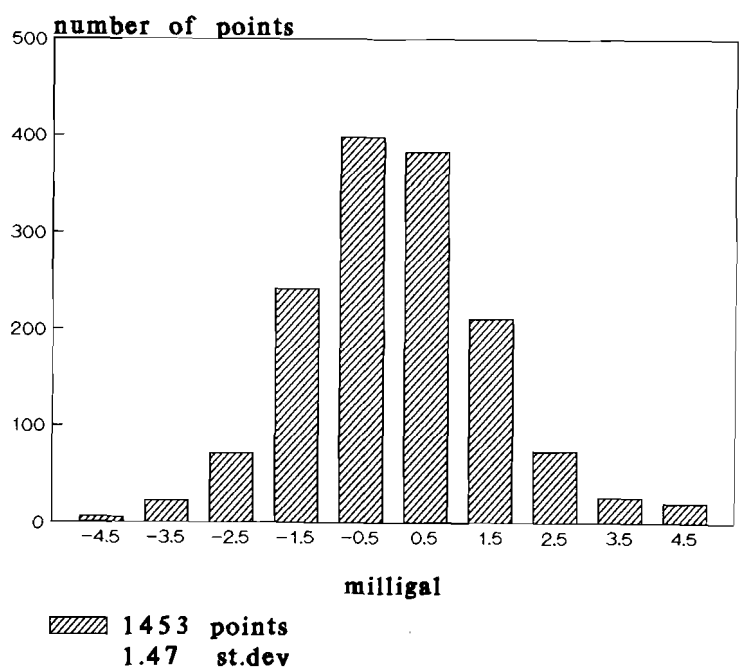

Figure 4

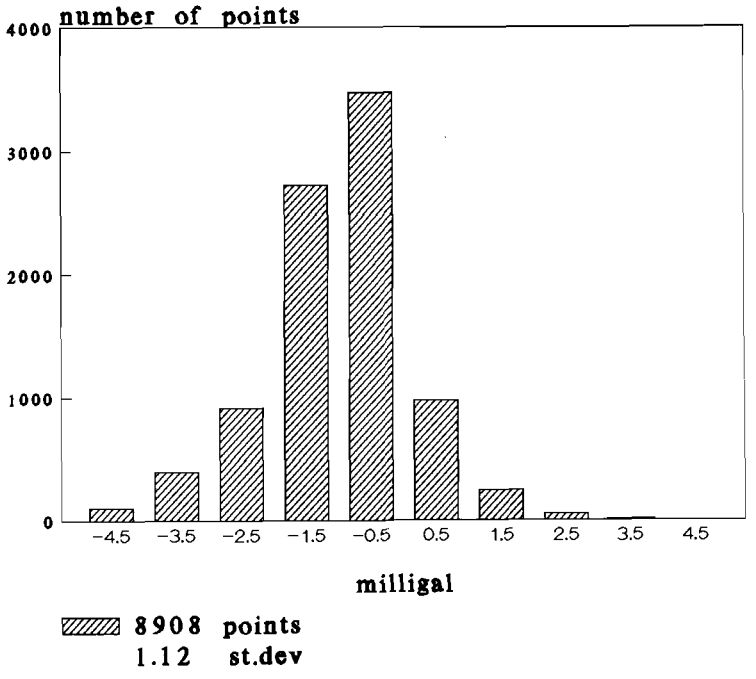

Figure 5

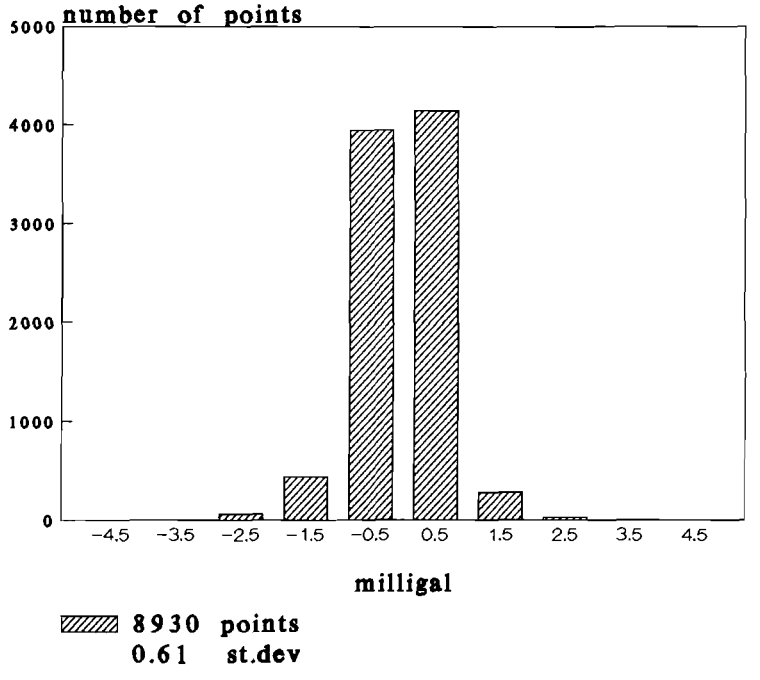

Figure 6

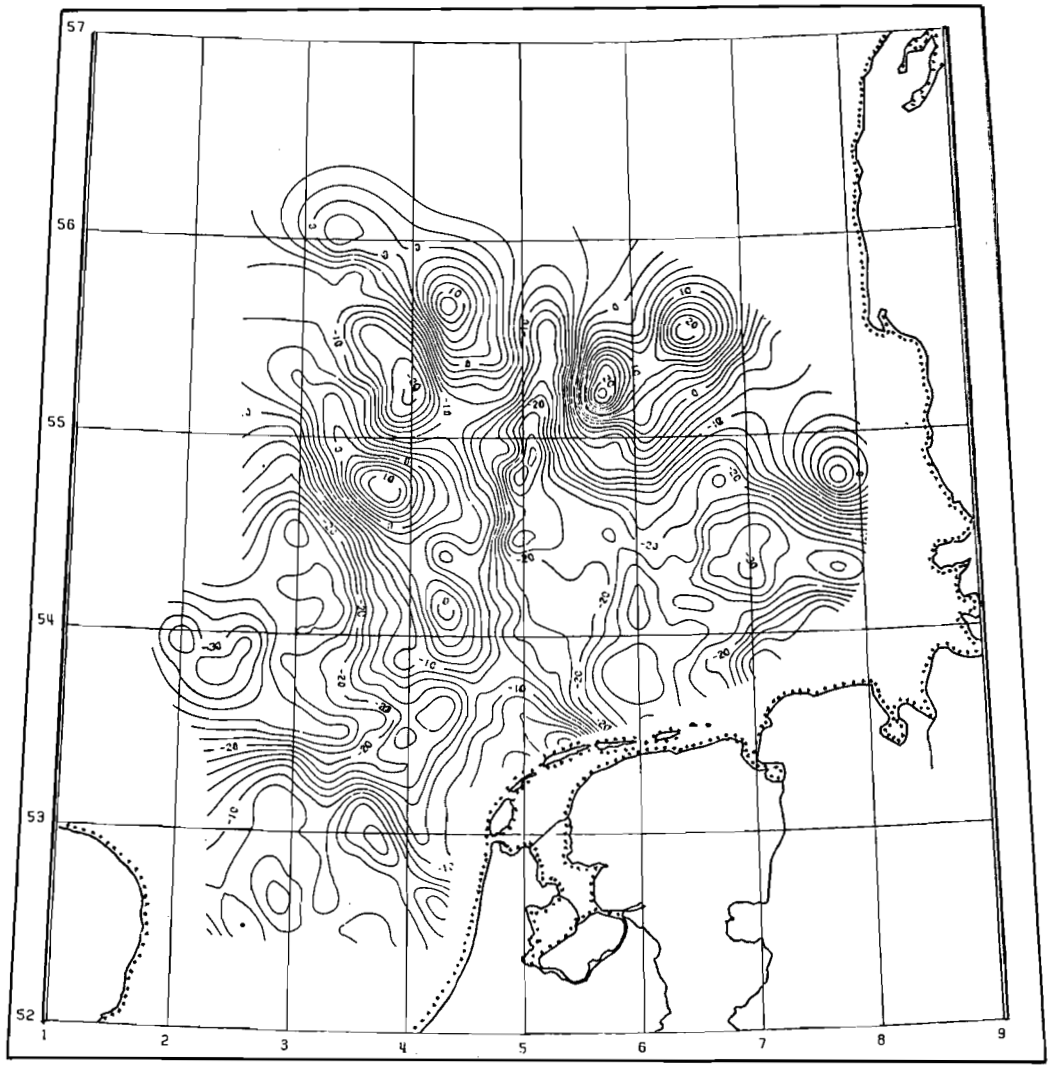

Figure 7. Free air gravity anomalies in mgal, measured in 1979

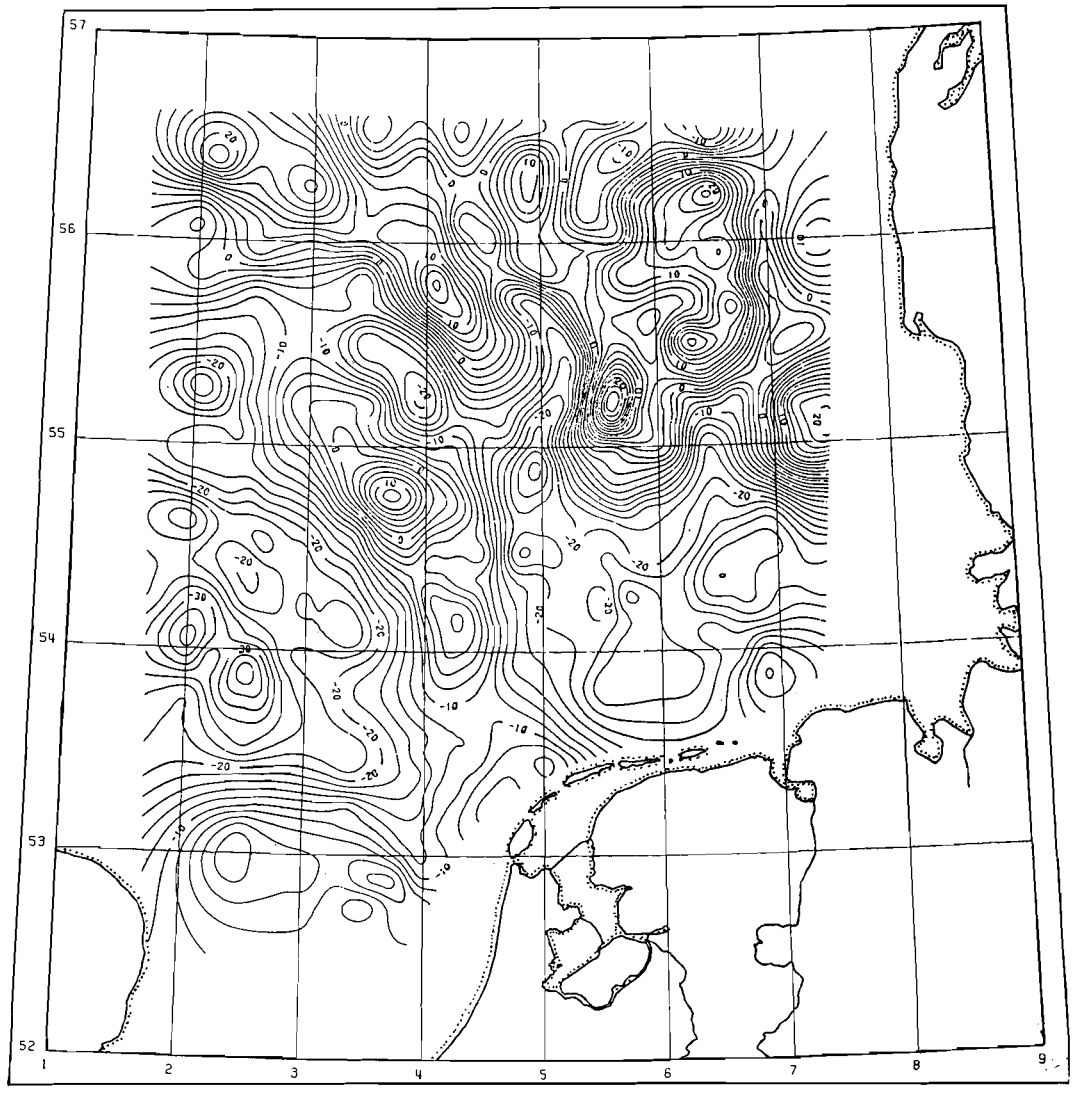

Figure 8. Free air gravity anomalies in mgal, measured in 1986

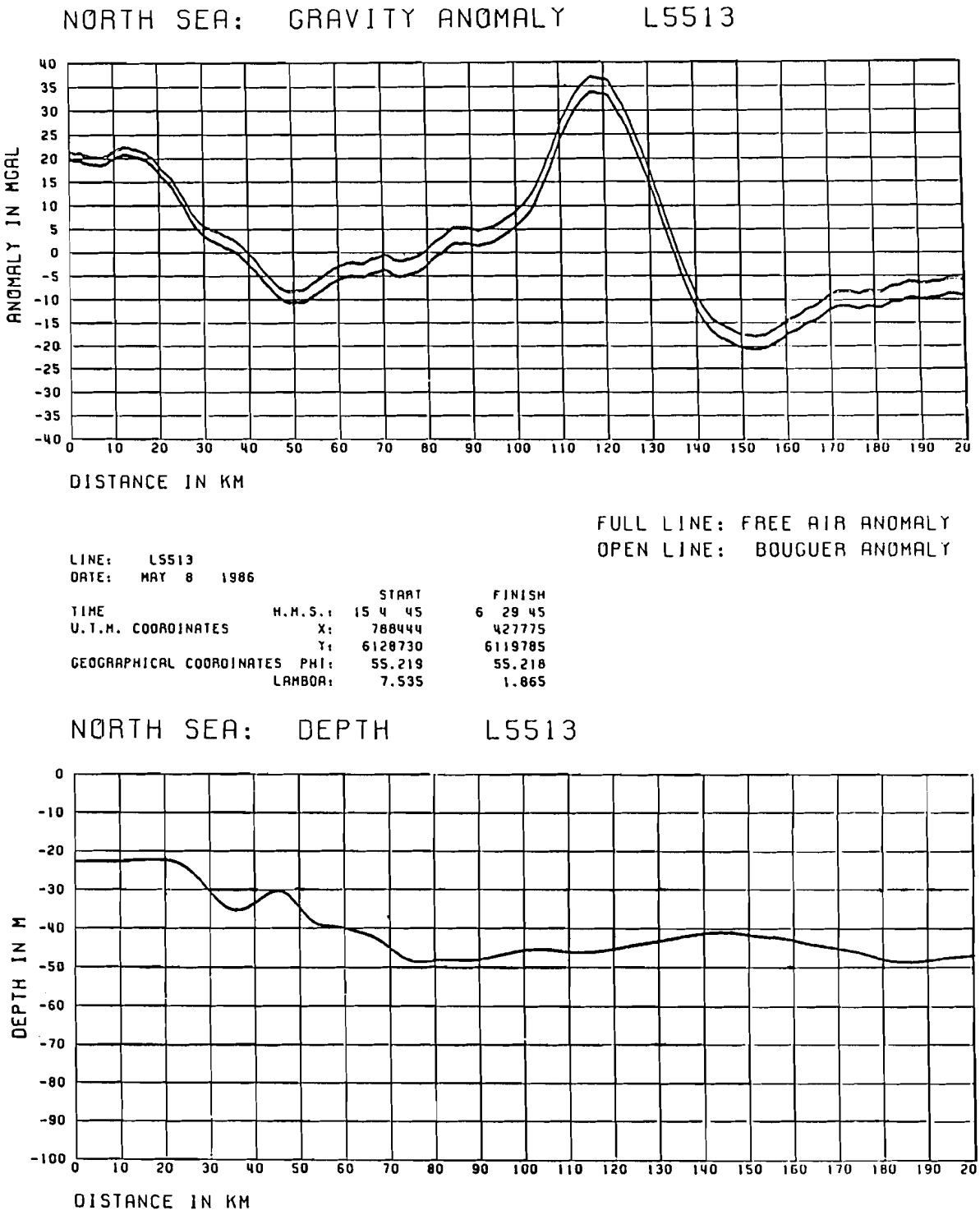

Figure 9. The largest gravity anomaly

8. Literature

Collette, B.J. (1960): The gravity field of the North Sea. Gravity expeditions 1948-1958, vol. V, part II, Netherlands Geodetic Commission.

Fleischer, U. (1974): Seegravimetrie. Journal of Geophysics, vol. 40, no. 1.

Strang van Hees, G.L. (1983): Gravity survey of the North Sea. Marine Geodesy, vol. 6, no. 2.

Vening Meinesz, F.A. (1932, 1934, 1941, 1948): Gravity expeditions at sea. Vol. I, II, III, IV, Netherlands Geodetic Commission.

USING GPS SHIP VELOCITY ESTIMATES FOR EÖTVÖS CORRECTION

J.H.M. Smit
Delft University of Technology
Faculty of Geodesy

1. Introduction

In sea gravimetry the nowadays realizable accuracy is limited by Eötvös correction errors. The Eötvös effect is caused by the motion of the ship relative to the rotating earth. This motion results in a coriolis acceleration which must be corrected for. To determine the Eötvös correction to better than 0.5 mgal ship velocity estimation with an accuracy of 0.1 knot (approximately 5 cm/s) is necessary. High precision HF or MF terrestrial navigation systems offer such accuracy, but only near shore. For ocean gravity surveys the Global Positioning System is almost the only possibility to obtain high precision ship velocity estimates.

The NAVGRAV navigation data was used to compare Eötvös corrections computed from Syledis and Hyperfix velocity estimates with those from GPS velocity estimates (Smit, 1988).

2. Eötvös correction

The Eötvös correction can be written:

$$\Delta g_E = 2\omega v_E \cos\varphi + \frac{v^2}{r} \qquad (1)$$

in which ω is the earth's rotation angular velocity, v_E the ship velocity east component, φ the latitude, v the ship velocity and r the earth radius. When the ship velocity is given in knots, the Eötvös correction in mgal is:

$$\Delta g_E = 7.503 \cdot v_E \cos\varphi + 0.00415 \cdot v^2 \qquad (2)$$

Formula (2) gives the correction to be added to the gravity measurements. For the ship heading east the gravity reading becomes too small and the Eötvös correction is positive. When the east velocity component is exactly zero, i.e. when the ship is heading north or south, the Eötvös correction is practically zero.

The Eötvös correction standard deviation is, when neglecting the second term on the right hand side of formula (2):

$$\sigma_E = 7.503 \cdot \cos\varphi \cdot \sigma_{V_E} \qquad (3)$$

in which σ_{V_E} is the standard deviation of the ship east velocity. Taking $\varphi = 52^\circ$ and the required Eötvös correction standard deviation $\sigma_E = 0.5$ mgal yields for the required east velocity standard deviation:

$$\sigma_{V_E} = 0.1 \text{ knot} \cong 0.05 \text{ ms}^{-1} \qquad (4)$$

Because of the velocity accuracy required the Eötvös correction is a restrictive factor in sea gravimetry.

The Global Positioning System, when fully deployed, will offer high velocity accuracy worldwide, 24 hours per day. Therefore, GPS is a promising development for sea gravimetry.

3. Ship velocity estimation with GPS

Ship velocity can be estimated with the Global Positioning System using pseudorange code measurements, carrier phase measurements or a combination of these measurement types. The pseudorange method and the combination method yield ship positions at every (receiver dependent) epoch. The positions can be converted to ship velocities by numerical differentiation. The carrier phase method yields ship velocities at every epoch.

3.1. GPS pseudoranging

Pseudorange positioning is realized by the measurement of four pseudoranges between the receiver and four satellites. These ranges are determined by cross-correlating the coded signal, transmitted by (and unique for) each satellite, with an identical signal generated in the receiver. The four unknowns are the receiver coordinates x, y, z (or φ, λ, h) and the time bias between the receiver clock and the GPS time frame.

The linearized model for pseudorange single point positioning can be written:

$$dr = ATdx \qquad (5)$$

where dr is the vector of observed minus computed pseudoranges, A the design matrix containing the partial derivatives of the pseudoranges with respect to receiver cartesian coordinates and clock bias, T the transformation matrix from geographical to cartesian coordinates, and dx the vector of corrections to the geographical coordinates and clock bias.

Solution of equation (5) by a collocation model is:

$$dx = (P_x + T^T A^T P_r A T)^{-1} T^T A^T P_r dr \qquad (6)$$

which allows one or more unknowns to be held fixed by giving it a large weight factor in the a priori weight matrix of unknowns P_x. This way any number of unknowns can be computed less than or equal to the number of satellites available.

The satellite cartesian coordinates are computed from a set of orbit parameters, an extension of the six Keplerian orbit parameters. They are found in the second and third subframe of the satellite navigation message (Van Dierendonck et al, 1978).

The algorithm described above yields position estimates φ, λ, h in a certain reference system at every (receiver dependent) epoch. The two systems used for GPS are the World Geodetic System 1972 and 1984. The positions, in WGS72 or WGS84, given e.g. every 3 seconds for a TI-4100 receiver, must now be converted to velocities, e.g. every 60 seconds, which is the observation period of the gravity meter. This can be done e.g. with a least squares second order polynomial fit of the latitude and longitude estimates. The second term of the polynomial represents the north velocity and the east velocity according to:

$$\bar{v}_N = r \cdot \frac{d\varphi}{dt} \qquad (7)$$

$$\bar{v}_E = r\cos\bar{\varphi} \cdot \frac{d\lambda}{dt} \qquad (8)$$

The mean Eötvös correction over 60 seconds is computed from:

$$\overline{\Delta g}_E = 7.503 \cdot \bar{v}_E \cos\bar{\varphi} + \frac{\bar{v}^2}{r} \qquad (9)$$

3.2. GPS Doppler smoothed pseudoranging

A combination of pseudorange code measurements and carrier phase measurements is used in the case of Doppler smoothed pseudoranging, as described by (Hatch, 1982), (Hatch, 1986), and (Lachapelle et al, 1987). Suppose that pseudorange measurements are available on both GPS carrier waves L1 and L2. The L1 carrier with a frequency of 1575.42 MHz is modulated with the C/A code, the P code and the satellite navigation message. The L2 carrier with a frequency of 1227.60 MHz is modulated with the P code and the satellite navigation message. The P code pseudorange measurements P_{L1} and P_{L2} on the L1 and L2 carriers, respectively, are combined into a frequency weighted average measurement:

$$P = (f_1 \cdot P_{L1} + f_2 \cdot P_{L2})/(f_1 + f_2) \tag{10}$$

With a TI-4100 receiver one finds the pseudorange code measurement centered in the interval of carrier phase measurement. The carrier start phase measurement preceeds the code measurement which itself is followed by the carrier end phase measurement. The interval of carrier phases is a constant 160 milliseconds. Averaging of carrier start phase and carrier end phase yields the carrier phases C_{L1} and C_{L2} on the L1 and L2 carrier respectively, which are combined by differencing:

$$C = C_{L1} - C_{L2} \tag{11}$$

The differencing results in a longer wavelength whose initial ambiguity is easier to resolve.

A smoothed pseudorange $\bar{P}$ can be formed by averaging the measured pseudorange P with its predicted value $\hat{P}$ in a recursive filter:

$$\hat{P}_n = \bar{P}_{n-1} + (C_n - C_{n-1}) \cdot \frac{c}{f_1 - f_2} \tag{12}$$

$$\sigma^2_{\bar{P}} = \frac{\sigma^2_{\hat{P}} \cdot \sigma^2_P}{\sigma^2_{\hat{P}} + \sigma^2_P} \tag{13}$$

$$\bar{P}_n = \sigma^2_{\bar{P}} \cdot \left(\frac{\hat{P}_n}{\sigma^2_{\hat{P}}} + \frac{P_n}{\sigma^2_P} \right) \qquad (14)$$

The second term on the right hand side of formula (12) is the integrated Doppler count over the time interval between epoch n-1 and n, converted to meters by multiplying with the velocity of light c divided by the difference of the two carrier frequencies f_1 and f_2 . The variance of the predicted pseudorange is given by:

$$\sigma^2_{\hat{P}} = \sigma^2_{\bar{P}} + 2 \cdot \sigma^2_C \cdot \frac{c^2}{(f_1 - f_2)^2} \qquad (15)$$

in which σ^2_C is the variance of the differenced carrier phase measurement C.

If a cycle slip is detected by evaluating the absolute value of the difference between the measured pseudorange P and its prediction $\hat{P}$, the filter is reset by taking $\sigma^2_{\bar{P}} = \sigma^2_P$.

The smoothed pseudoranges are used in the linearized model of formula (5) in the same way as described in chapter 3.1. , again yielding position estimates φ, λ, h in WGS72 or WGS84 at every (receiver dependent) epoch. The positions are converted to velocities every 60 seconds by a least squares second order polynomial fit of latitude and longitude estimates, compare formulae (7) and (8). The mean Eötvös corrections per 60 seconds can be computed with (9).

3.3. GPS carrier velocities

The linear model for carrier frequency velocity estimation can be written, see (Kleusberg et al, 1985):

$$-\lambda_c \Delta f + a_0 = A T \dot{x} \qquad (16)$$

in which λ_c is the carrier wavelength, Δf is the vector of observed carrier frequency shifts, a_0 a function of satellite cartesian coordinates, satellite velocity and clock drift, A the design matrix containing the partial derivatives of the pseudoranges with respect to receiver cartesian coordinates and clock bias, T the transformation matrix from geographical to

cartesian coordinates and $\dot{x}$ the vector of unknown time derivatives of geographical coordinates and unknown receiver clock drift or frequency offset:

$$\dot{x} = \begin{bmatrix} \dot{\varphi}(M+h) \\ (\dot{\lambda}+\omega)(N+h)\cos\varphi \\ \dot{h} \\ c\delta f \end{bmatrix} = \begin{bmatrix} v_N \\ v_E + (N+h)\omega\cos\varphi \\ v_H \\ c\delta f \end{bmatrix} \qquad (17)$$

Here v_N , v_E , v_H are the velocity components in north, east and upward direction respectively. The east velocity component v_E must be corrected for the earth rotation effect $(N+h)\omega\cos\varphi$.

Solution of equation (16) by a collocation model is:

$$\dot{x} = (P_{\dot{x}} + T^T A^T P_{\lambda_c \Delta f} AT)^{-1} T^T A^T P_{\lambda_c \Delta f} (a_0 - \lambda_c \Delta f) \qquad (18)$$

which allows one or more unknowns to be held fixed by giving it a large weight factor in the a priori weight matrix of unknowns $P_{\dot{x}}$. This way any number of unknowns can be computed less than or equal to the number of satellites available. When estimating ship velocities one can usually constrain the height component to zero by selecting a proper weight.

With a TI-4100 receiver one finds a carrier velocity measurement centered in the interval of carrier phase measurements. The carrier start phase measurement preceeds the carrier velocity measurement (or carrier phase time derivative) which itself is followed by the carrier end phase measurement. The interval of carrier phases is a constant 160 milliseconds (compare chapter 3.2.). Differencing of carrier start phase and carrier end phase and dividing by the time interval of 160 milliseconds yields carrier velocities on L1 and L2 which are both equal to the direct carrier velocity readout:

$$\dot{\phi} = \frac{\left[\phi_{end} - \phi_{start}\right]_{L1}}{0.160} = \frac{\left[\phi_{end} - \phi_{start}\right]_{L2}}{0.160} \qquad (19)$$

As the noise level is much higher in the direct carrier velocity readout (Wells et al, 1985), the L1 carrier start phase and end

phase measurements are used to compute the carrier frequency shift:

$$\lambda_c \Delta f = \frac{\left[\phi_{end} - \phi_{start}\right]_{L1}}{0.160} \cdot \frac{c}{f_1} \qquad (20)$$

The satellite velocity vector can be found by time differentiation of the formulae for computing the satellite cartesian coordinates.

The algorithm described above yields velocity estimates v_N and v_E in WGS72 or WGS84 at every (receiver dependent) epoch. The mean values of v_N and v_E over 60 seconds are computed and from them the mean Eötvös corrections with formula (9).

4. Comparison of Eötvös corrections

By comparing the available terrestrial and GPS navigation data for the available gravity lines of the NAVGRAV project the following lines could be selected to analyse the Eötvös corrections:

line id	start time	end time	date 1986	radio navigation	GPS receiver	ship course
L5430a	2:05	4:33	April 24	Hyperfix	TI-4100	270°
L0330a	4:39	6:12	April 24	Syledis	TI-4100	180°
L0430d	15:53	18:39	April 25	Syledis	TI-4100	0°
L5415a	2:24	5:12	April 26	Hyperfix	TI-4100	90°
L0600a	15:36	17:18	April 26	Syledis	TI-4100	0°

Table 1. Gravity lines selected for analysis

The main selection criterion was the required GPS satellite coverage of at least two satellites, which was the case during two periods per day, the first being from 1:35 h to 8:50 h, the second from 13:45 h to 20:25 h (periods are given for April 24 in GMT, the pattern shifts approximately 4 minutes per day). The selected lines can be found in figure 1 and are all from the first (navigation) part of the NAVGRAV project, because the Syledis and

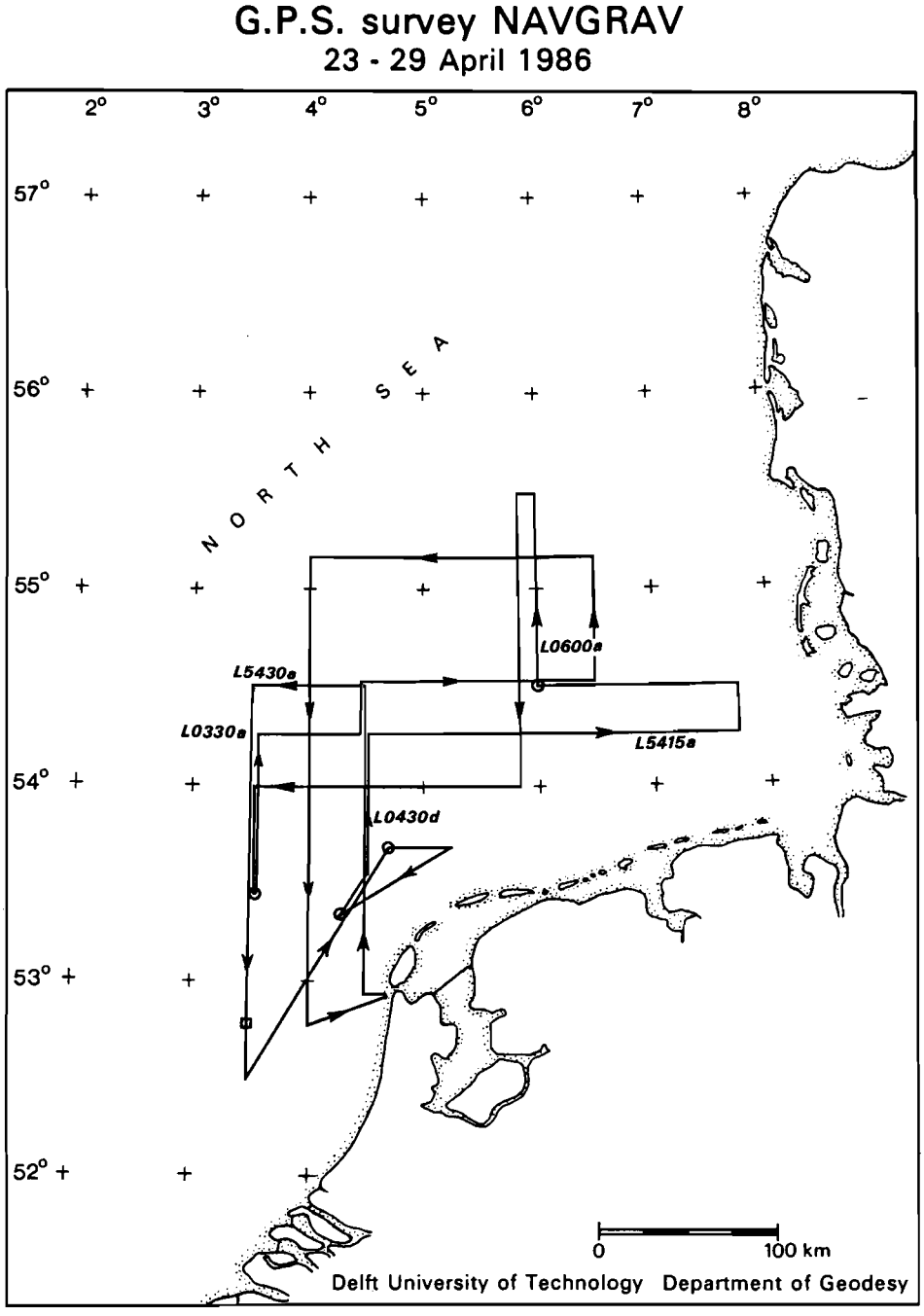

Figure 1. The first period of NAVGRAV with five gravity lines selected for analysis

Hyperfix navigation systems, used as a reference, were part of the navigation experiment only.

The available velocity estimates are:

- numerical differentiation of Syledis position
- numerical differentiation of Hyperfix position
- numerical differentiation of GPS pseudoranging position (chapter 3.1.)
- numerical differentiation of GPS Doppler smoothed pseudo-ranging position (chapter 3.2.)
- averaging of GPS carrier frequency velocity (chapter 3.3.)

The numerical differentiation of Syledis and Hyperfix position is analogous to the numerical differentiation of GPS position and will therefore not be dealt with here. The Syledis and Hyperfix velocity estimates, used as reference, are given every 60 seconds and are corrected for outliers and filtered. The GPS velocity estimates were computed every 60 seconds as described in chapter 3. Outlier detection of GPS pseudoranging and Doppler smoothed pseudoranging velocity estimates was done by means of the estimated standard deviation of the Eötvös correction, which should be less than 1 mgal. The outlier detection of GPS carrier frequency velocity estimates is achieved by means of the absolute value of the difference of each velocity estimate per 3 seconds with the averaged velocity per 60 seconds. The difference should be within a 99.9 percent confidence region of 3.29 times the standard deviation of the single velocity estimate. All GPS derived velocity estimates were left unfiltered in order to establish the achievable resolution and accuracy.

Figures 2, 3, 4, 5 and 6 show Eötvös corrections for gravity lines L5430a, L0330a, L0430d, L5415a and L0600a, respectively, computed from GPS and Syledis or Hyperfix navigation data. All Eötvös corrections are given in mgal.

The comparison of the three GPS derived Eötvös corrections with the Syledis or Hyperfix derived Eötvös corrections shows sometimes poor performance of GPS. The intervals meant here are of line L5430a, figure 2 between 12000 and 14000, line L0430d, figure 4 between 64000 and 67000, and line L5415a, figure 5 between 12000 and 14000. The reason can be found in the satellite configuration.

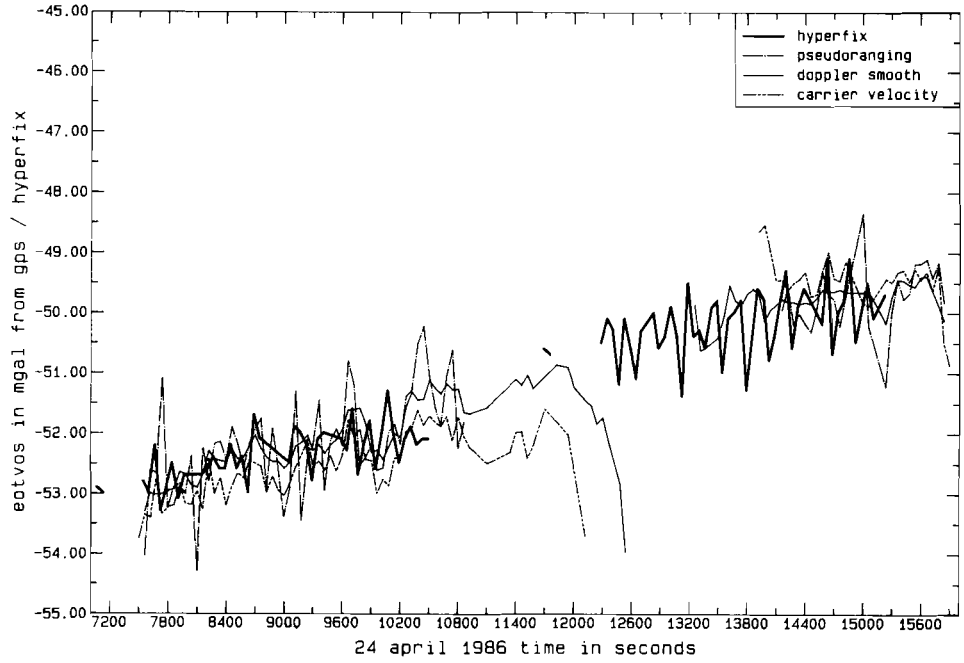

Figure 2. Eötvös corrections for line L5430a from GPS pseudoranging, Doppler smoothed pseudoranging, carrier velocity, and Hyperfix

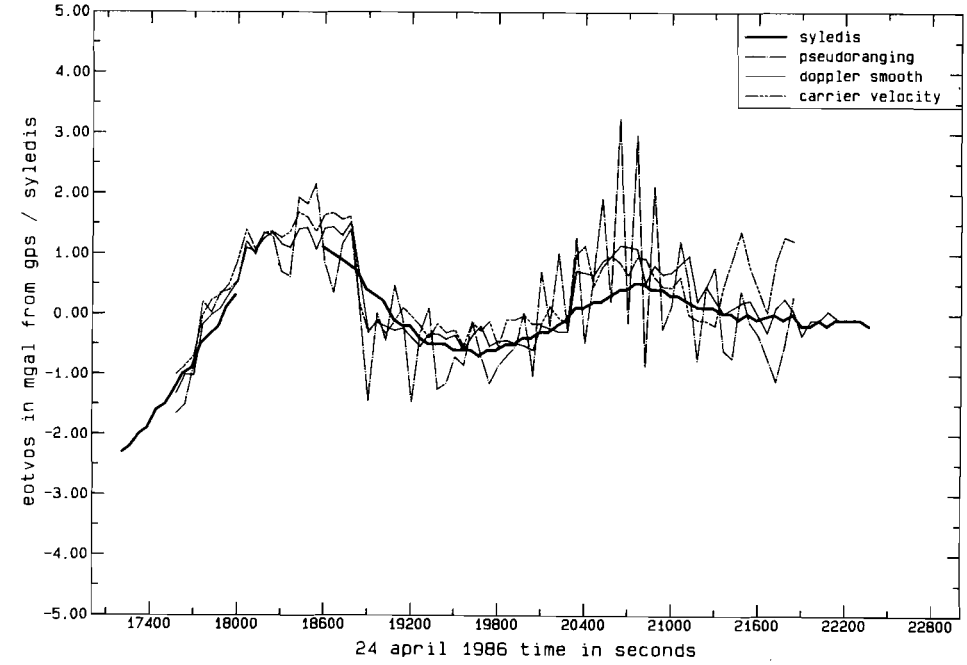

Figure 3. Eötvös corrections for line L0330a from GPS pseudoranging, Doppler smoothed pseudoranging, carrier velocity, and Syledis

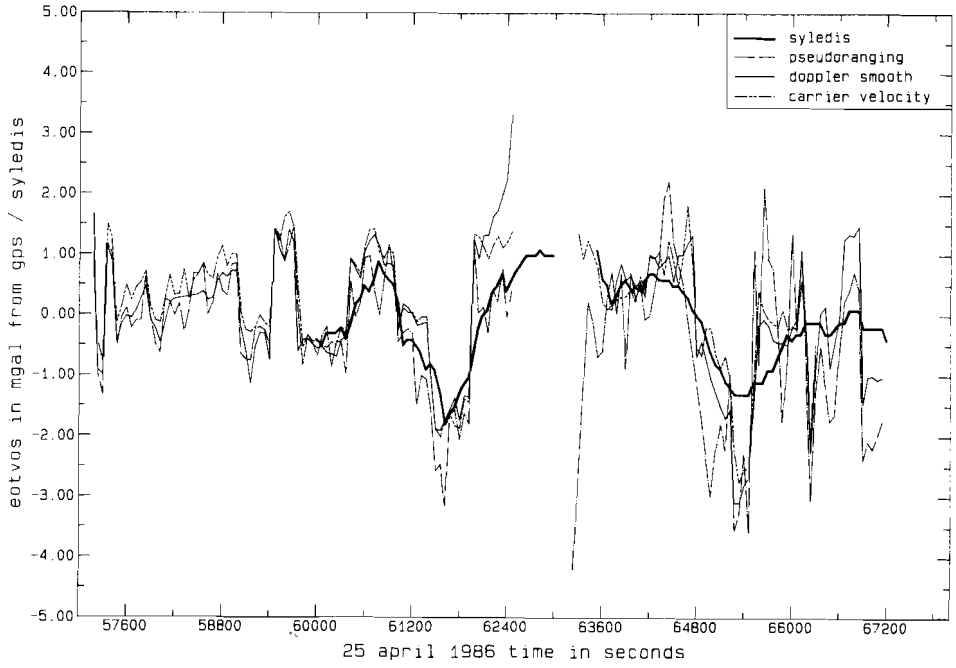

Figure 4. Eötvös corrections for line L0430d from GPS pseudoranging, Doppler smoothed pseudoranging, carrier velocity, and Syledis

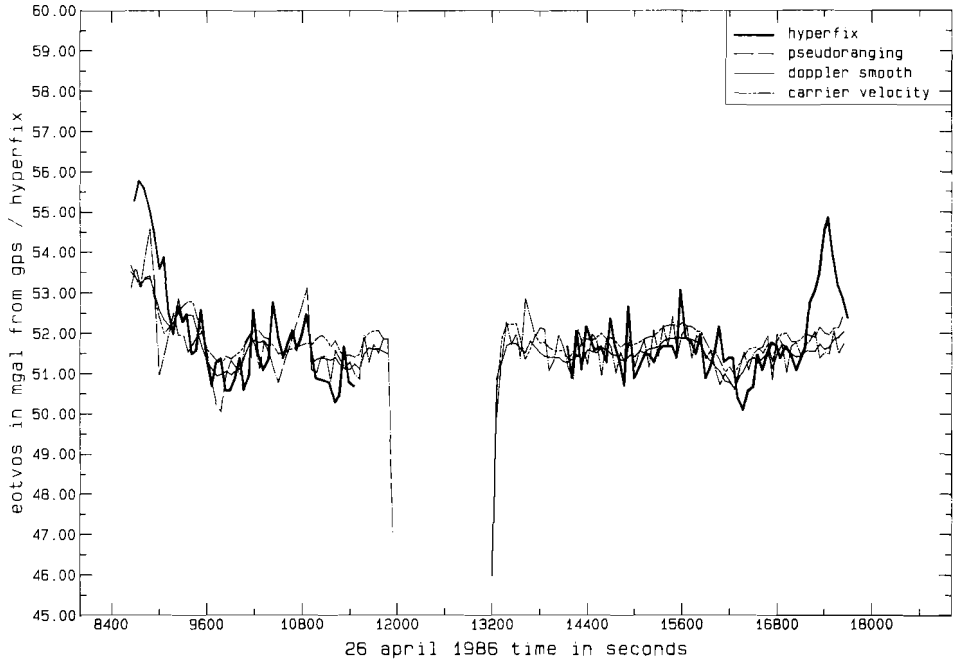

Figure 5. Eötvös corrections for line L5415a from GPS pseudoranging, Doppler smoothed pseudoranging, carrier velocity, and Hyperfix

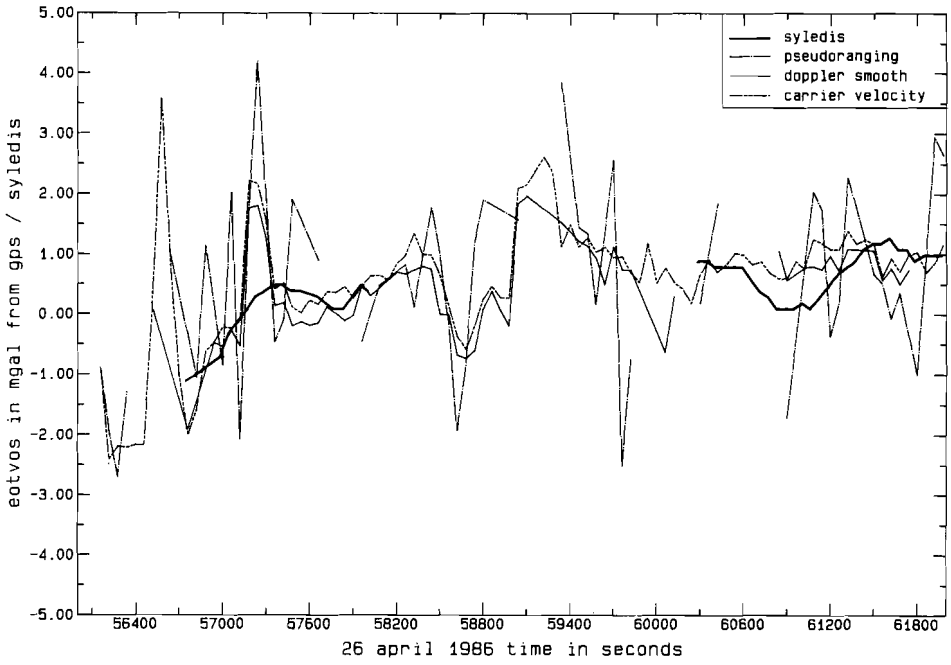

Figure 6. Eötvös corrections for line L0600a from GPS pseudoranging, Doppler smoothed pseudoranging, carrier velocity, and Syledis

line	radio nav	GPS pseudorange	GPS Doppler psr	GPS carrier vel
L5430a	Hyperfix	n= 54	n= 70	n= 58
		m= 0.130 mgal	m=-0.002 mgal	m=-0.057 mgal
		σ= 0.737 mgal	σ= 0.712 mgal	σ= 0.543 mgal
L0330a	Syledis	n= 66	n= 57	n= 59
		m=-0.531 mgal	m= 0.159 mgal	m= 0.322 mgal
		σ= 2.267 mgal	σ= 0.292 mgal	σ= 0.439 mgal
L0430d	Syledis	n= 92	n= 90	n= 84
		m=-0.320 mgal	m= 0.120 mgal	m= 0.181 mgal
		σ= 1.086 mgal	σ= 0.807 mgal	σ= 0.681 mgal
L5415a	Hyperfix	n= 92	n= 91	n= 93
		m=-0.244 mgal	m=-0.239 mgal	m= 0.026 mgal
		σ= 0.891 mgal	σ= 0.827 mgal	σ= 0.873 mgal
L0600a	Syledis	n= 26	n= 30	n= 47
		m= 0.142 mgal	m= 0.033 mgal	m= 0.198 mgal
		σ= 1.515 mgal	σ= 0.621 mgal	σ= 0.556 mgal

Table 2. Comparison of GPS derived Eötvös corrections

During these intervals the dilution of precision appears to be considerably worse than 10 and therefore not representative. In the future, when more satellites are available, the choice of another set of satellites with a better dilution of precision will avoid the problem encountered here.

Comparison of the three GPS derived Eötvös corrections in figures 2 to 6 yields the impression that the Doppler smoothed pseudoranging velocity estimates are best. In order to further compare the three GPS derived Eötvös corrections to the Syledis or Hyperfix derived Eötvös corrections the mean differences and the standard deviations of the differences are computed for each gravity line. All data was used unless marked as outlier. The results can be found in table 2. In the table are given the number of Eötvös differences, n, the mean Eötvös difference m in mgal, and the standard deviation of the differences, σ, in mgal.

The mean differences are smallest for Eötvös corrections as derived from Doppler smoothed pseudoranging, a little larger for those based on carrier velocity and largest for those from pseudoranging, but all mean differences are small enough to justify the conclusion that no systematic effects are present. The standard deviations are best when using Doppler smoothed pseudoranging and carrier velocity as compared to pseudoranging.

Figures 7, 8 and 9 show distributions of absolute values of differences between Eötvös corrections as derived from Hyperfix and GPS pseudoranging, those from GPS Doppler smoothed pseudoranging and those from GPS carrier velocity for gravity line L5430a. Figures 10, 11 and 12 show distributions of absolute differences between Syledis and GPS derived Eötvös corrections for line L0330a. The histograms justify a conclusion of the maximum values of the Eötvös correction differences as given in table 3.

GPS Doppler smoothed pseudoranging	1.0 mgal
GPS carrier velocity	1.5 mgal
GPS pseudoranging	2.0 mgal

Table 3. Maximum differences of GPS and Syledis/Hyperfix derived Eötvös corrections

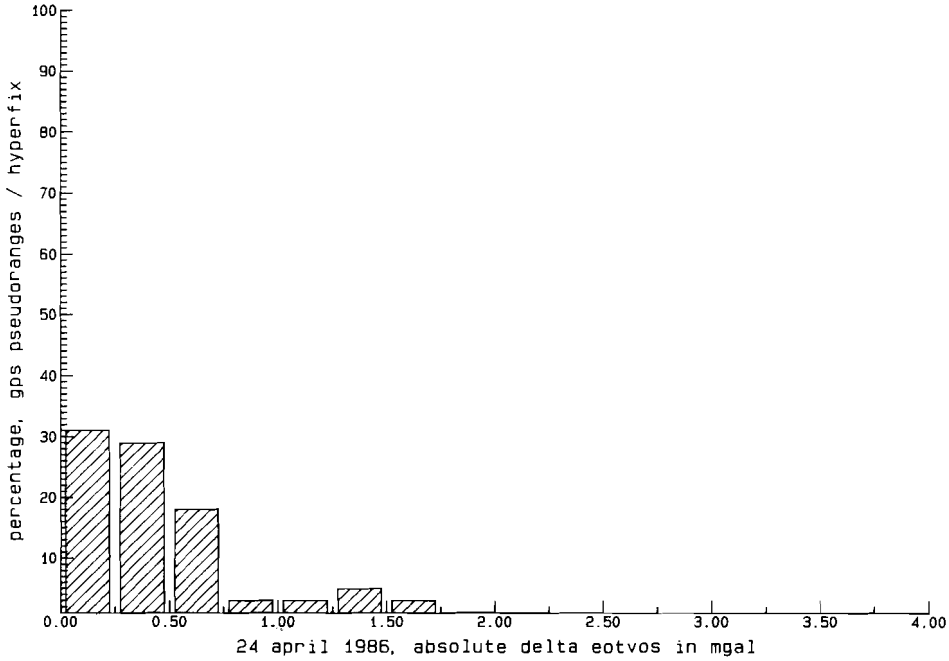

Figure 7. Distribution of absolute values of Eötvös correction differences for line L5430a from GPS pseudoranging and Hyperfix

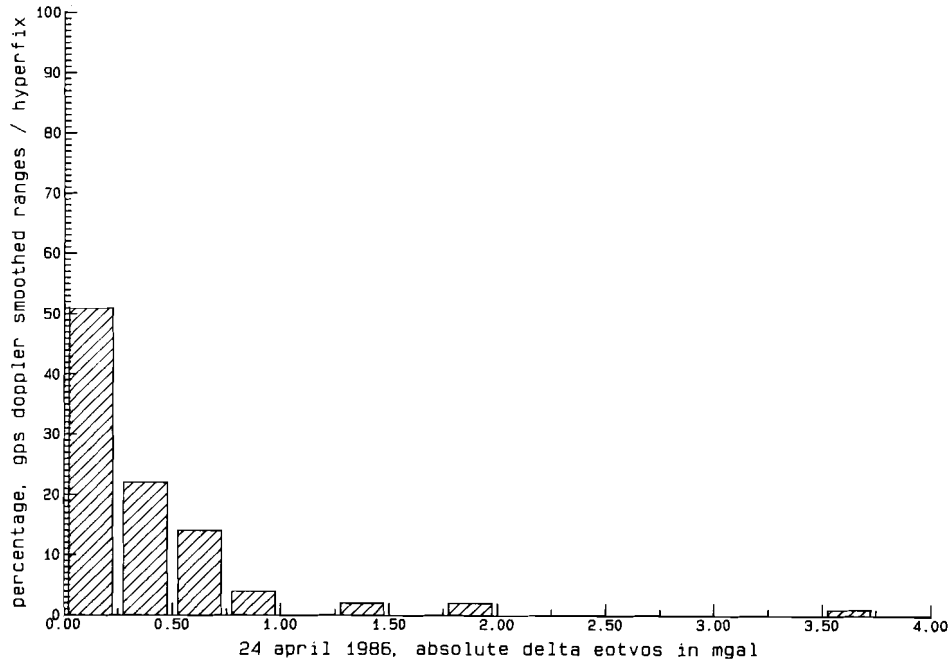

Figure 8. Distribution of absolute values of Eötvös correction differences for line L5430a from GPS Doppler smoothed pseudoranging and Hyperfix

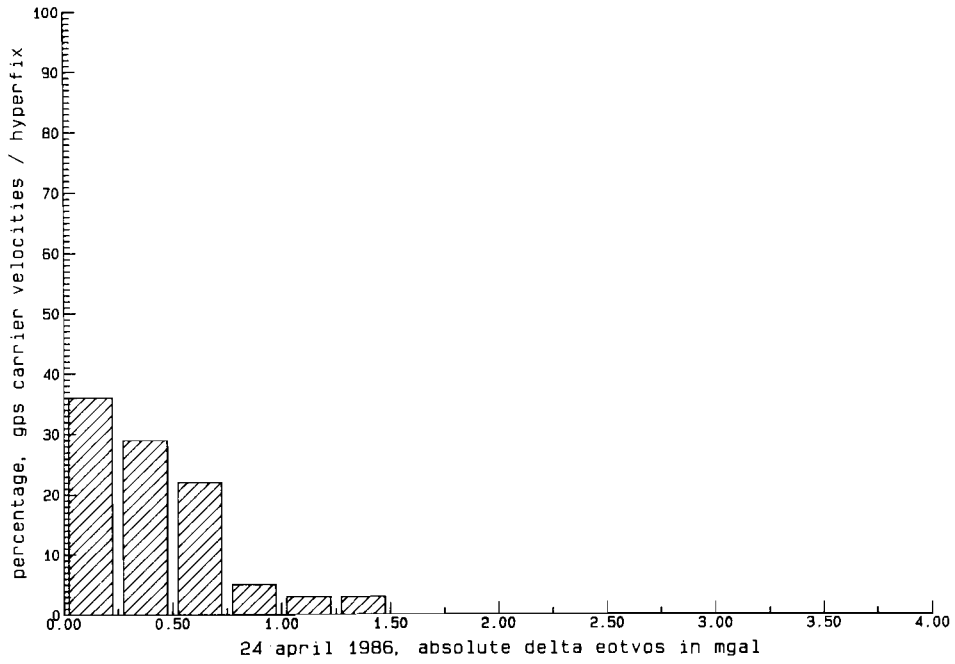

Figure 9. Distribution of absolute values of Eötvös correction differences for line L5430a from GPS carrier velocity and Hyperfix

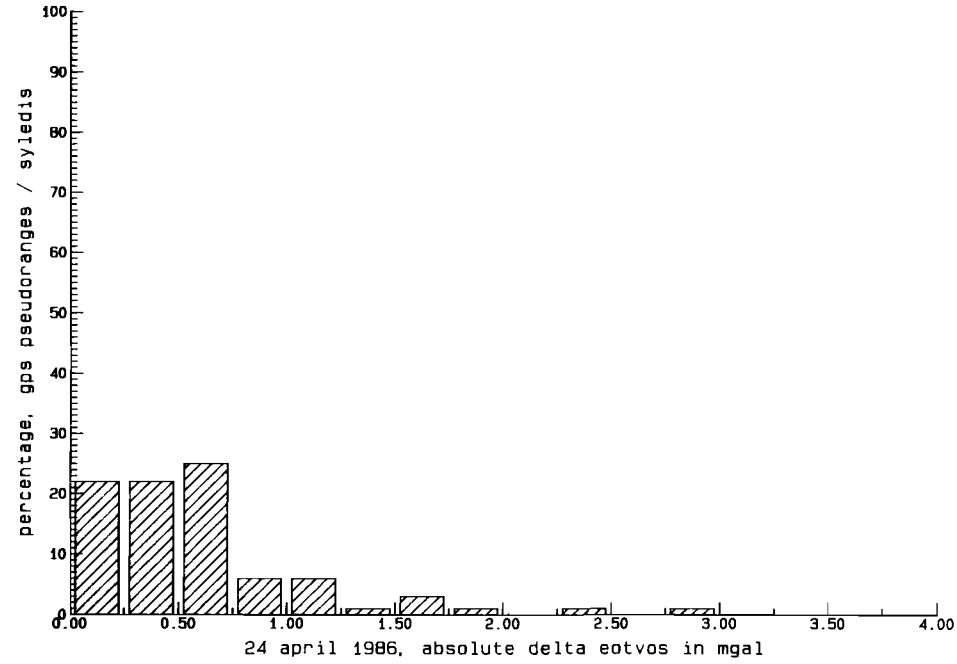

Figure 10. Distribution of absolute values of Eötvös correction differences for line L0330a from GPS pseudoranging and Syledis

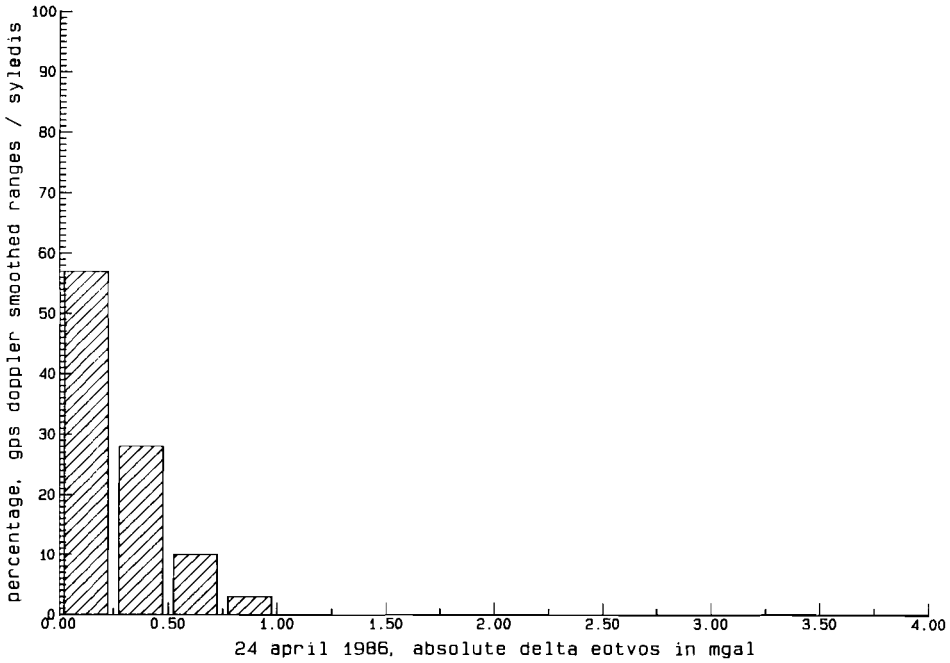

Figure 11. Distribution of absolute values of Eötvös correction differences for line L0330a from GPS Doppler smoothed pseudoranging and Syledis

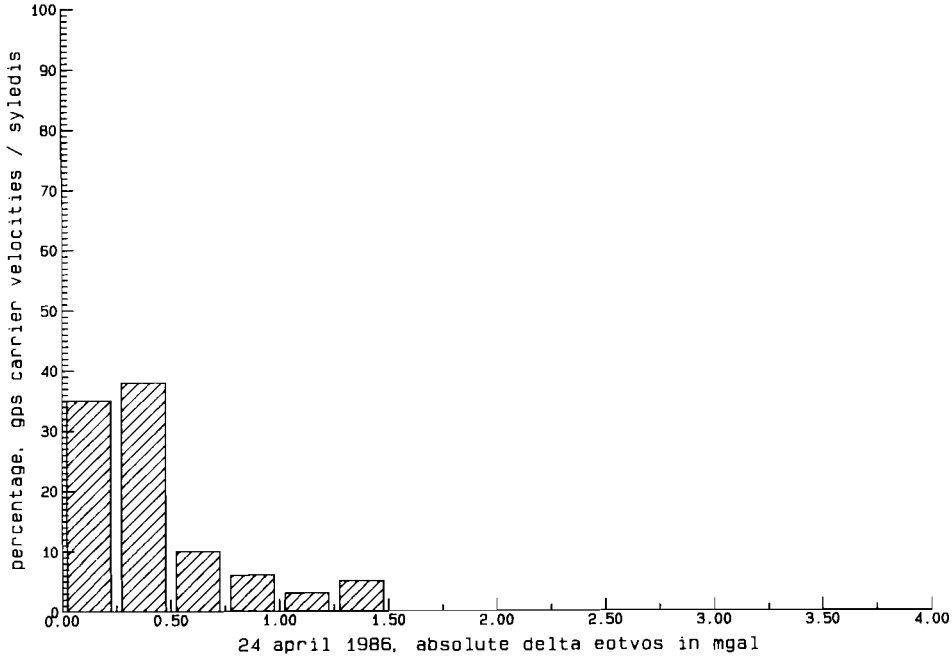

Figure 12. Distribution of absolute values of Eötvös correction differences for line L0330a from GPS carrier velocity and Syledis

5. Conclusions

The analysis of the Eötvös corrections for the five gravity lines shows that the Global Positioning System yields excellent velocity estimates. It shall be clear that no perfect reference exists and that the comparison of Eötvös corrections derived from GPS and radio navigation velocities is affected by the imperfection of both systems. Comparison which velocity estimation method actually yields best results can be done by correcting the gravity measurements for the Eötvös effect and analysing the cross-over differences. However, since the five gravity lines available for this analysis do not intersect a cross-over analysis was not possible.

Although the analysis was carried out with measurements under ideal and controlled circumstances (no heavy wind and excellent radio positioning), the conclusions about the possibilities of the Global Positioning System remain valid for less favourable conditions. In near future, when more satellites will be available, GPS will provide high accuracy ship velocity estimates worldwide, also in open oceans where terrestrial navigation systems are not available. Hence we expect that the effect of Eötvös correction errors in sea gravimetry can be reduced significantly.

6. References

Hatch, R.R. (1982): The synergism of GPS code and carrier measurements. Proceedings of the Third International Symposium on Satellite Doppler Positioning, Las Cruces, New Mexico.

Hatch, R.R. (1986): Dynamic differential GPS at the centimeter level. Proceedings of the Fourth International Geodetic Symposium on Satellite Positioning, Austin, Texas.

Kleusberg, A., S.H. Quek, D.E. Wells, J. Hagglund (1985): Comparison of INS and GPS ship velocity determination. Proceedings of the Third International Symposium on Inertial Technology for Surveying and Geodesy, Banff, Canada.

Lachapelle, G., W. Falkenberg, M. Casey (1987): Use of phase data for accurate differential GPS kinematic positioning. Bulletin Géodésique, vol. 61, no. 4.

Smit, J.H.M. (1988): Sea gravimetry and Eötvös correction. Graduate thesis, Delft University of Technology, Faculty of Geodesy.

Van Dierendonck, A.J., S.S. Russell, E.R. Kopitzke, M. Birnbaum (1978): The GPS Navigation Message. Navigation, vol. 25, no. 2.

Wells, D.E., S.H. Quek, J. McCullough, J. Hagglund (1985): Precise Ship's Velocity from GPS: Some Test Results. Proceedings of the First International Symposium on Precise Positioning with the Global Positioning System, Rockville, Maryland.

ALTIMETRY DERIVED GRAVITY COMPARED WITH NAVGRAV OBSERVED GRAVITY

R.H.N. Haagmans
Delft University of Technology
Faculty of Geodesy

1. Introduction

The only way to obtain information at sea before the satellite era was to collect shipborne measurements during expensive and time consuming expeditions. Think of Vening Meinesz' pioneering work, (1941) or (1948). As a result only relatively small areas could be covered, with different accuracies, while large parts of the oceans remained unexplored.

Nowadays the characteristics of the "wet part" of our globe are better known due to the launch of various earth observing satellites. One of the earth observing techniques is satellite altimetry which provides us with sea surface heights of uniform quality covering large ocean areas on a global scale. The analysis of altimeter data yields worldwide oceanographic and geophysical information, such as currents, eddies, sea surface variabilities, geoid heights and gravity anomalies.

In this study gravity anomalies are computed from the observed sea surface heights. At first sight the idea looks paradoxical because one of the main objectives of physical geodesy is just the opposite, the determination of geoid heights from gravity anomalies. In this respect one would rather prefer to think of an altimetric-gravimetric boundary value problem combining gravity on land with altimetry in ocean areas (cf. Sacerdote and Sansò, 1983 or Sansò and Stock, 1985). However for many purposes one still wants to derive gravity from altimetry, either for geophysical purposes or for merging it with land gravity to one global data set. In our case the purpose is to compare altimetry derived with measured gravity.

For the computation of gravity anomalies two different methods are considered here, collocation known from geodetic practice (cf.

Tscherning, 1974 or Moritz, 1980) and a method using the relations between the Fourier spectra of the geoid heights and the gravity anomalies developed by geophysicists (cf. Roest, 1987).

The results can be compared with very accurate shipborne free air gravity anomalies in the North Sea which are computed from ship gravimetry during the NAVGRAV experiment (cf. Strang van Hees, this issue). This accurate reference data set allows a judgement on the accuracy of the altimetry derived gravity anomalies as obtained from both approximation methods (cf. Haagmans, 1988).

2. The SEASAT altimeter

The altimeter on board of the SEASAT satellite observed ranges to the sea surface during its three months operational time in 1978. These raw observations need to be corrected for disturbing effects caused by the ionosphere, the troposphere and the instrument. Combining the corrected ranges with information about the satellite position results in sea surface heights above a chosen reference ellipsoid (for example the GRS80).

The instantaneous sea state is influenced by various time variable effects. For several of these, such as ocean and earth tides, surface pressure and significant wave heights model corrections are provided to the user on the Geophysical Data Records (Lorell et al, 1980) and can be applied to the raw sea surface height. The principle of satellite altimetry is shown in figure 1.

Two other effects remain and need to be eliminated in order to achieve meaningful geoid heights. The first is the residual sea surface topography which, again, can be divided into a stationary and a time variable part. For the stationary part estimates up to degree and order 20 of a spherical harmonic expansion result in gravity anomaly corrections smaller than 0.5 mgal for the North Sea region (cf. Rapp, 1985). The time variable part is even smaller but more difficult to model. Both effects are neglected in our computations which implies that they constitute an error source in the final gravity anomaly solution.

Secondly the radial orbit error needs to be eliminated from

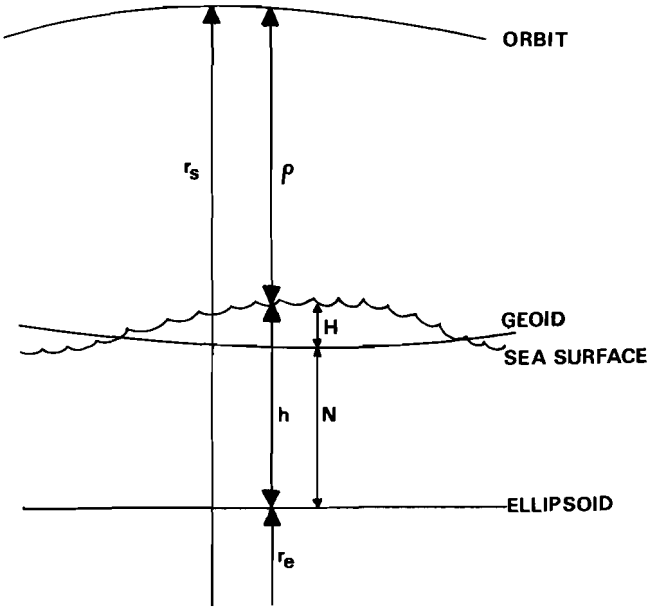

Figure 1. The Principle of an altimeter measurement.

the satellite positions. Although the sea surface heights are rather well determined relative to the satellite position (to better than 10 cm) an uncertainty in the absolute position of the satellite remains as large as ± 1.5 m r.m.s.. This rather large radial orbit error is a result of uncertainties in the initial conditions of the satellite orbit and, predominately, in the uncertainties of the gravity field parameters (cf. Colombo, 1984 or Rummel, 1986).

The problem of the orbit errors is treated in different ways for the two gravity field approximation methods considered here. For the case of the geophysical method it is more of a trend removal than an orbit error removal. For each individual arc segment a linear trend is removed which models the difference between the arc and a reference geoid based upon the GEM10B set of potential coefficients (cf. Roest, 1987 or Haagmans, 1988). The result is a rather arbitrary fit of each arc to the GEM10B reference independent from other arcs within a larger configuration.

For the case of the collocation method the orbit errors are

treated in a more sophisticated way. Using cross-over conditions the errors are minimized in an adjustment in two steps.
The first step consists of a cross-over minimization of the orbit error fitting to each ascending and descending arc a linear function in a large diamond shaped area in the Northern Atlantic. The result is a relative solution (Haagmans, 1988). In a second step an optimal fit connects the relative solution to a GEM10B reference geoid (Schrama, 1988).

Both approaches are considered to result in geoid heights, which can be expressed as:

$$N(P) = r_s - r_e + \varepsilon_s - \rho_{cor} - H \qquad (1)$$

where N(P) is the geoid height at point P, r_s is the satellite position, r_e is the position of the projection of P (cf. figure 1) onto the reference ellipsoid, ε_s is a linear trend or orbit error correction, ρ_{cor} is the corrected range (i.e. corrected for ionosphere, troposphere, the instrumental effect, ocean and solid earth tides, barotropic effects and significant waveheight effects) and H is the modelled sea surface topography.
Once these geoid heights are determined the gravity anomalies can be computed.

3. Gravity anomalies

The geoid height of the earth's gravity field at a point P can be linked to the gravity anomaly at the same point by the fundamental equation of geodesy combined with Bruns' formula (cf. Heiskanen and Moritz, 1967) yielding in spherical approximation:

$$\Delta g(P) = -\left(\frac{\partial}{\partial r} + \frac{2}{R} \right) \gamma \, N(P) \qquad (2)$$

where Δg is the gravity anomaly, R is the mean earth's radius and γ is the mean gravity over the earth.
Two discrete approximation methods will be used in the sequel in order to compute the local gravity anomaly field. A problem may

arise if observed geoid heights are used as input, since the transform from geoid heights to gravity anomalies is a differentiating operation or a kind of high-pass filter. Or if there is noise in the observations it will be amplified together with the higher frequency content of the geoid height signal which may result in unstable or even meaningless gravity anomaly estimates.
This problem is handled in both methods by carefully selecting the sample point distribution and by noise modelling and filtering (cf. Haagmans, 1988).

3.1 Least squares collocation

The first method is least squares collocation which is a space domain technique where (signal) covariance functions play a very important role in field representation and filter design. It is a sophisticated and rather complex approach which derives from the measurements any desired linear functional of the earth's disturbing potential in the least squares, minimum norm sense.

Under the assumption that the data can be considered homogeneous (independent of the position) and isotropic (independent of the azimuth) a model is introduced treating gravity field quantities as stochastic signals. The estimated gravity anomaly is computed from (cf. Rapp, 1977):

$$\hat{\Delta g}(P) = C_{gN} \left[C_{NN} + D \right]^{-1} \left[N - N_{ref} \right] + \Delta g_{ref} \qquad (3)$$

where $\hat{\Delta g}$ refers to the chosen ellipsoidal normal field, N is a column vector of altimeter implied geoid heights, N_{ref} is a column vector of approximate geoid heights and Δg_{ref} a point gravity anomaly both implied by a GEM10B reference field up to degree and order 36 of a spherical harmonic expansion (refering to the same ellipsoidal field), D is a diagonal a priori noise variance-covariance matrix whose elements correspond to the square of the standard deviation (± 7.5 - 10 cm) of the altimeter geoid heights, C_{NN} is a square symmetric matrix containing the (signal) covariances between the given geoid heights and C_{gN} is a row vector containing the (signal) covariance between the gravity

anomaly being predicted at point P and the given geoid heights.

In equation (3) the solution of the problem is split into a trend contribution implied by the GEM10B reference field and a collocation solution coming from the remaining signal and assumed to have zero expectation.

For the collocation solution (signal) covariance functions are used for the definition of the approximation function space. A local autocovariance function for gravity anomalies is derived for the North Sea area from a global Tscherning/Rapp model (cf. Tscherning and Rapp, 1974). Error degree variances for the GEM10B coefficient set were not at our disposal, so the first 36 terms of the local function are set to zero. Hence the local covariance function for gravity anomalies can be expressed as:

$$C_{gg} = \sum_{n=37}^{\infty} c_n^g \, S^{n+2} \, P_n(\cos \psi) \qquad (4)$$

where $P_n(\cos \psi)$ are the Legendre polynomials, and S is the ratio between a Bjerhammar radius and the earth radius, where S is:

$$S = \left[\frac{R_B^2}{R^2} \right] = 0.999617 \qquad (5)$$

and where one of the empirical degree variance models is used (cf. Tscherning and Rapp, 1974):

$$c_n^g = \frac{A \, (n-1)}{(n-2)(n+24)} \qquad \text{for } n \geq 37 \qquad (6)$$

with A = 161.3 $mgal^2$ corresponding to a signal variance of 420 $mgal^2$ (cf. Haagmans, 1988).

Once this covariance function is chosen the autocovariance functions of other gravity field quantities or their cross-covariance functions can easily be derived by covariance propagation using the functional relations (cf. Moritz, 1980).

The actual collocation computations are performed with the

GEOCOL program which was originally developed by C.C. Tscherning at the Department of Geodetic Science and Surveying of the Ohio State University. Meanwhile the original program has been modified and extended with new options at the Danish Geodetic Institute and the latest update has been provided to us (cf. Tscherning, 1974 and Tscherning and Knudsen, 1986).

3.2 The geophysical approach

This second method of discrete gravity field approximation describes and relates the frequencies which are present in the geoid height and gravity anomaly signal. The space domain filtering as we know it from collocation is replaced by frequency domain filtering. The relation between the amplitude spectra of geoid height and gravity anomaly is derived following the procedure described in (Chapman, 1979) and (Roest, 1987).

In case of satellite altimetry geoid heights are provided at regular intervals along observed profiles. Assuming a two dimensional world for each profile, the gravity field depends only on the along track x-coordinate and the height z and Laplace' equation becomes:

$$\frac{\partial^2 T}{\partial x^2} + \frac{\partial^2 T}{\partial z^2} = 0 \qquad (7)$$

where T represents the disturbing potential which is harmonic outside the geoid.

If our main subject of interest is the high frequency part of the gravity anomaly signal, a planar approximation of the gravity field can be applied subtracting first the GEM10B reference field up to degree and order 36 in terms of a spherical harmonic expansion. The remaining gravity anomaly signal in (2) may be approximated by the gravity disturbance and reflects the mentioned high frequencies. Hence:

$$\Delta g \approx \partial g = - \frac{\partial T}{\partial z} \qquad (8)$$

Using Bruns' equation and inserting (8) into (7) results in:

$$\gamma \frac{\partial^2 N}{\partial x^2} - \frac{\partial \Delta g}{\partial z} = 0 \qquad (9)$$

The quantities N and Δg in (9) can be expressed by a Fourier series in a planar approximation (Haagmans, 1988). Combining both series with equation (9) yields identical phase spectra for geoid height and gravity anomaly but different amplitude (or Fourier) spectra. It is:

$$\mathbb{F}[\Delta g] = \gamma k \omega_0 \, \mathbb{F}[N] \quad \text{with} \quad k = 1,2,3,\ldots,\frac{K-1}{2} \qquad (10)$$

where $\mathbb{F}[\ ]$ denotes the Fourier transform, γ the mean earth's gravity, ω_0 the fundamental frequency of the profile and K the number of discrete observations in a profile.

A Butterworth filter is implemented in the transform in order to control the effect of possible instabilities caused by noise. It is a low-pass filter which approximates very well the ideal (magnitude) filter characteristics (Lynn, 1973) and can be expressed as:

$$|B(\omega)|^2 = \frac{1}{1 + \left[\frac{\omega}{\omega_B}\right]^{2b}} \qquad (11)$$

where $B(\omega)$ represents the magnitude of the filter, b the order of the filter and ω_B the band frequency (0.25 cps cf. Roest, 1987).

The Butterworth filter applied to the transform of eq. (10) gives:

$$\mathbb{F}[\Delta g] = |B(\omega)| \, \gamma k \omega_0 \, \mathbb{F}[N] \qquad (12)$$

In (12) $|B(\omega)|$ is the amplitude filter (not the power spectrum version of (11)).
The transforms of eq. (10) and (11) are illustrated in figure 2.

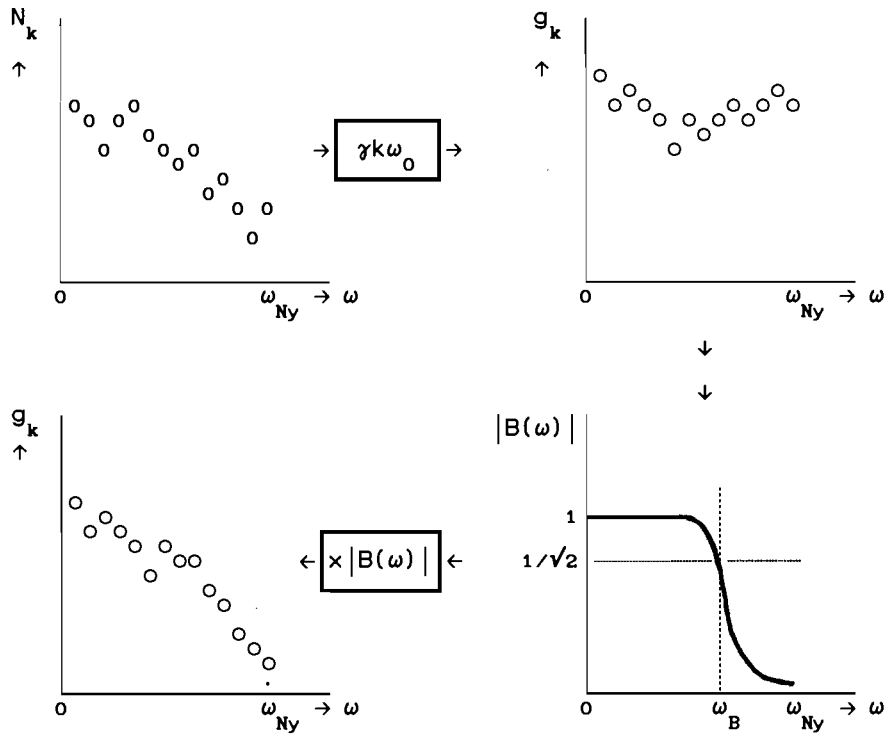

Figure 2. Geoid spectrum - Gravity spectrum relation and the effect of amplitude filtering. ω_{Ny} is the Nyquist frequency (here 0.5 cps). N_k and g_k are the geoid resp. gravity amplitudes per degree k.

By taking the inverse Fourier transform one can subsequently obtain the desired gravity anomaly signal along an altimeter profile.

4. Altimetry derived results compared with NAVGRAV gravity anomalies

The results from altimetry computed with the methods from chapters **3.1** and **3.2** can be compared with the 1986 NAVGRAV results (cf. Strang van Hees, this issue). For this purpose all three sets of gravity anomalies are finally computed in identical grid points. Each set results in a ϕ,λ-grid ($0.125^0 \times 0.25^0$) with gravity anomalies within the following bounds:
$54^0 \leq \phi \leq 56^0$ and $2.125^0 \leq \lambda \leq 7.125^0$.

The 357 gridded NAVGRAV anomalies are computed from the free

air anomalies along the profiles of figure 2 in (NAVGRAV (introduction), this issue). An interpolation program for irregularly spaced data using difference equations for minimum curvature (Swain, 1976) produces the gridded values with an estimated accuracy of better than 1.75 mgal (cf. Haagmans, 1988).

4.1 The collocation results

As input for the collocation a quite regular pattern with altimeter geoid heights was selected as represented in figure 3. Two other attemps with different patterns were less satisfactory, one due to two almost coinciding altimeter tracks which disturbe the numerical stability of the solution of the normal equations (cf. Tscherning, 1985) yielding a poorly determined gridded solution. The second gave problems due to a large cross-over discrepancy (± 25 cm) which caused a kind of clover leaf pattern with useless gravity anomaly values. It is a very tricky solution which may lead to misinterpretations of the altimeter results! After comparison of contour maps of this latter altimetric solution and the NAVGRAV results the at first sight promising statistics appeared to be useless. The descending track on which the cross-over was situated was replaced by another descending arc which was better connected to the configuration of figure 3. The

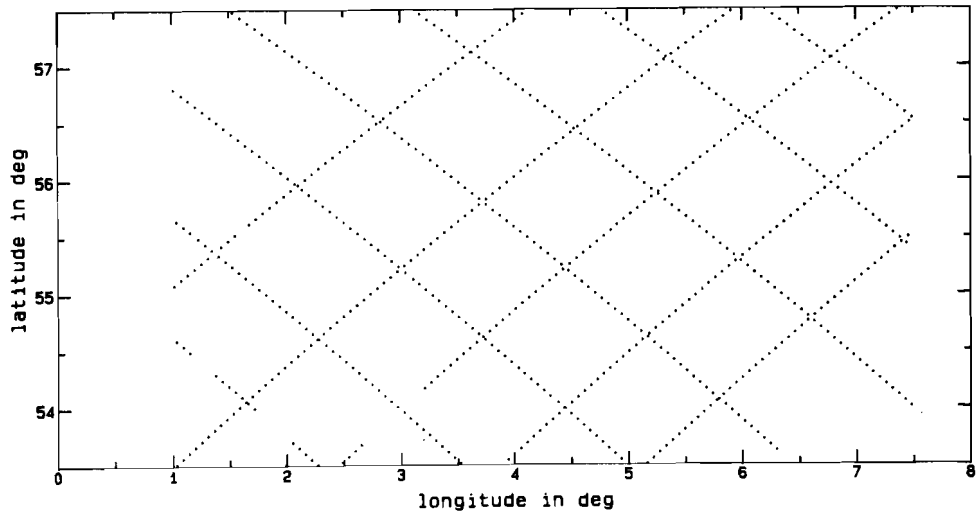

Figure 3. Selected geoid heights from altimetry which serve as input for collocation.

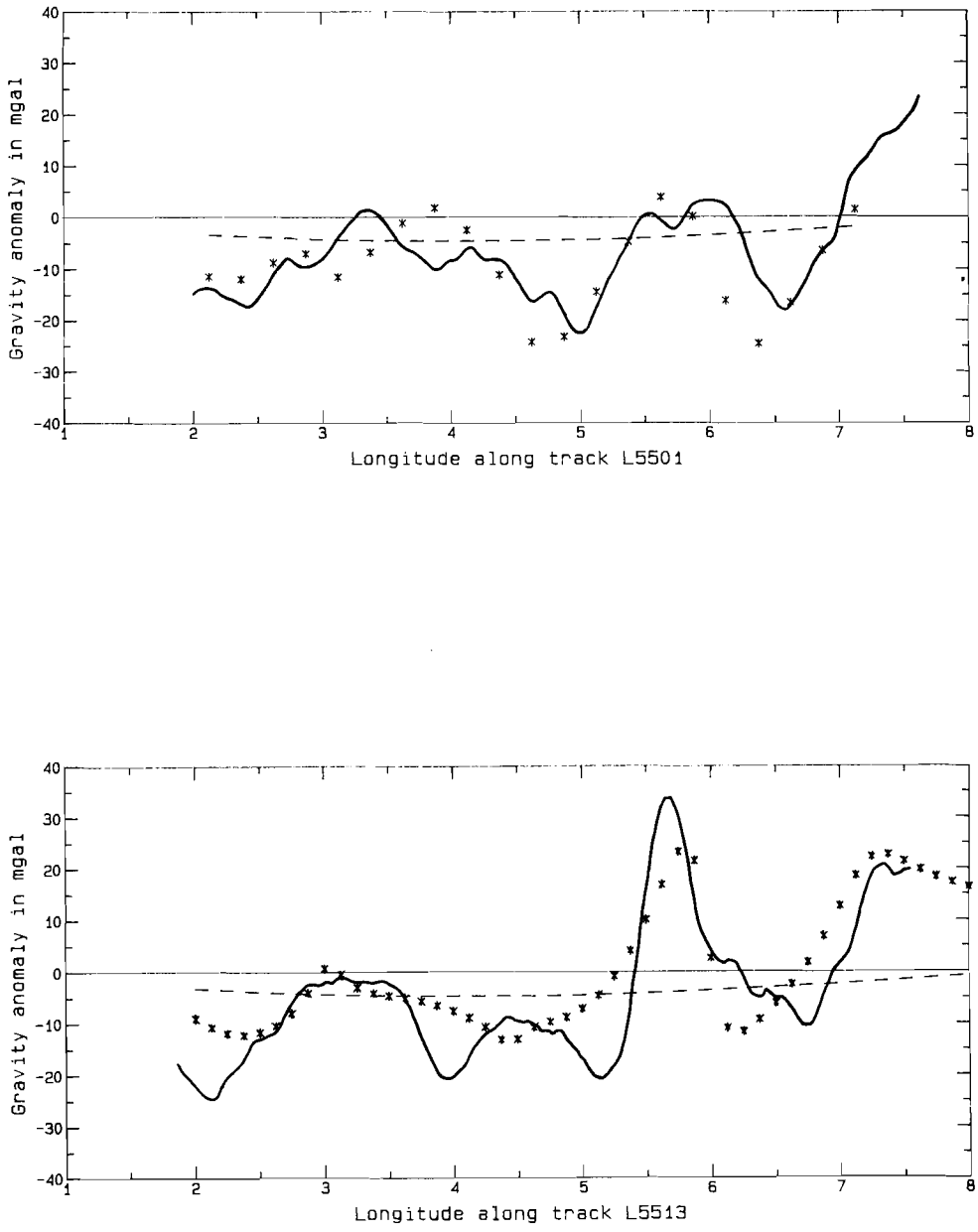

Figure 4. Two predicted solutions from altimetry. The continuous line represents the NAVGRAV free air gravity anomalies in GRS67, *the stars the predicted free air anomalies in* GRS80 *based on the SEASAT data and the dashed line the anomaly contribution in* GRS80 *implied by the* GEM10B *reference field (all in mgal).*

gridded results are tested against the NAVGRAV solution in chapter **4.3**.

The advantage of the collocation prediction is that a result can be provided at any desired point. Using this property gravity anomalies are predicted along some sailed NAVGRAV profiles. The results are presented in figure 4 where NAVGRAV and altimeter anomalies show good resemblance except for the highest frequencies.

4.2 The results of the geophysical method

Different from the collocation procedure where the transformation into gravity anomalies and the gridding is done at once, the geophysical method requires two steps.
During the first step the transformation of, eq. (12), is applied to the geoid heights along 16 selected SEASAT profiles, each ± 630 km long (cf. figure 5). A descending arc, for example the second arc counted from the East side, is transformed into a gravity

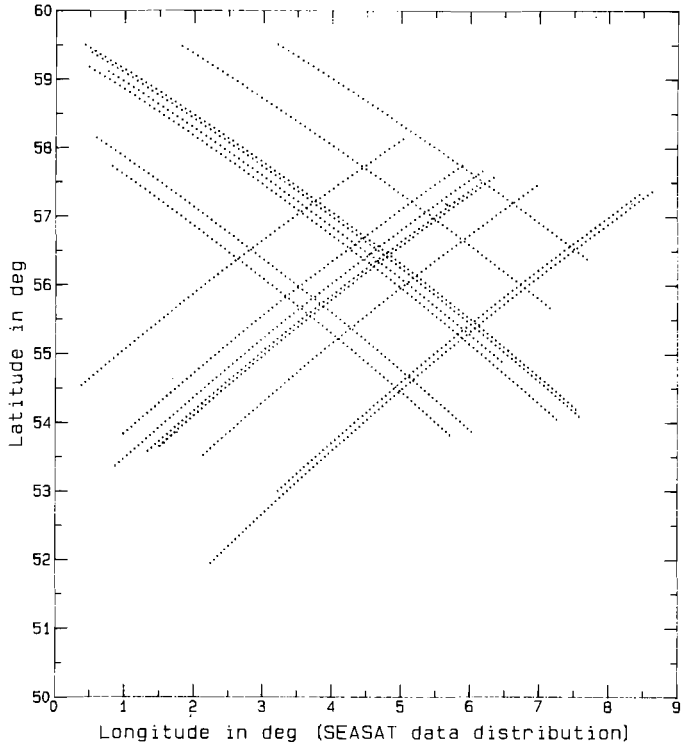

Figure 5. SEASAT tracks in the North Sea selected for the geophysical method.

profile using a tenth order Butterworth filter (equation (11)). The geoid height and the gravity anomaly signal are shown in figure 6. The gravity signal is reflecting the amplified high frequencies from the geoid height signal as a result of the differentiating operation.

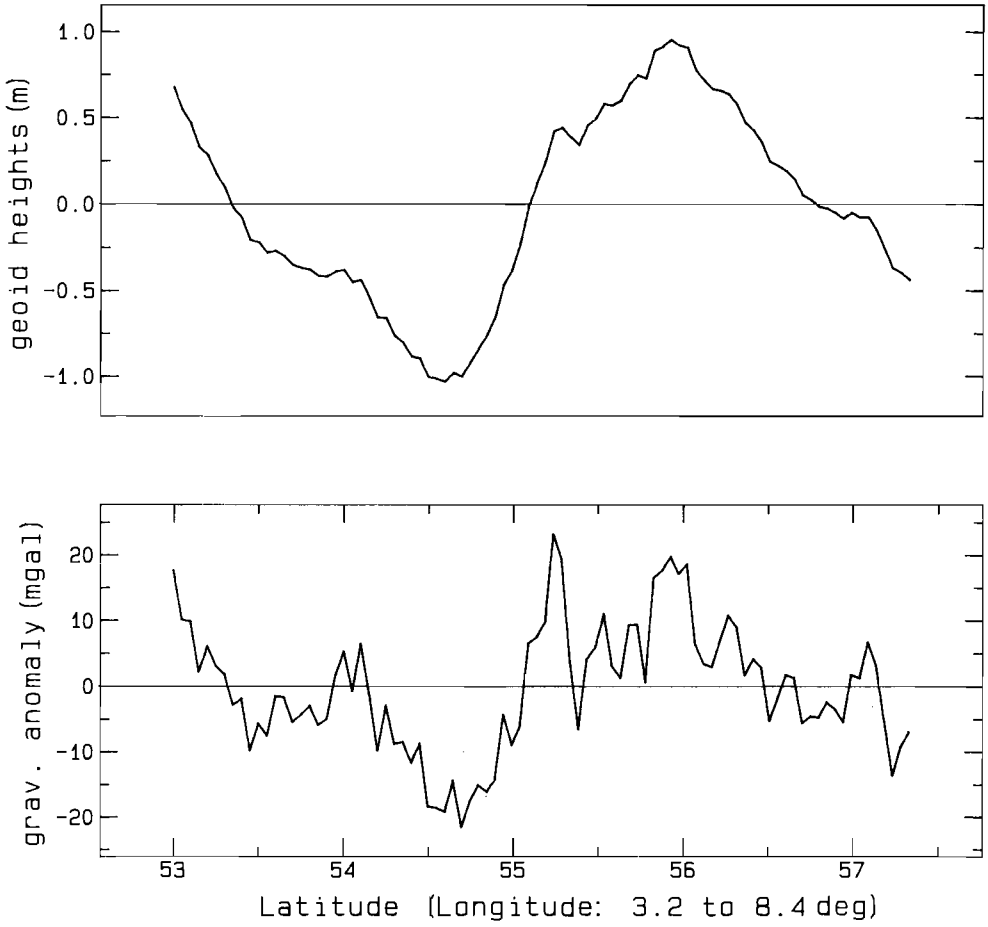

Figure 6. Along track geoid height-gravity anomaly relation using the spectral operator of equation (12) with a tenth order Butterworth filter.

Once all individual arcs are transformed into gravity profiles a serious disadvantage of the method, as applied by Roest (1987), becomes clear. Every cross over point (cf. 83 cross overs in figure 5) should have identical gravity anomaly values for the descending as well as the ascending arc. However the mean cross-over difference between ascending and descending values is

2.43 mgal with a standard deviation of 8.28 mgal. This is obviously a result of the arbitrariness in the trend removal as discussed in chapter 2.
A gridded solution is computed in a second step using the same method as applied for the NAVGRAV gridding.

4.3 Statistics, comparison and conclusion

Some statistics are obtained from both altimetric and the NAVGRAV gridded solutions. The similarity between both altimetric results in GRS80 and the NAVGRAV grid in GRS67 is examined by comparing contour plots obtained with GSPP (Sünkel, 1980) and by computing the correlation coefficient between the grids (Haagmans, 1988). Furthermore each set of gridded values is statistically represented by a mean and a r.m.s. value together with its gravity anomaly distribution. The latter are shown as histograms in figure 7. Also the differences between the solutions areanalysed in the same way. A histogram of the differences between the best solution (collocation) and the NAVGRAV gridded anomalies is shown in figure 8.
In fact the results of NAVGRAV should be converted to GRS80 by applying (13) (cf. Moritz, 1980b):

$$\Delta g_{1967} = \Delta g_{1980} + 0.8316 + 0.0782 \sin^2\varphi - 0.0007 \sin^4\varphi \text{ [mgal]} \quad (13)$$

yielding within the North Sea area:

$$\varphi = 51^0 \quad \rightarrow \quad \Delta g_{1967} = \Delta g_{1980} + 0.8785 \text{ [mgal]}$$

$$\varphi = 58^0 \quad \rightarrow \quad \Delta g_{1967} = \Delta g_{1980} + 0.8874 \text{ [mgal]}$$

The effect within the relative small area can be regarded as a bias in the mean of the anomaly differences of about 0.88 mgal, while the standard deviation remains the same.
All statistical results are presented in table 1. The contribution of the GEM10B reference field is left out of consideration in the statistics because its contribution is equal to all three grids.

From the results of table 1 as well as from the distributions of figure 7 it appears that the collocation and the NAVGRAV solution show most resemblance. Not only the statistics but also

the contour plots of both solutions (cf. figure 9 and 10) justify the conclusion that the collocation solution can be denoted as acceptable.

The FFT solution contains a clear systematic difference and a rather small signal variance compared to both other solutions. The smaller variance may partly result from smoothing effects from the Butterworth filter and of the interpolation and partly of the signal information loss during the trend removal where probably some physically correct signal is eliminated. For the case of the technique presented in (Roest, 1987) which led to more disappointing results some minor modifications may lead to better ones. The differences with the NAVGRAV results which are an

gridded solutions without GEM10B contribution	**mean (mgal)**	**r.m.s. (mgal)**
357 FFT gravity anomalies* (10^{th} order filter)	-0.28	7.32
357 collocation gravity anomalies*	-6.67	13.15
357 NAVGRAV gravity anomalies+	-5.76	11.88
differences between SEASAT and NAVGRAV	**mean (mgal)**	**σ (mgal)**
357 FFT* minus NAVGRAV+ anomalies	5.48	8.11
357 collocation* minus NAVGRAV+ anomalies	-0.91	7.10
357 collocation* minus NAVGRAV* anomalies	-0.03	7.10
similarity between both SEASAT and the NAVGRAV solution		
correlation coefficient (FFT* and NAVGRAV+)		0.74
correlation coefficient (collocation* and NAVGRAV+)		0.83

* Computed in GRS80
\+ Computed in GRS67

Table 1. Statistics of three gridded gravity anomaly solutions. The solution of the geophysical method is denoted as FFT, i.e. Fast Fourier Technique.

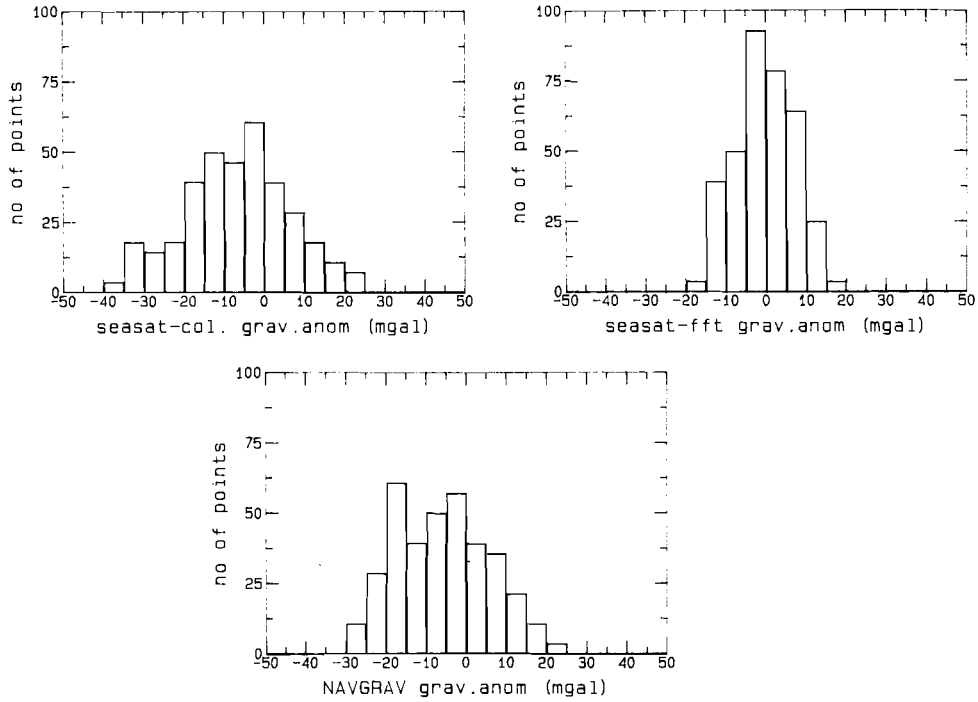

Figure 7. Distributions of the gravity anomaly signal in mgal, each computed from 357 grid points. They represent respectively the collocation solution, the geophysical solution (both in GRS80) and the NAVGRAV solution (in GRS67).

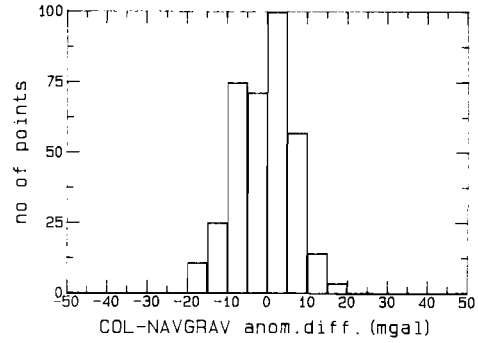

Figure 8. Distribution of the differences between the collocation solution (in GRS80) and the NAVGRAV solution (in GRS67) in mgal.

accumulated effect of the cross-over differences and of the trend removal can be reduced by using the same orbit error removal process as used for collocation. Furthermore an adequate description of noise and signal in higher frequency ranges could result in an optimal filter and thus a less smooth and more realistic gravity anomaly signal. If these drawbacks are eliminated the advantages of the geophysical method could be fully exploited. The method is easy to handle and extremely fast.

Considering the collocation results (with a precision of better than 7.4 mgal for gridded anomalies) it seems to be very well feasible that gravity anomalies obtained from SEASAT altimeter data are employed for large scale exploration surveys e.g. for oil compagnies in order to detect areas of interest. These areas can subsequently be examined with dedicated ship expeditions in order to obtain additional geophysical information within the area e.g. by seismic surveys and/or detailed high precision gravity surveys. However one has to be careful when applying the collocation and the geophysical method in areas where the gravity field is highly anisotropic because both methods imply a rather isotropic gravity field. Also the collocation results can be improved by using a more complete data selection of SEASAT data within an area, by applying a better local covariance function and by carefully modelling the sea surface topography so that even better results may be expected in the near future.

5. Acknowledgements

We gratefully acknowledge the support of C.C. Tscherning of the Danish Geodetic Institute for providing the Danish collocation software and for his valuable advice during the installation of the software on our computer. Many thanks to E.J.O. Schrama for performing the local cross-over adjustment of SEASAT altimeter data.

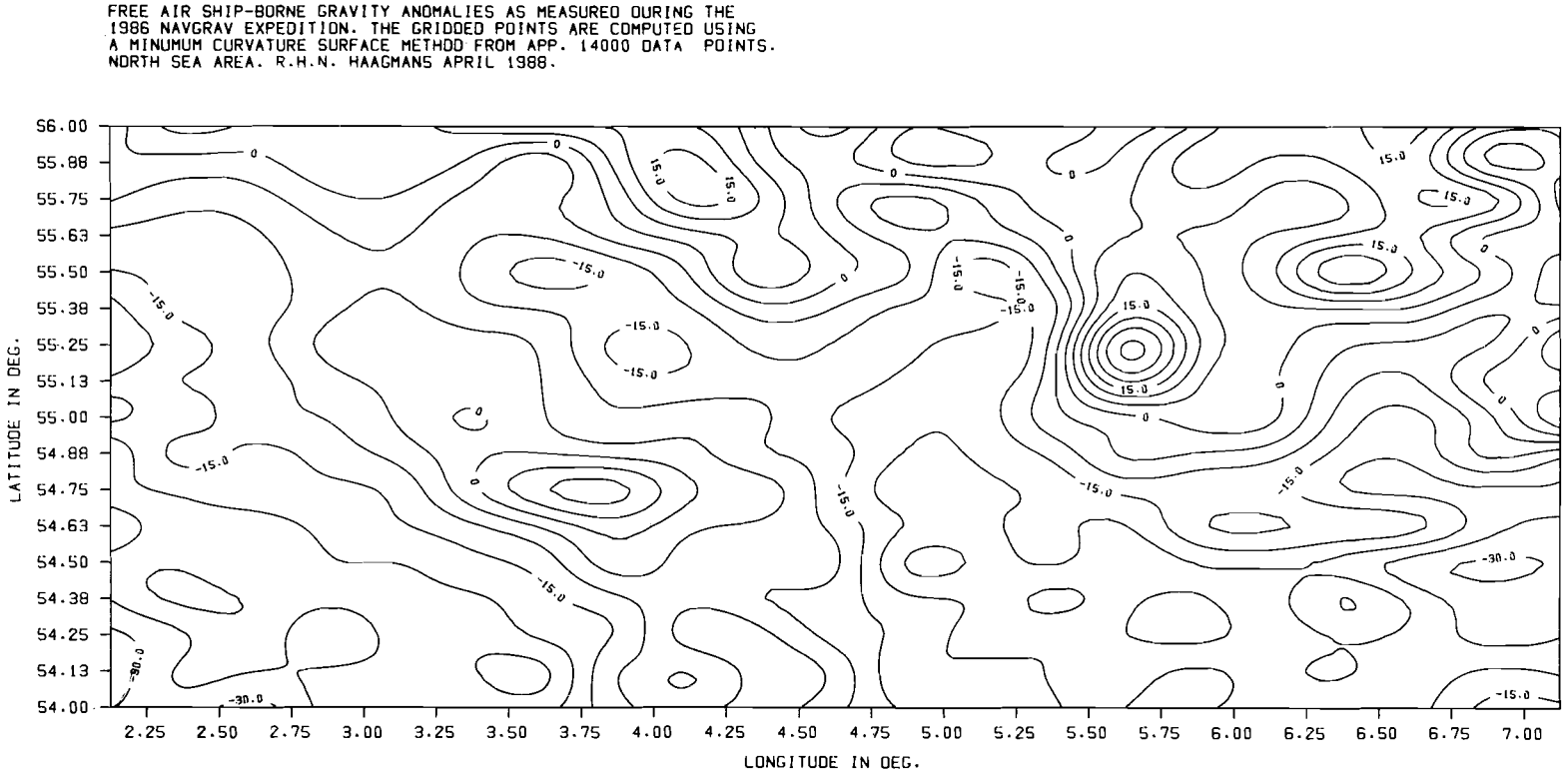

Figure 9. Contour plot in mgal obtained from a gridded set NAVGRAV free air gravity anomalies (in GRS67).

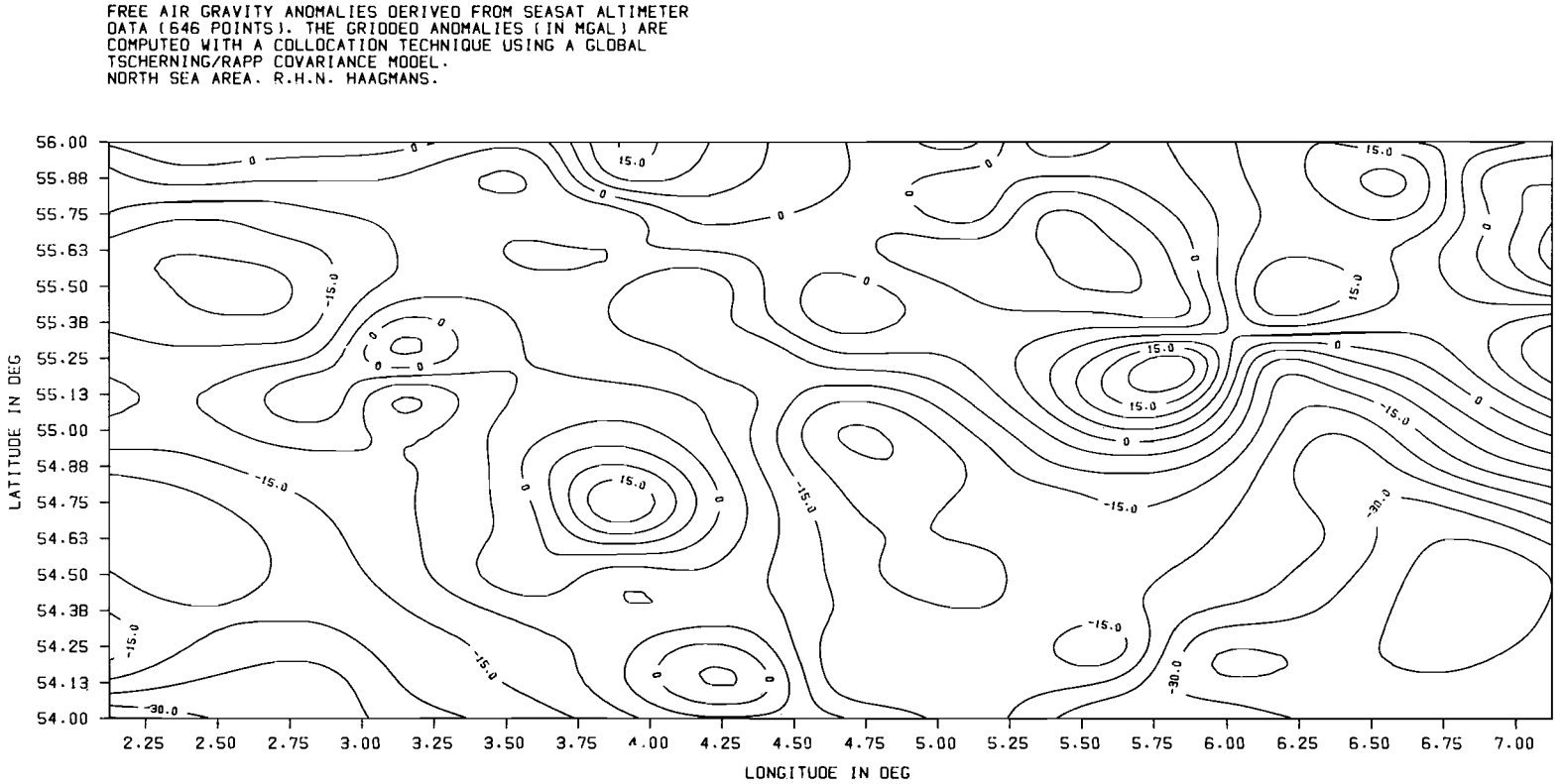

Figure 10. Contour plot in mgal obtained from a gridded set SEASAT free air gravity anomalies (in GRS80). The anomalies are computed with collocation from the data of figure 3.

6. References

Chapman, M.E. (1979): Techniques for interpretation of geoid anomalies. Journal of Geophysical Research 84, B8, 3793-3801.

Colombo, O.L. (1984): Altimetry, orbits and tides. TM86180, Goddard Space Flight Center, NASA, Greenbeld, Maryland.

Haagmans, R.H.N. (1988): Detailed gravity anomalies derived from SEASAT altimeter data (A comparison of two alternative approaches: least squares collocation and a method based on FFT). Graduate thesis, Delft University of Technology, Faculty of Geodesy.

Heiskanen, W.A. and H. Moritz (1967): Physical Geodesy. Freem. and Company, San Francisco.

Lorell, J., M. Parke and J. Scott (1980): SEASAT geophysical data record (GDR) users handbook. Doc. 622-97, Jet Propulsion Laboratory, Pasadena, California.

Lynn, P.A. (1973): An introduction to the analysis and processing of signals. MacMillan, London.

Moritz, H. (1980): Advanced physical geodesy. H. Wichmann Verlag, Karlsruhe.

Moritz, H. (1980b): Geodetic Reference System 1980. Bulletin Géodésique, vol. 54, no. 3, Paris.

Rapp, R.H., R. Rummel, L. Sjöberg (1977): The determination of gravity anomalies from geoid heights using least squares collocation. Reports of the Department of Geodetic Science and Surveying, no. 269, OSU, Columbus, Ohio.

Rapp, R.H. (1985): Detailed gravity anomalies and sea surface heights derived from GEOS-3/SEASAT altimeter data. Reports of the Department of Geodetic Science and Surveying, no. 365, OSU, Columbus, Ohio.

Roest, W. (1987): Seafloor spreading pattern of the North Atlantic between 10^0 and 40^0 N. Geologica ultraiectina, no. 48, Elinkwijk BV, Utrecht.

Rummel, R. (1986): Satellite altimetry as a part of a geodetic model. Proceedings 1^{st} Hotine-Marussi symposium on mathematical geodesy, 757-786, Rome 3-6 June 1985.

Sacerdote, F. and F. Sansò (1983): A contribution to the analysis of the altimetry-gravimetry problem. Bulletin Géodésique,

vol. 57, no. 3, Paris.

Sansò, F and B. Stock (1985): A numerical experiment in the altimetry-gravimetry problem II. Manuscripta Geodaetica, vol. 10, no. 1, Springer Verlag, Berlin.

Schrama, E.J.O. (1988): Documentation on software handling regional adjustment of SEASAT altimeter data. Internal Report, Delft University of Technology, Faculty of Geodesy.

Swain, C.J. (1976): A Fortran IV program for interpolating irregularly spaced data using difference equations for minimum curvature. Computer & Geosciences, vol. 1, 231-240, Pergamon Press.

Sünkel, H. (1980): A general surface representation module designed for geodesy. Reports of the Department of Geodetic Science and Surveying, no 292, OSU, Columbus, Ohio.

Tscherning, C.C. (1974): A Fortran IV program for the determination of the anomalous potential using stepwise least squares collocation. Reports of the Department of Geodetic Science and Surveying, no. 212, OSU, Columbus, Ohio.

Tscherning, C.C. and R.H. Rapp (1974): Closed covariance expressions for gravity anomalies, geoid undulations and deflections of the vertical implied by anomaly degree variance models. Reports of the Department of Geodetic Science and Surveying, no. 208, OSU, Columbus, Ohio.

Tscherning, C.C. (1985): Local approximation of the gravity potential by least squares collocation. Proceedings "Local gravity field approximation", Beijing, 277-362.

Tscherning, C.C. and P. Knudsen (1986): Determination of bias parameters for satellite altimetry by least squares collocation. In Proceedings 1st Hotine-Marussi symposium on mathematical geodesy, 833-852, Rome 3-6 June 1985.

Vening Meinesz, F.A. (1941): Gravity expeditions at sea 1934-1939. Volume III, Waltman, Delft.

Vening Meinesz, F.A. (1948): Gravity expeditions at sea 1923-1938. Volume IV, DUM, Delft.

APPENDIX A

Gravity profiles

The following gravity profiles show detailed gravity field variations along the sailed NAVGRAV tracks of figure 2 (NAVGRAV (introduction), this issue). Bouguer and free air gravity anomalies have been computed and are represented in the upper part of the graphs. Underneath, the corresponding depth profiles are shown.

The line numbers are expressed in degrees and seconds e.g. L5513 means an East-West line along the parallel $55^{o}13'$ or L0630 means a North-South line along the meridian $6^{o}30'$.

The software for testing, filtering and plotting the data is written by R.P.E. van Rossem (student of the Faculty of Geodesy).

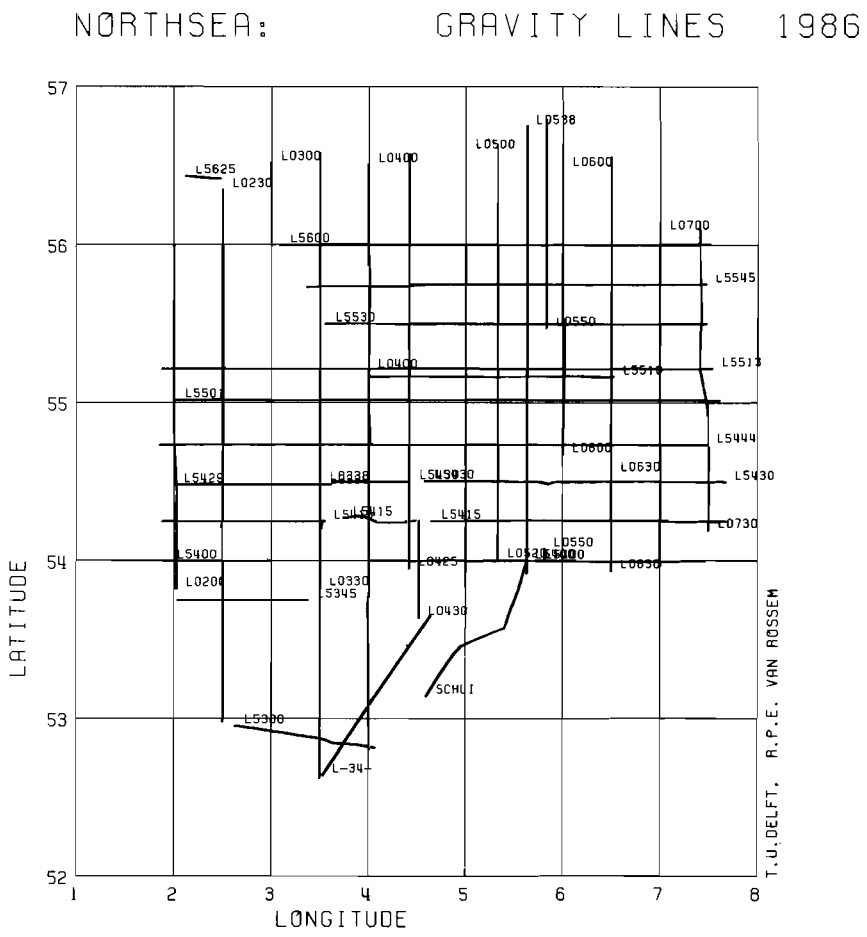

Gravity line numbering

NORTH SEA: GRAVITY ANOMALY L0200

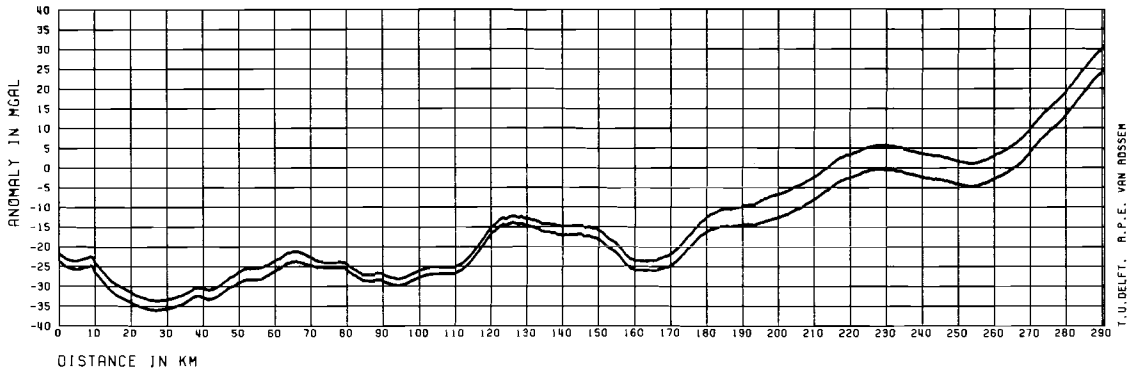

FULL LINE: FREE AIR ANOMALY
OPEN LINE: BOUGUER ANOMALY

LINE: L0200
DATE: MAY 11 1986

		START	FINISH
TIME	H.M.S.:	17 59 44	6 29 52
U.T.M. COORDINATES	X:	435857	438331
	Y:	5963395	6254104
GEOGRAPHICAL COORDINATES	PHI:	53.814	56.426
	LAMBDA:	2.026	2.000

NORTH SEA: DEPTH L0200

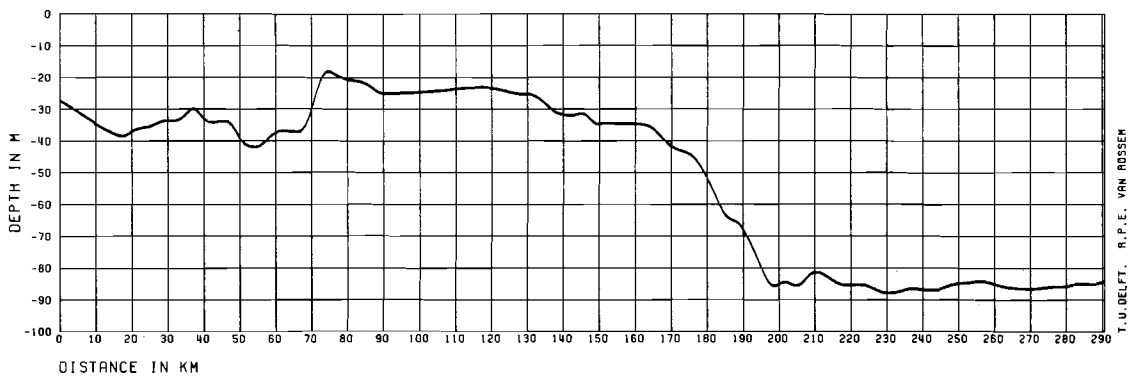

NORTH SEA: GRAVITY ANOMALY L0230

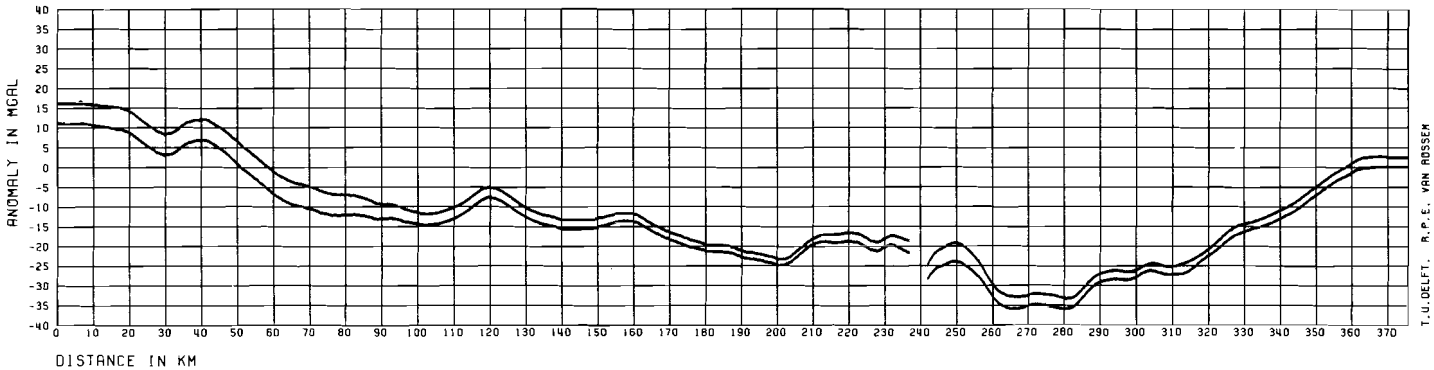

FULL LINE: FREE AIR ANOMALY
OPEN LINE: BOUGUER ANOMALY

LINE: L0230
DATE: MAY 12 1986

		START	FINISH
TIME	H.M.S.:	8 9 43	0 54 42
U.T.M. COORDINATES	X:	469097	466406
	Y:	6245360	5869576
GEOGRAPHICAL COORDINATES	PHI:	56.351	52.974
	LAMBDA:	2.500	2.500

NORTH SEA: DEPTH L0230

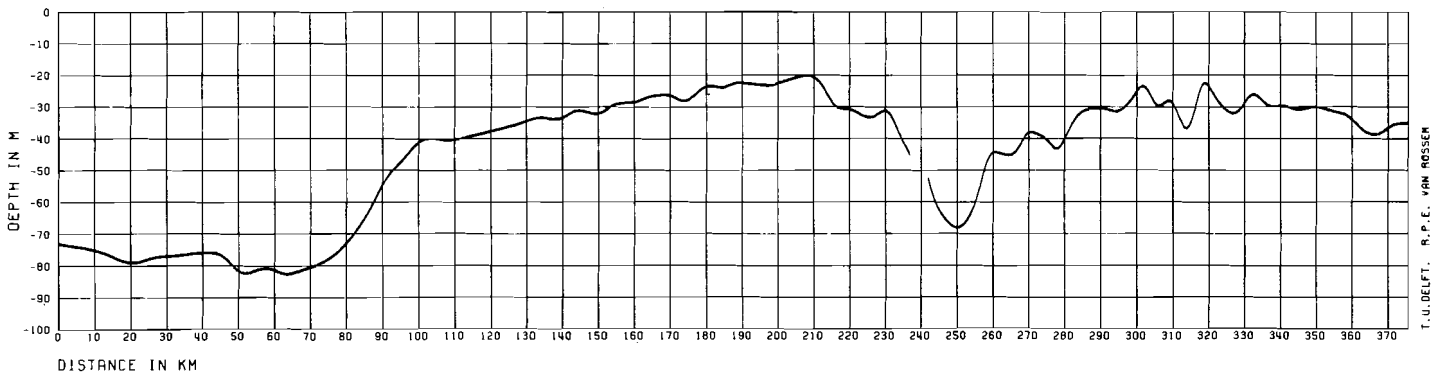

NORTH SEA: GRAVITY ANOMALY L0300

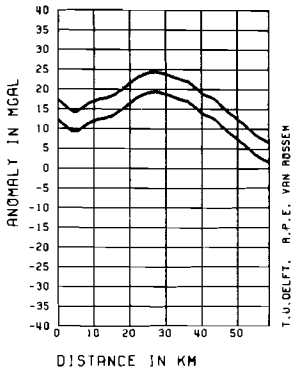

FULL LINE: FREE AIR ANOMALY
OPEN LINE: BOUGUER ANOMALY

LINE: .L0300
DATE: MAY 6 1986

		START	FINISH
TIME	H.M.S.:	21 29 46	23 54 46
U.T.M. COORDINATES	X:	498920	500001
	Y:	6265159	6206364
GEOGRAPHICAL COORDINATES	PHI:	56.530	56.001
	LAMBDA:	2.999	3.000

NORTH SEA: DEPTH L0300

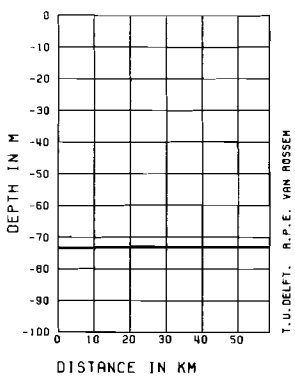

NORTH SEA: GRAVITY ANOMALY L0330

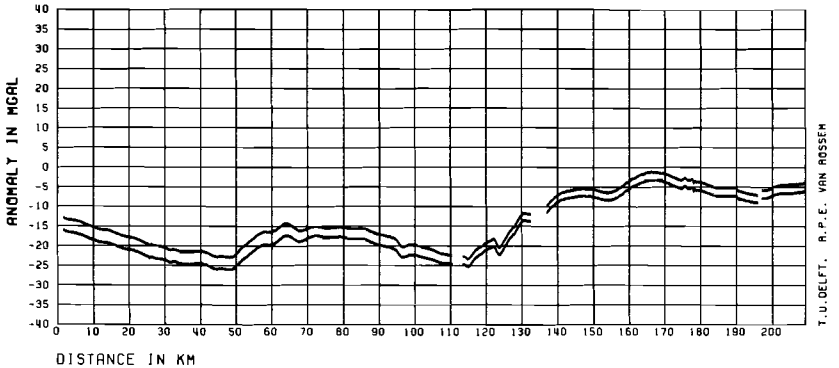

FULL LINE: FREE AIR ANOMALY
OPEN LINE: BOUGUER ANOMALY

LINE: L0330
DATE: APRIL 24 1986

		START	FINISH
TIME	H.M.S.:	4 45 48	18 29 42
U.T.M. COORDINATES	X:	532438	533766
	Y:	6036954	5829661
GEOGRAPHICAL COORDINATES	PHI:	54.478	52.615
	LAMBDA:	3.501	3.499

NORTH SEA: DEPTH L0330

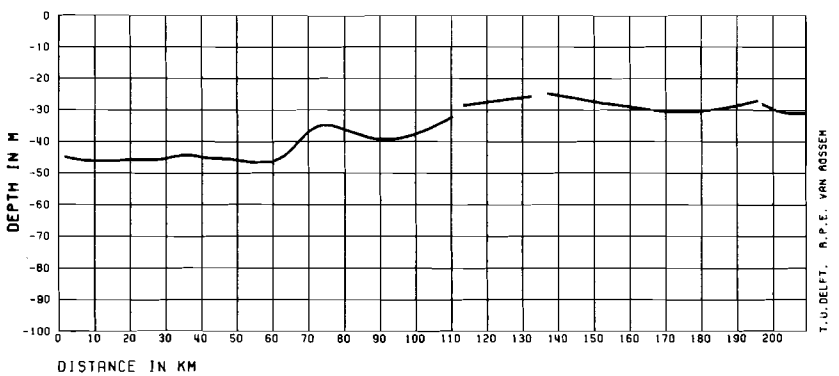

NORTH SEA: GRAVITY ANOMALY L0330

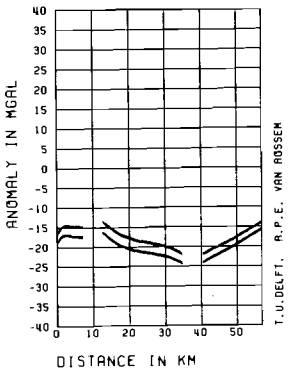

FULL LINE: FREE AIR ANOMALY
OPEN LINE: BOUGUER ANOMALY

LINE: L0330
DATE: APRIL 27 1986

		START	FINISH
TIME	M.M.S.:	11 19 42	13 39 42
U.T.M. COORDINATES	X:	532902	533304
	Y:	5965645	5908665
GEOGRAPHICAL COORDINATES	PHI:	53.837	53.325
	LAMBDA:	3.500	3.500

NORTH SEA: DEPTH L0330

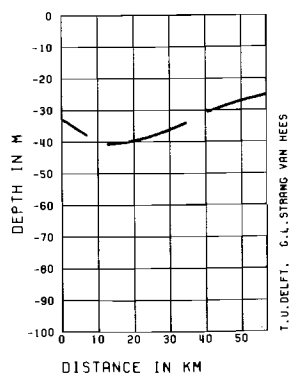

NORTH SEA: GRAVITY ANOMALY L0330

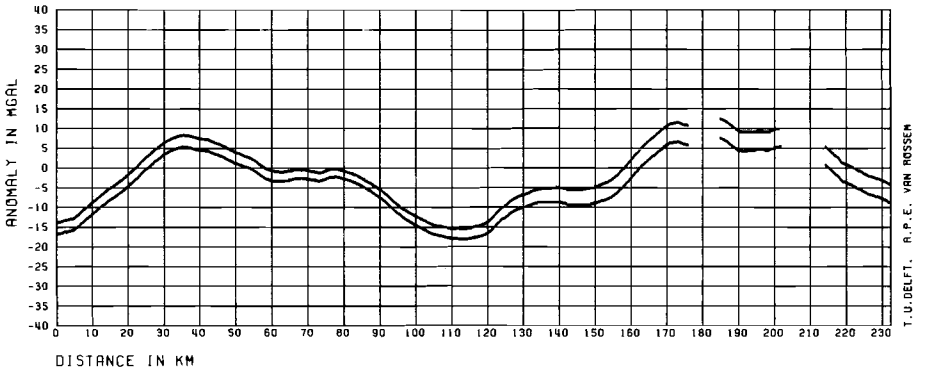

FULL LINE: FREE AIR ANOMALY
OPEN LINE: BOUGUER ANOMALY

LINE: L0330
DATE: MAY 6 1986

		START	FINISH
TIME	M.M.S.:	10 17 42	19 55 45
U.T.M. COORDINATES	X:	532362	530713
	Y:	6038539	6271028
GEOGRAPHICAL COORDINATES	PHI:	54.492	56.581
	LAMBDA:	3.500	3.500

NORTH SEA: DEPTH L0330

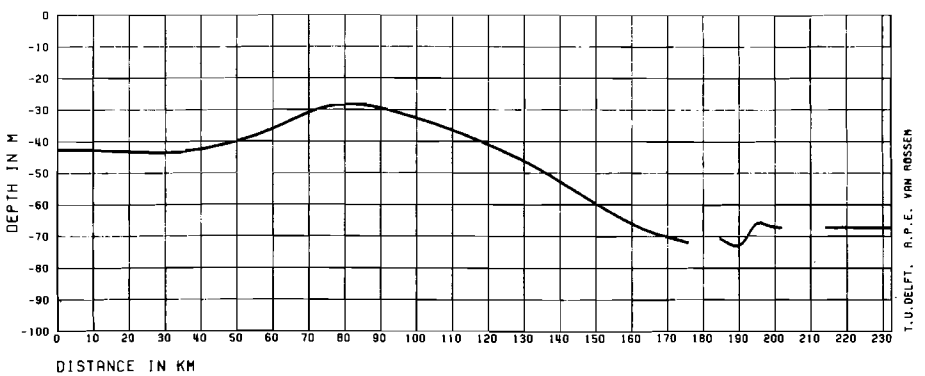

NORTH SEA: GRAVITY ANOMALY L0400

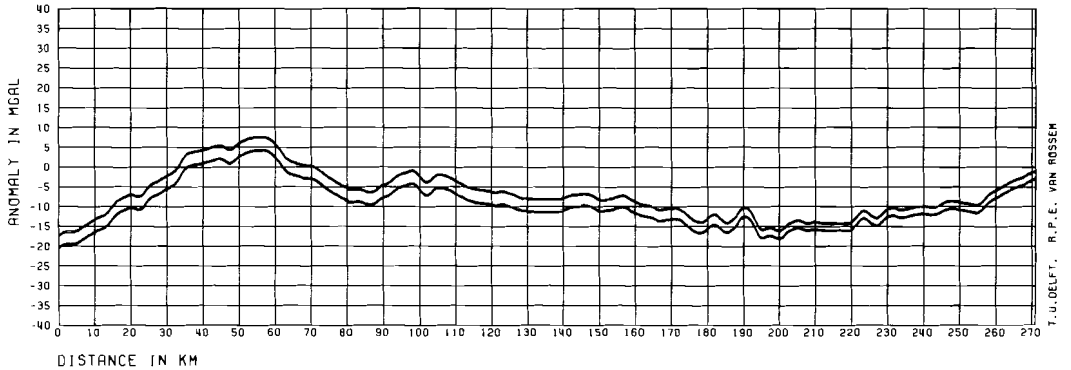

DISTANCE IN KM

FULL LINE: FREE AIR ANOMALY
OPEN LINE: BOUGUER ANOMALY

LINE: L0400
DATE: APRIL 28 1986

		START	FINISH
TIME	H.M.S.:	17 59 40	5 39 42
U.T.M. COORDINATES	X:	563585	567506
	Y:	6118134	5848136
GEOGRAPHICAL COORDINATES	PHI:	55.213	52.778
	LAMBDA:	3.999	4.001

NORTH SEA: DEPTH L0400

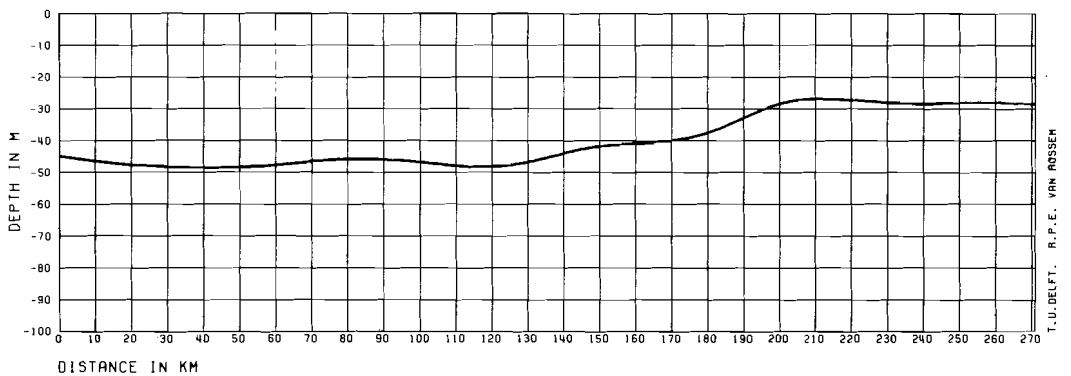

DISTANCE IN KM

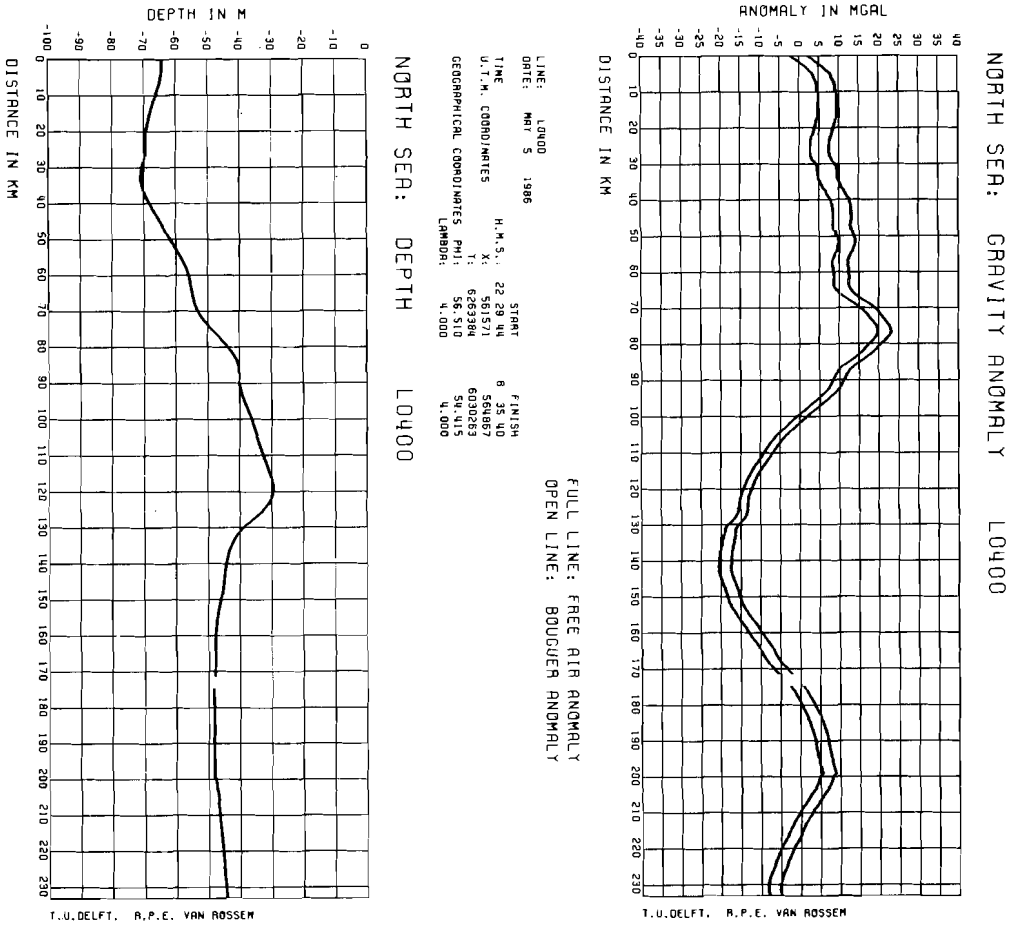
NORTH SEA: GRAVITY ANOMALY L0400
ANOMALY IN MGAL
DISTANCE IN KM
T.U.DELFT. R.P.E. VAN ROSSEM
FULL LINE: FREE AIR ANOMALY
OPEN LINE: BOUGUER ANOMALY
LINE: L0400
DATE: MAY 5 1986
TIME H.M.S.:
U.T.M. COORDINATES
X:
Y:
GEOGRAPHICAL COORDINATES PHI:
LAMBDA:
START
22 28 44
5611571
6263384
56.510
4.000
FINISH
8 35 40
5649867
6030263
54.415
4.000
NORTH SEA: DEPTH L0400
DEPTH IN M
DISTANCE IN KM
T.U.DELFT. R.P.E. VAN ROSSEM

NORTH SEA: GRAVITY ANOMALY L0425

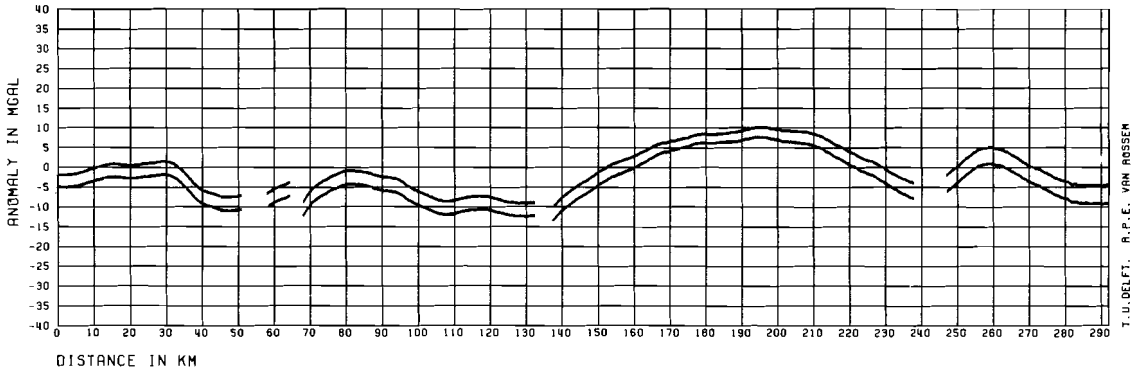

DISTANCE IN KM

FULL LINE: FREE AIR ANOMALY
OPEN LINE: BOUGUER ANOMALY

LINE: L0425
DATE: MAY 5 1986

		START	FINISH
TIME	H.M.S.:	7 9 42	21 7 43
U.T.M. COORDINATES	X:	592994	587052
	Y:	5979481	6271594
GEOGRAPHICAL COORDINATES	PHI:	53.954	56.579
	LAMBDA:	4.417	4.417

NORTH SEA: DEPTH L0425

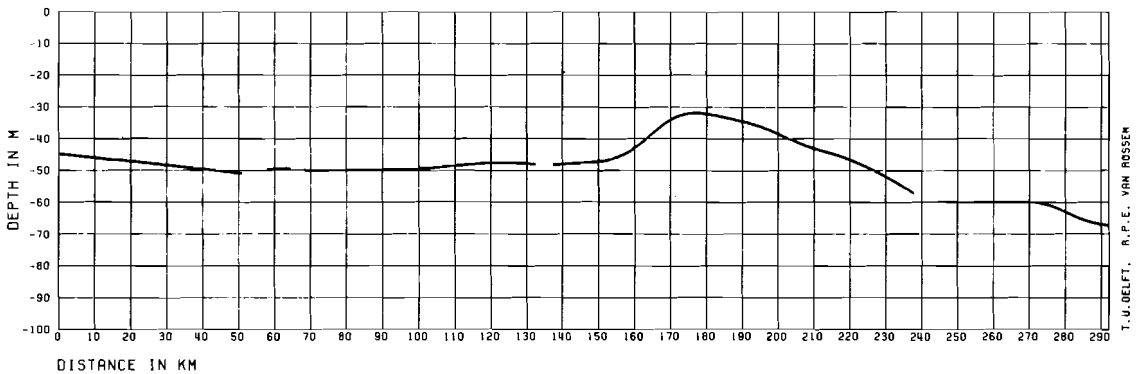

DISTANCE IN KM

NORTH SEA: GRAVITY ANOMALY L0430

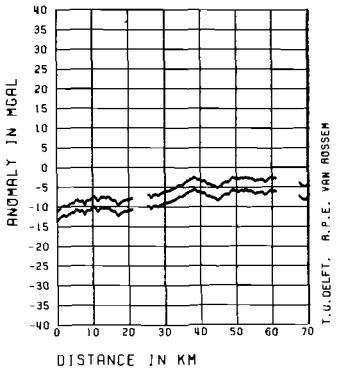

FULL LINE: FREE AIR ANOMALY
OPEN LINE: BOUGUER ANOMALY

LINE: L0430
DATE: APRIL 25 1986

		START	FINISH
TIME	H.M.S.:	16 38 49	19 29 38
U.T.M. COORDINATES	X:	600338	598903
	Y:	5943492	6013784
GEOGRAPHICAL COORDINATES	PHI:	53.629	54.261
	LAMBDA:	4.517	4.518

NORTH SEA: DEPTH L0430

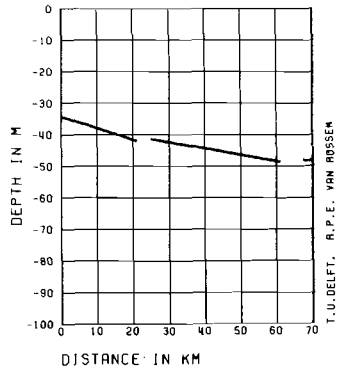

NORTH SEA: GRAVITY ANOMALY L0500

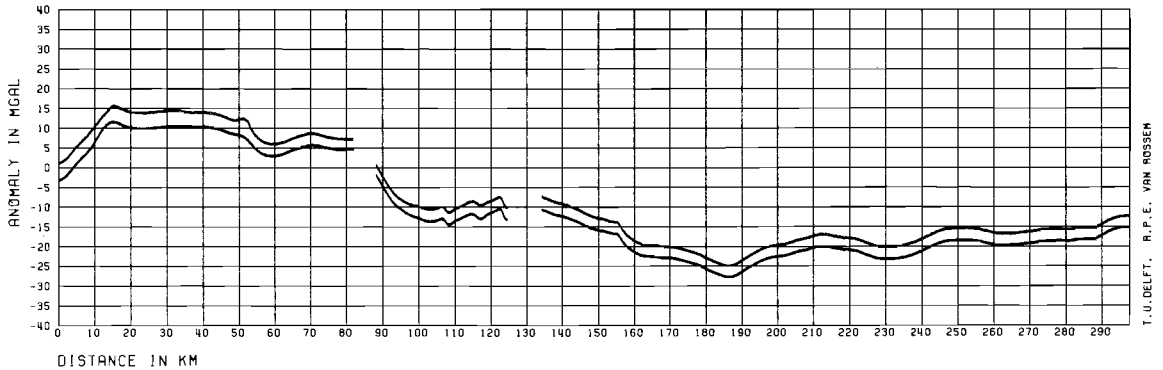

DISTANCE IN KM

FULL LINE: FREE AIR ANOMALY
OPEN LINE: BOUGUER ANOMALY

LINE: L0500
DATE: MAY 4 1986

		START	FINISH
TIME	H.M.S.:	16 9 38	5 4 44
U.T.M. COORDINATES	X:	622861	631509
	Y:	6273955	5976235
GEOGRAPHICAL COORDINATES	PHI:	56.592	53.917
	LAMBDA:	5.001	5.002

NORTH SEA: DEPTH L0500

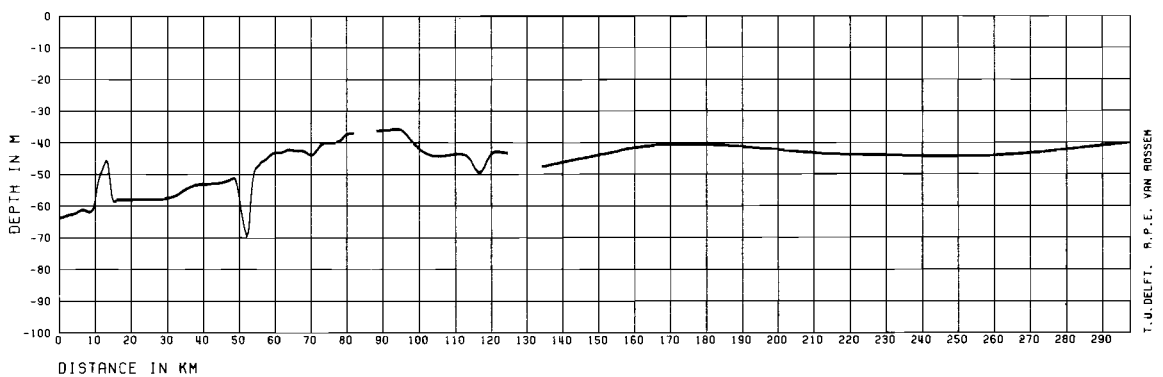

DISTANCE IN KM

NORTH SEA: GRAVITY ANOMALY L0520

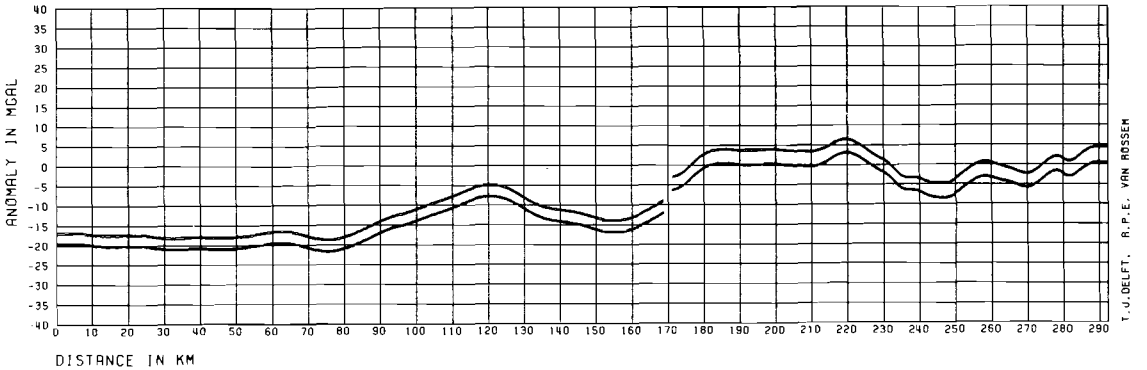

DISTANCE IN KM

FULL LINE: FREE AIR ANOMALY
OPEN LINE: BOUGUER ANOMALY

LINE: L0520
DATE: MAY 3 1986

		START	FINISH
TIME	H.M.S.:	22 59 44	11 28 40
U.T.M. COORDINATES	X:	652955	643167
	Y:	5985927	6278208
GEOGRAPHICAL COORDINATES	PHI:	53.998	56.625
	LAMBDA:	5.333	5.333

NORTH SEA: DEPTH L0520

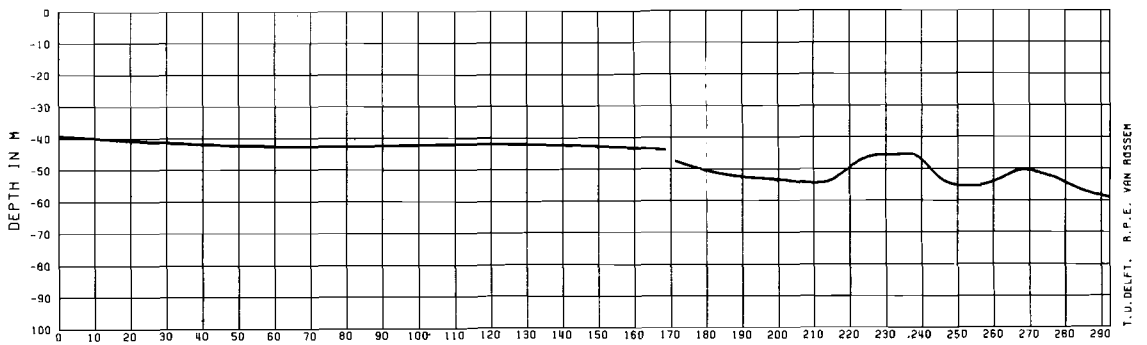

DISTANCE IN KM

NØRTH SEA: GRAVITY ANØMALY L0538

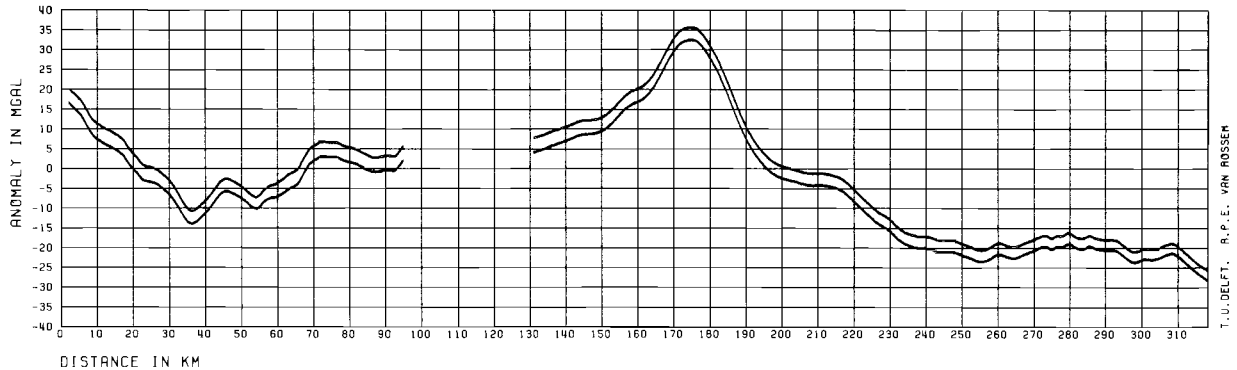

FULL LINE: FREE AIR ANOMALY
OPEN LINE: BOUGUER ANOMALY

LINE: L0538
DATE: MAY 3 1986

		START	FINISH
TIME	H.M.S.:	8 20 44	21 49 45
U.T.M. COORDINATES	X:	660417	672925
	Y:	6293819	5977966
GEOGRAPHICAL COORDINATES	PHI:	56.759	53.920
	LAMBDA:	5.624	5.633

NØRTH SEA: DEPTH L0538

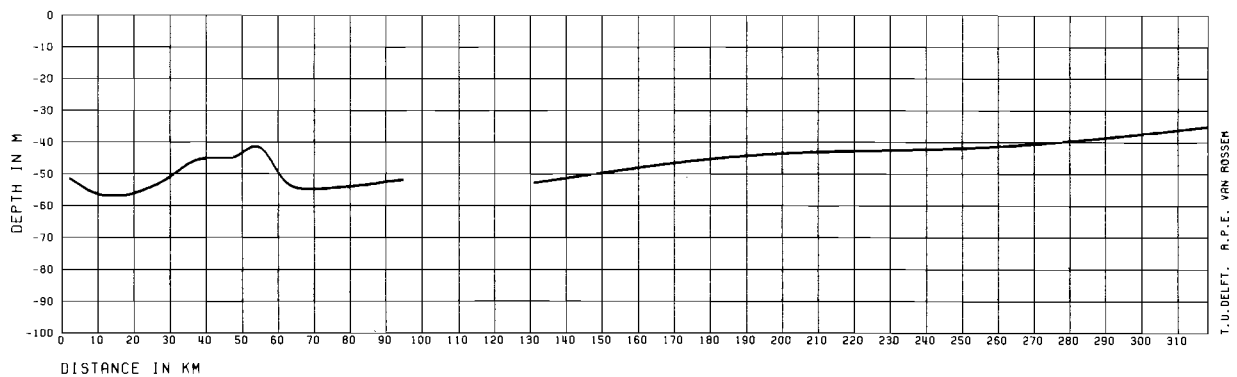

NORTH SEA: GRAVITY ANOMALY LO550

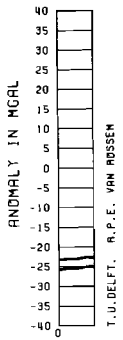

DISTANCE IN KM

FULL LINE: FREE AIR ANOMALY
OPEN LINE: BOUGUER ANOMALY

LINE: LO550
DATE: APRIL 27 1986

		START	FINISH
TIME	H.M.S.:	3 11 47	3 36 43
U.T.M. COORDINATES	X:	683853	684621
	Y:	5996844	5987022
GEOGRAPHICAL COORDINATES	PHI:	54.086	53.997
	LAMBDA:	5.811	5.817

NORTH SEA: DEPTH LO550

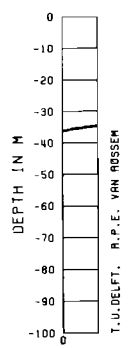

DISTANCE IN KM

NORTH SEA: GRAVITY ANOMALY LO550

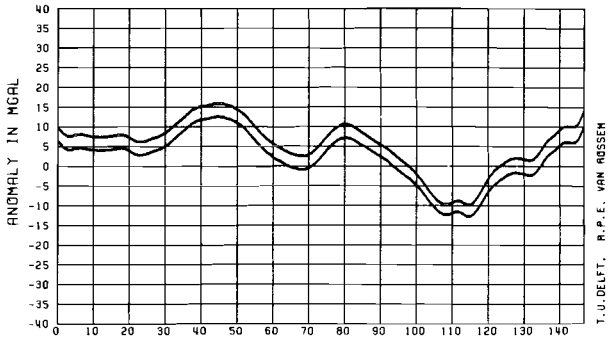

DISTANCE IN KM

FULL LINE: FREE AIR ANOMALY
OPEN LINE: BOUGUER ANOMALY

LINE: LO550
DATE: MAY 3 1986

		START	FINISH
TIME	H.M.S.:	1 31 40	7 39 45
U.T.M. COORDINATES	X:	679061	672953
	Y:	6151307	6298108
GEOGRAPHICAL COORDINATES	PHI:	55.474	56.793
	LAMBDA:	5.833	5.832

NORTH SEA: DEPTH LO550

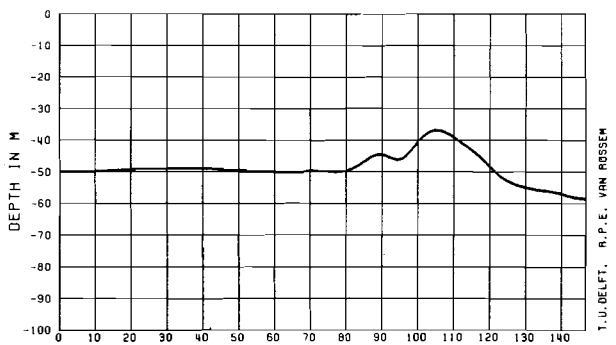

DISTANCE IN KM

NORTH SEA: GRAVITY ANOMALY LO600

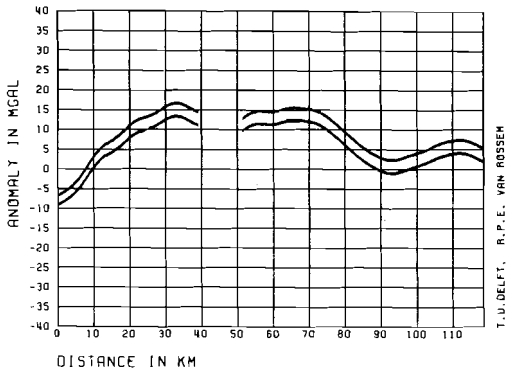

FULL LINE: FREE AIR ANOMALY
OPEN LINE: BOUGUER ANOMALY

LINE: LO600
DATE: MAY 2 1986

		START	FINISH
TIME	H.M.S.:	19 34 37	0 44 41
U.T.M. COORDINATES	X:	684754	689837
	Y:	6263830	6145395
GEOGRAPHICAL COORDINATES	PHI:	56.481	55.417
	LAMBDA:	6.000	5.999

NORTH SEA: DEPTH LO600

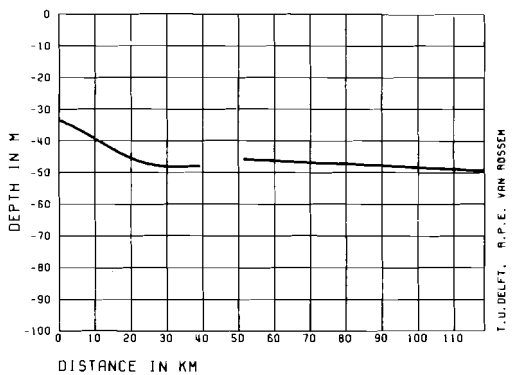

NORTH SEA: GRAVITY ANOMALY LO600

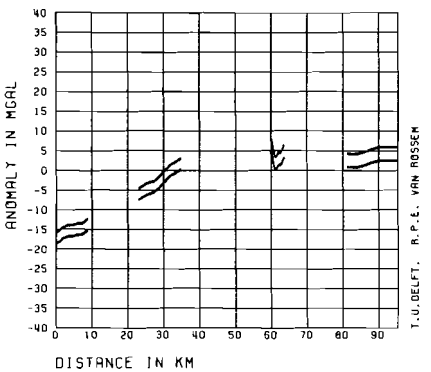

FULL LINE: FREE AIR ANOMALY
OPEN LINE: BOUGUER ANOMALY

LINE: LO600
DATE: APRIL 26 1986

		START	FINISH
TIME	H.M.S.:	15 44 48	19 44 35
U.T.M. COORDINATES	X:	693506	690611
	Y:	6061471	6156916
GEOGRAPHICAL COORDINATES	PHI:	54.662	55.520
	LAMBDA:	6.000	6.019

NORTH SEA: DEPTH LO600

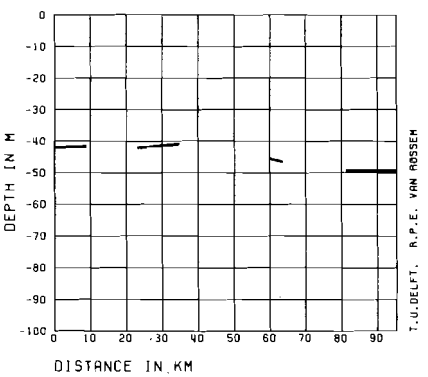

NØRTH SEA: GRAVITY ANØMALY L0630

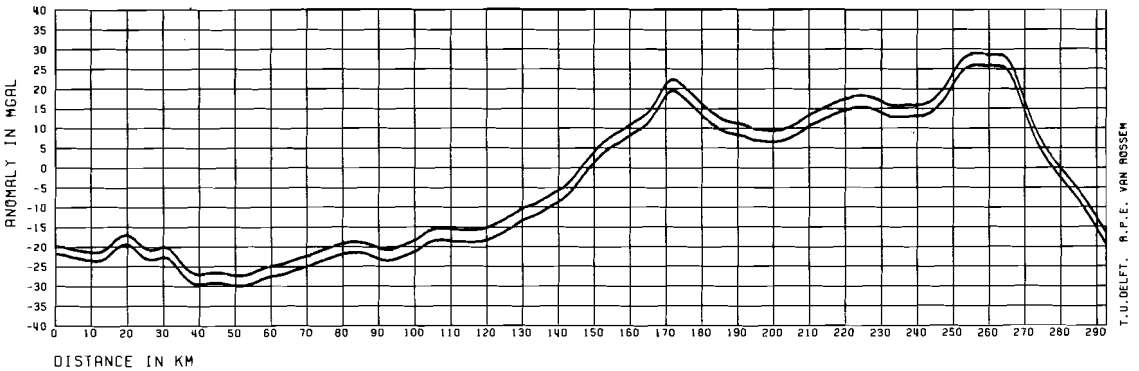

FULL LINE: FREE AIR ANØMALY
ØPEN LINE: BØUGUER ANØMALY

LINE: L0630
DATE: MAY 2 1986

		START	FINISH
TIME	H.M.S.:	5 33 46	17 44 45
U.T.M. CØØRDINATES	X:	729748	715050
	Y:	5982344	6274629
GEØGRAPHICAL CØØRDINATES	PHI:	53.937	56.565
	LAMBDA:	6.500	6.500

NØRTH SEA: DEPTH L0630

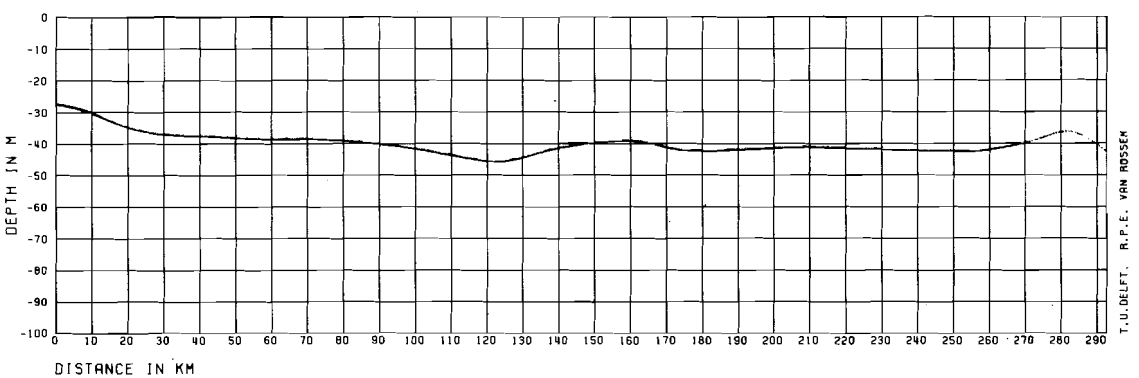

NORTH SEA: GRAVITY ANOMALY L0630

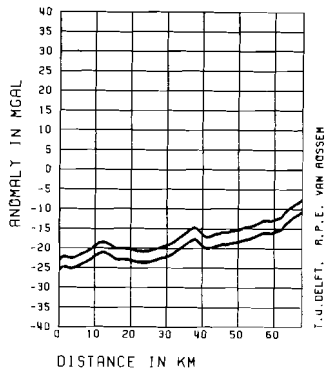

FULL LINE: FREE AIR ANOMALY
OPEN LINE: BOUGUER ANOMALY

LINE: L0630
DATE: APRIL 28 1986

		START	FINISH
TIME	H.M.S.:	6 51 41	9 39 45
U.T.M. COORDINATES	X:	726260	722948
	Y:	6051020	6118858
GEOGRAPHICAL COORDINATES	PHI:	54.555	55.265
	LAMBDA:	6.499	6.500

NORTH SEA: GRAVITY ANOMALY L0700

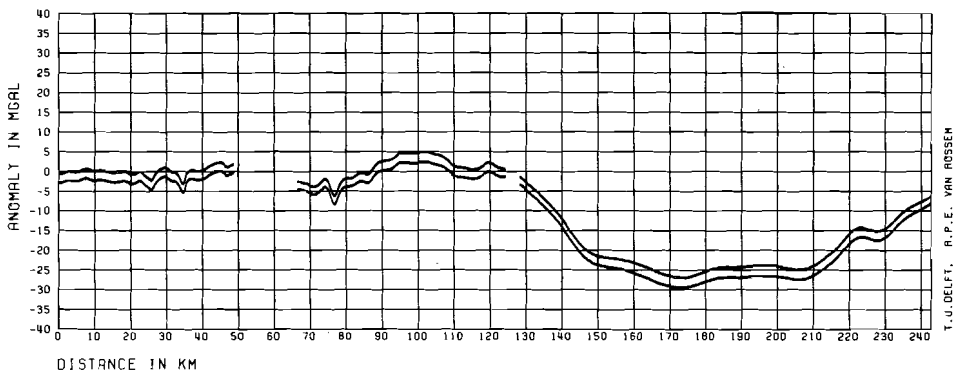

FULL LINE: FREE AIR ANOMALY
OPEN LINE: BOUGUER ANOMALY

LINE: L0700
DATE: MAY 1 1986

		START	FINISH
TIME	H.M.S.:	17 9 34	3 44 38
U.T.M. COORDINATES .	X:	748786	762499
	Y:	6223854	5981392
GEOGRAPHICAL COORDINATES	PHI:	56.094	53.913
	LAMBDA:	7.000	6.997

NORTH SEA: DEPTH L0630

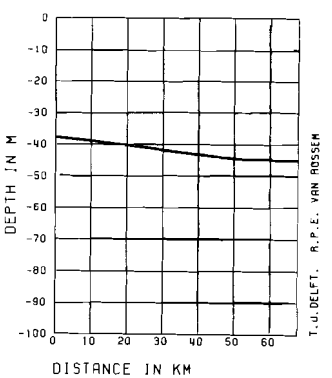

NORTH SEA: DEPTH L0700

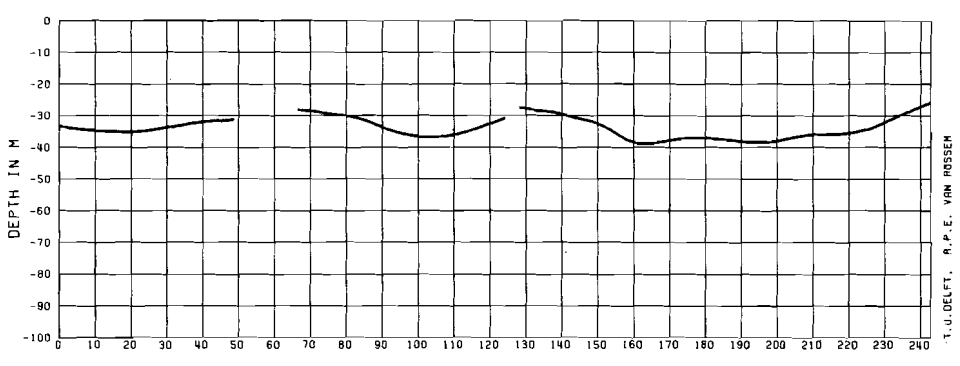

NORTH SEA: GRAVITY ANOMALY L0730

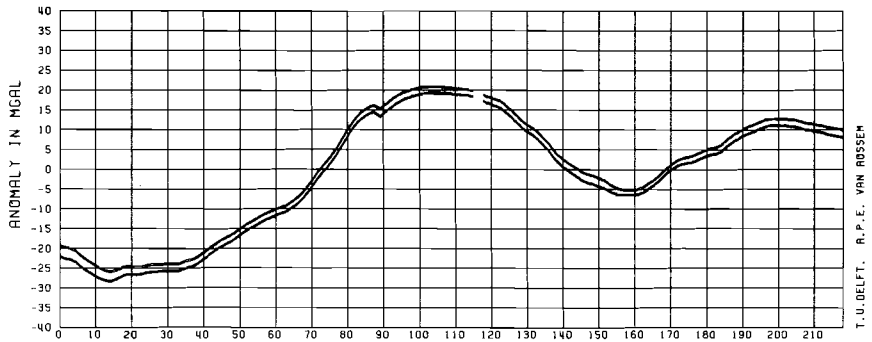

FULL LINE: FREE AIR ANOMALY
OPEN LINE: BOUGUER ANOMALY

LINE: L0730
DATE: MAY 1 1986

		START	FINISH
TIME	H.M.S.:	6 19 43	15 34 42
U.T.M. COORDINATES	X:	793500	773766
	Y:	6014400	6231599
GEOGRAPHICAL COORDINATES	PHI:	54.192	56.149
	LAMBDA:	7.500	7.408

NORTH SEA: DEPTH L0730

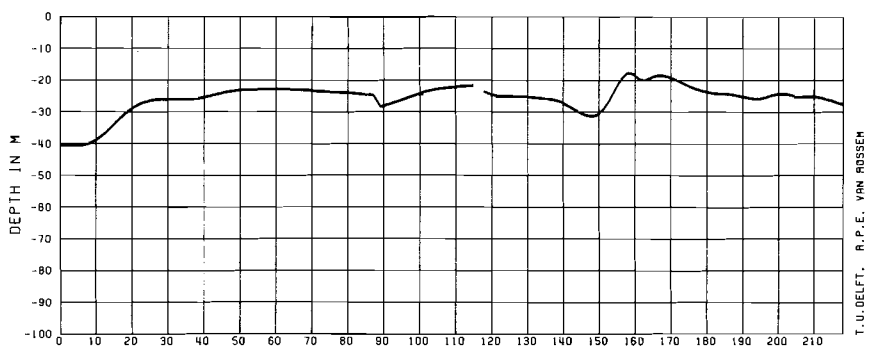

NORTH SEA: GRAVITY ANOMALY L5300

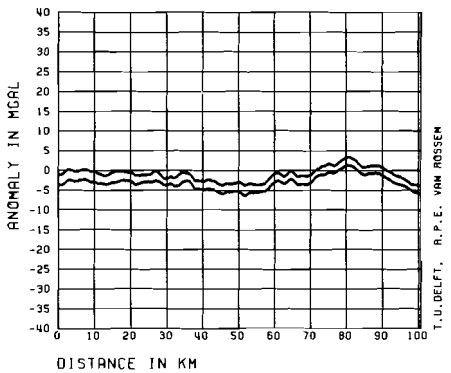

FULL LINE: FREE AIR ANOMALY
OPEN LINE: BOUGUER ANOMALY

LINE: L5300
DATE: MAY 13 1986

		START	FINISH
TIME	H.M.S.:	1 29 40	5 59 45
U.T.M. COORDINATES	X:	474315	573878
	Y:	5867302	5852182
GEOGRAPHICAL COORDINATES	PHI:	52.954	52.813
	LAMBDA:	2.618	4.096

NORTH SEA: DEPTH L5300

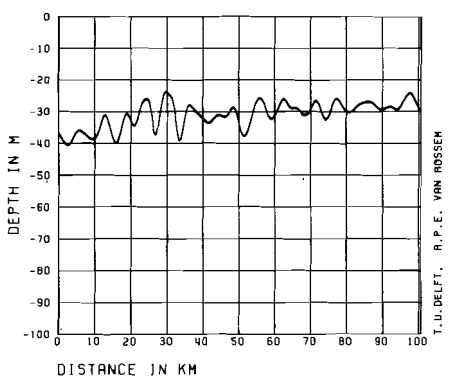

NORTH SEA: GRAVITY ANOMALY L5345

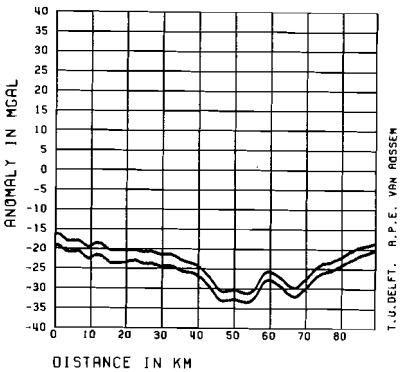

FULL LINE: FREE AIR ANOMALY
OPEN LINE: BOUGUER ANOMALY

LINE: L5345
DATE: MAY 11 1986

		START	FINISH
TIME	H.M.S.:	13 39 52	17 39 49
U.T.M. COORDINATES	X:	525717	436271
	Y:	5956088	5956247
GEOGRAPHICAL COORDINATES	PHI:	53.752	53.750
	LAMBDA:	3.390	2.034

NORTH SEA: DEPTH L5345

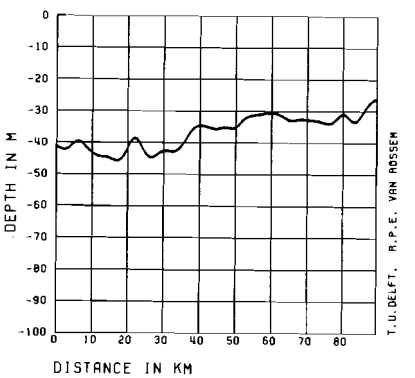

NORTH SEA: GRAVITY ANOMALY L5400

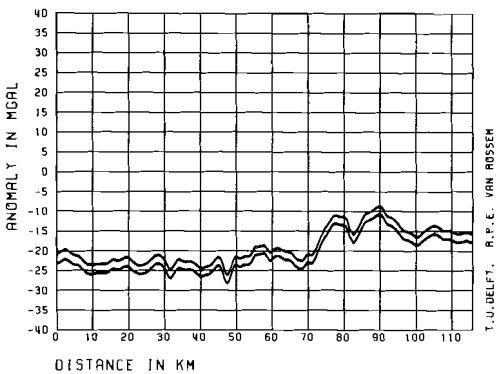

FULL LINE: FREE AIR ANOMALY
OPEN LINE: BOUGUER ANOMALY

LINE: L5400
DATE: MAY 1 1986

		START	FINISH
TIME	M.M.S.:	0 44 38	5 19 37
U.T.M. COORDINATES	X:	677042	792776
	Y:	5987117	5992778
GEOGRAPHICAL COORDINATES	PHI:	54.001	53.999
	LAMBDA:	5.701	7.468

NORTH SEA: DEPTH L5400

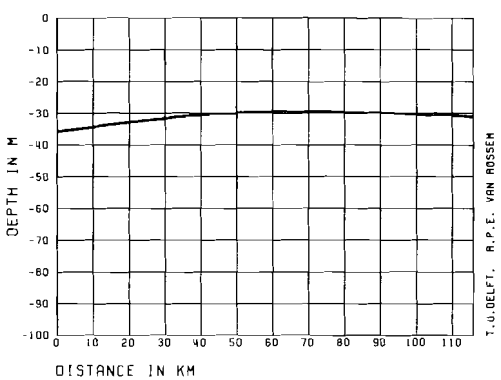

NORTH SEA: GRAVITY ANOMALY L5400

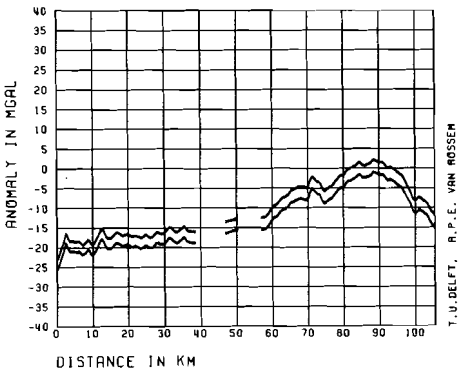

FULL LINE: FREE AIR ANOMALY
OPEN LINE: BOUGUER ANOMALY

LINE: L5400
DATE: APRIL 27 1986

		START	FINISH
TIME	M.M.S.:	4 11 43	8 36 42
U.T.M. COORDINATES	X:	671871	786169
	Y:	5987068	5984270
GEOGRAPHICAL COORDINATES	PHI:	54.002	54.001
	LAMBDA:	5.619	4.009

NORTH SEA: DEPTH L5400

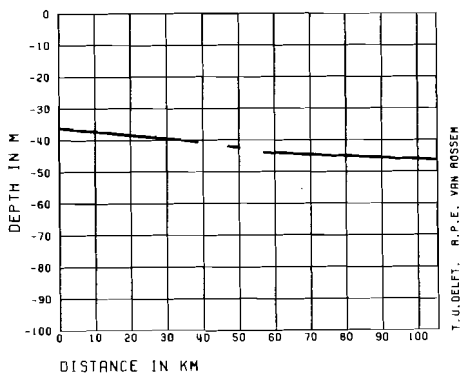

NORTH SEA: GRAVITY ANOMALY L5400

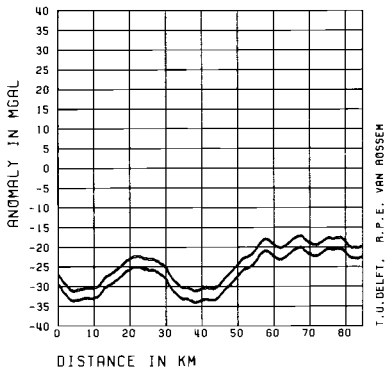

FULL LINE: FREE AIR ANOMALY
OPEN LINE: BOUGUER ANOMALY

LINE: L5400
DATE: MAY 11 1986

		START	FINISH
TIME	H.M.S.:	6 59 52	10 20 45
U.T.M. COORDINATES	X:	429643	514501
	Y:	5984111	5983698
GEOGRAPHICAL COORDINATES	PHI:	53.999	54.000
	LAMBDA:	1.927	3.221

NORTH SEA: DEPTH L5400

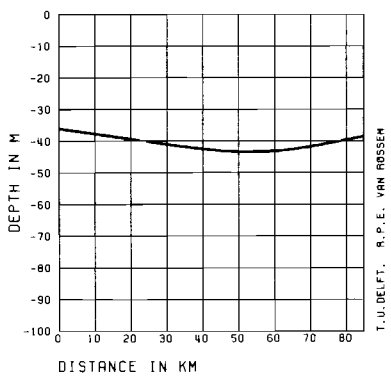

NORTH SEA: GRAVITY ANOMALY L5415

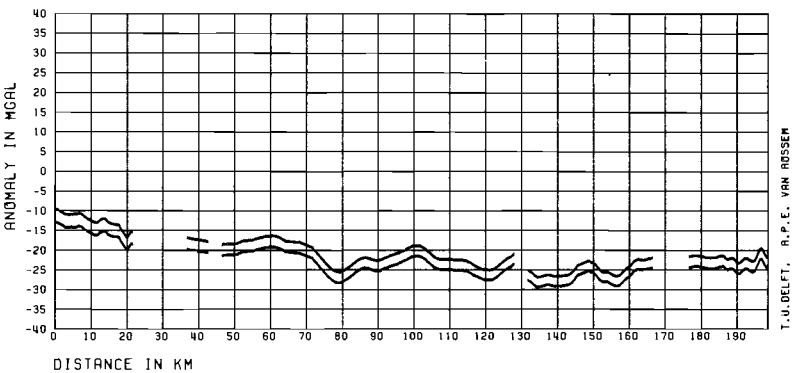

FULL LINE: FREE AIR ANOMALY
OPEN LINE: BOUGUER ANOMALY

LINE: L5415
DATE: APRIL 25 1986

		START	FINISH
TIME	H.M.S.:	20 14 52	4 54 48
U.T.M. COORDINATES	X:	606942	805410
	Y:	6012975	6021672
GEOGRAPHICAL COORDINATES	PHI:	54.252	54.250
	LAMBDA:	4.641	7.689

NORTH SEA: DEPTH L5415

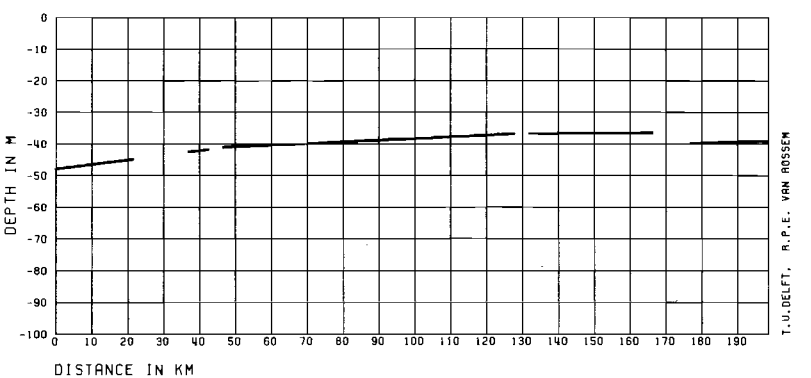

NORTH SEA: GRAVITY ANOMALY L5415

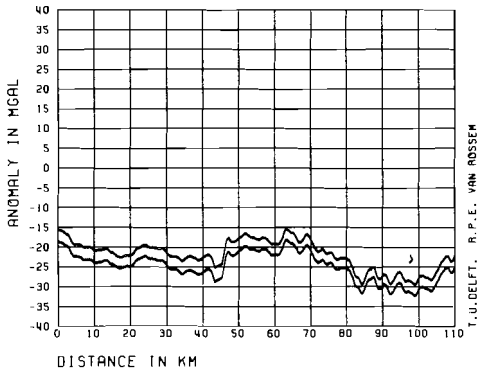

DISTANCE IN KM

FULL LINE: FREE AIR ANOMALY
OPEN LINE: BOUGUER ANOMALY

LINE: L5415
DATE: MAY 11 1986

		START	FINISH
TIME	H.M.S.:	0 9 47	5 19 48
U.T.M. COORDINATES	X:	536155	425931
	Y:	6011758	6012055
GEOGRAPHICAL COORDINATES	PHI:	54.251	54.250
	LAMBDA:	3.555	1.863

NORTH SEA: DEPTH L5415

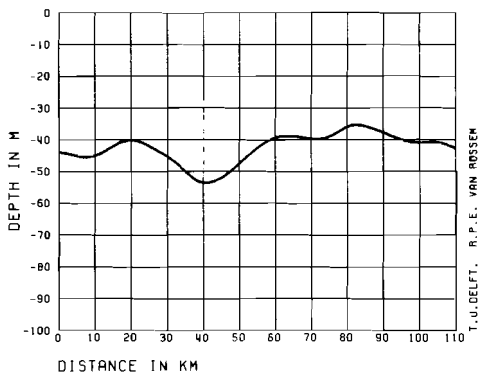

DISTANCE IN KM

NORTH SEA: GRAVITY ANOMALY L5415

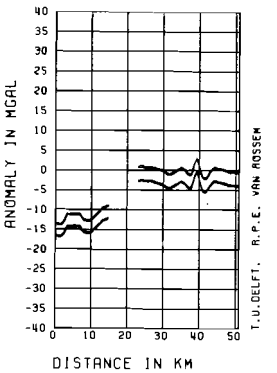

DISTANCE IN KM

FULL LINE: FREE AIR ANOMALY
OPEN LINE: BOUGUER ANOMALY

LINE: L5415
DATE: APRIL 27 1986

		START	FINISH
TIME	H.M.S.:	20 27 42	22 29 48
U.T.M. COORDINATES	X:	546972	597933
	Y:	6014153	6013343
GEOGRAPHICAL COORDINATES	PHI:	54.272	54.257
	LAMBDA:	3.721	4.503

NORTH SEA: DEPTH L5415

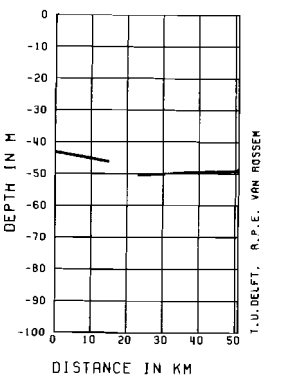

DISTANCE IN KM

NORTH SEA: GRAVITY ANOMALY L5429

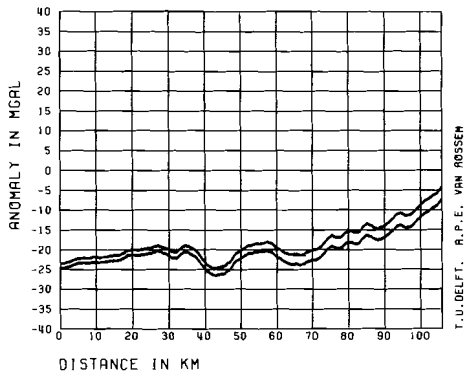

FULL LINE: FREE AIR ANOMALY
OPEN LINE: BOUGUER ANOMALY

LINE: L5429
DATE: MAY 10 1986

		START	FINISH
TIME	H.M.S.:	18 19 44	22 32 42
U.T.M. COORDINATES	X:	434409	540394
	Y:	6037473	6037649
GEOGRAPHICAL COORDINATES	PHI:	54.479	54.484
	LAMBDA:	1.988	3.623

NORTH SEA: DEPTH L5429

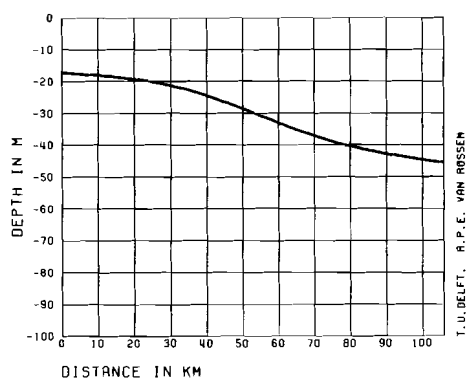

NORTH SEA: GRAVITY ANOMALY L5430

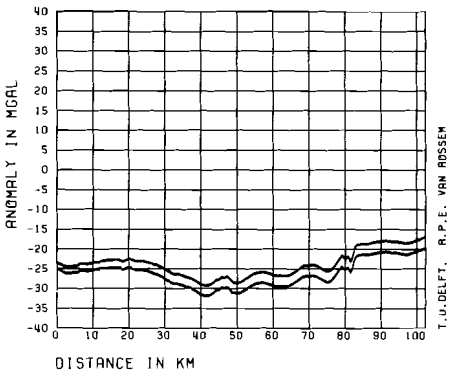

FULL LINE: FREE AIR ANOMALY
OPEN LINE: BOUGUER ANOMALY

LINE: L5430
DATE: APRIL 26 1986

		START	FINISH
TIME	H.M.S.:	8 9 43	12 39 44
U.T.M. COORDINATES	X:	802797	700531
	Y:	6049157	6043687
GEOGRAPHICAL COORDINATES	PHI:	54.498	54.500
	LAMBDA:	7.677	6.097

NORTH SEA: DEPTH L5430

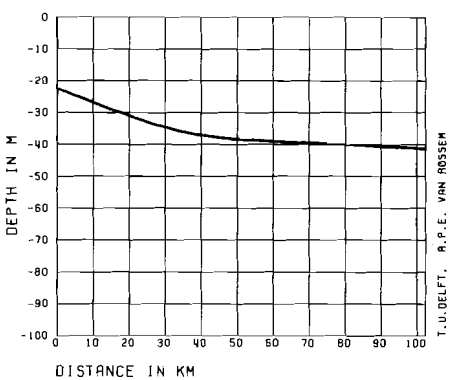

NORTH SEA: GRAVITY ANOMALY L5430

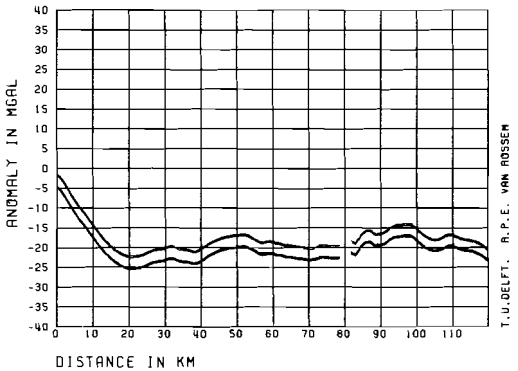

DISTANCE IN KM

FULL LINE: FREE AIR ANOMALY
OPEN LINE: BOUGUER ANOMALY

LINE: L5430
DATE: APRIL 28 1986

		START	FINISH
TIME	H.M.S.:	0 44 48	5 56 44
U.T.M. COORDINATES	X:	602090	721877
	Y:	6040929	6044691
GEOGRAPHICAL COORDINATES	PHI:	54.504	54.500
	LAMBDA:	4.577	6.427

NORTH SEA: DEPTH L5430

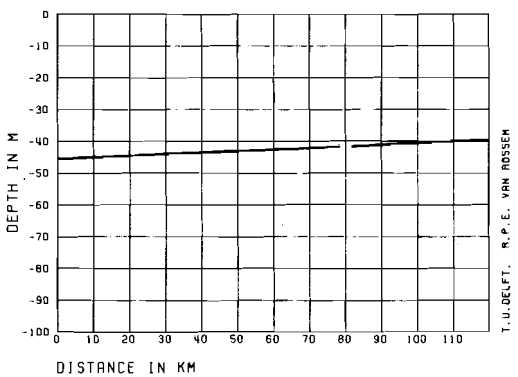

DISTANCE IN KM

NORTH SEA: GRAVITY ANOMALY L5430

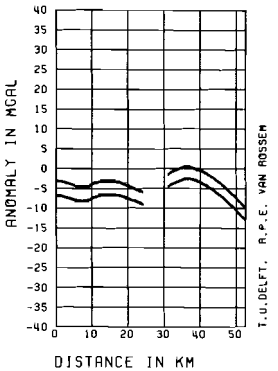

DISTANCE IN KM

FULL LINE: FREE AIR ANOMALY
OPEN LINE: BOUGUER ANOMALY

LINE: L5430
DATE: APRIL 24 1986

		START	FINISH
TIME	H.M.S.:	1 49 44	4 13 42
U.T.M. COORDINATES	X:	592322	539690
	Y:	6040509	6039525
GEOGRAPHICAL COORDINATES	PHI:	54.503	54.501
	LAMBDA:	4.426	3.613

NORTH SEA: DEPTH L5430

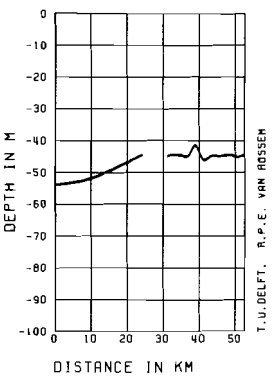

DISTANCE IN KM

NORTH SEA: GRAVITY ANOMALY L5444

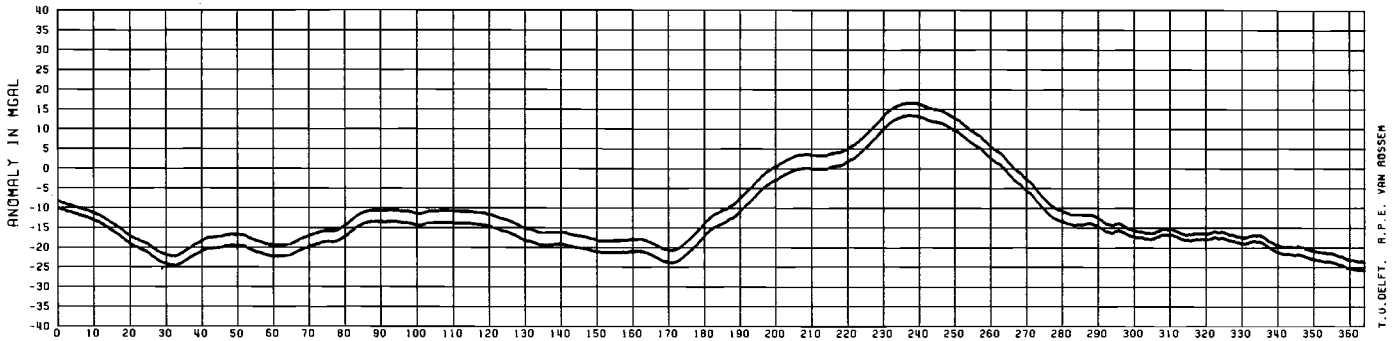

FULL LINE: FREE AIR ANOMALY
OPEN LINE: BOUGUER ANOMALY

LINE: L5444
DATE: MAY 10 1986

		START	FINISH
TIME	H.M.S.:	0 49 44	16 39 48
U.T.M. COORDINATES	X:	789486	425419
	Y:	6074708	6065738
GEOGRAPHICAL COORDINATES	PHI:	54.735	54.732
	LAMBDA:	7.497	1.842

NORTH SEA: DEPTH L5444

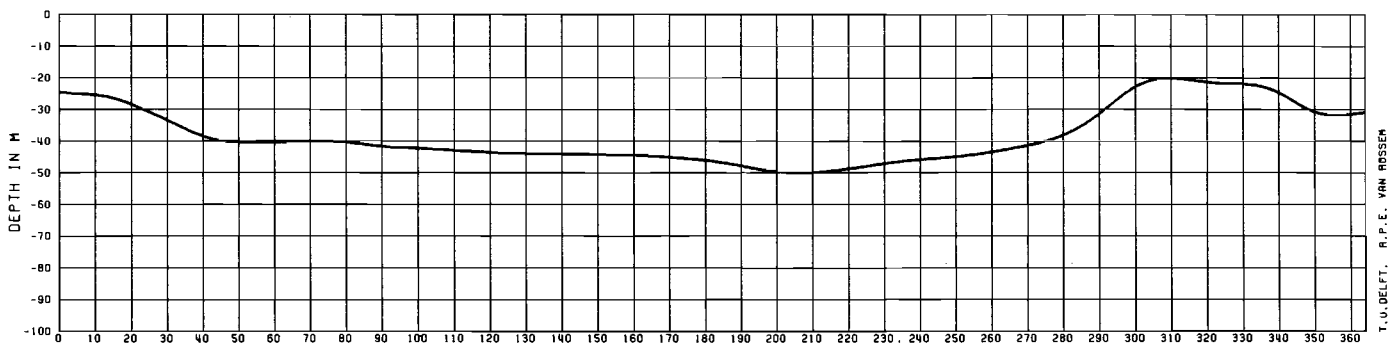

NORTH SEA: GRAVITY ANOMALY L5501

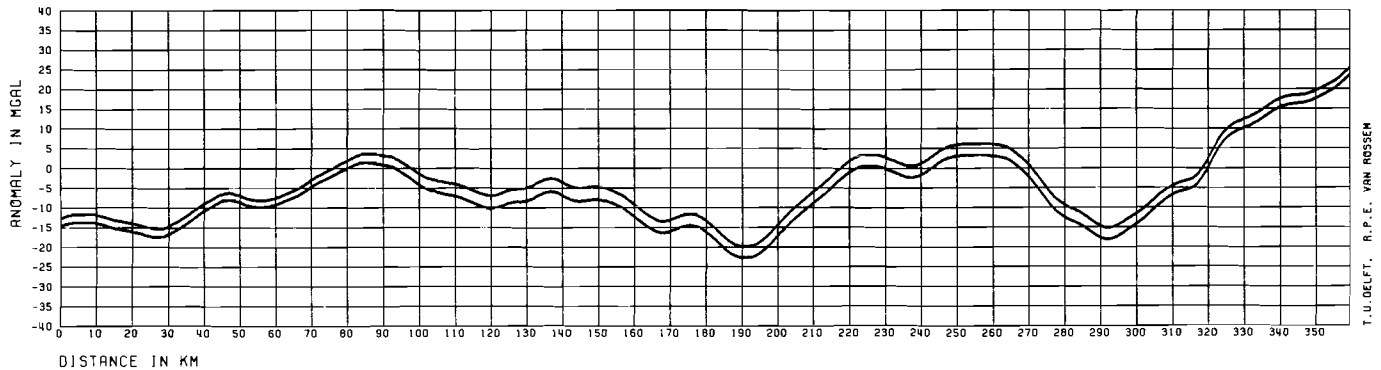

FULL LINE: FREE AIR ANOMALY
OPEN LINE: BOUGUER ANOMALY

LINE: L5501
DATE: MAY 9 1986

		START	FINISH
TIME	H.M.S.:	7 59 50	22 51 53
U.T.M. COORDINATES	X:	436496	795903
	Y:	6097277	6106658
GEOGRAPHICAL COORDINATES	PHI:	55.017	55.017
	LAMBDA:	2.007	7.629

NORTH SEA: DEPTH L5501

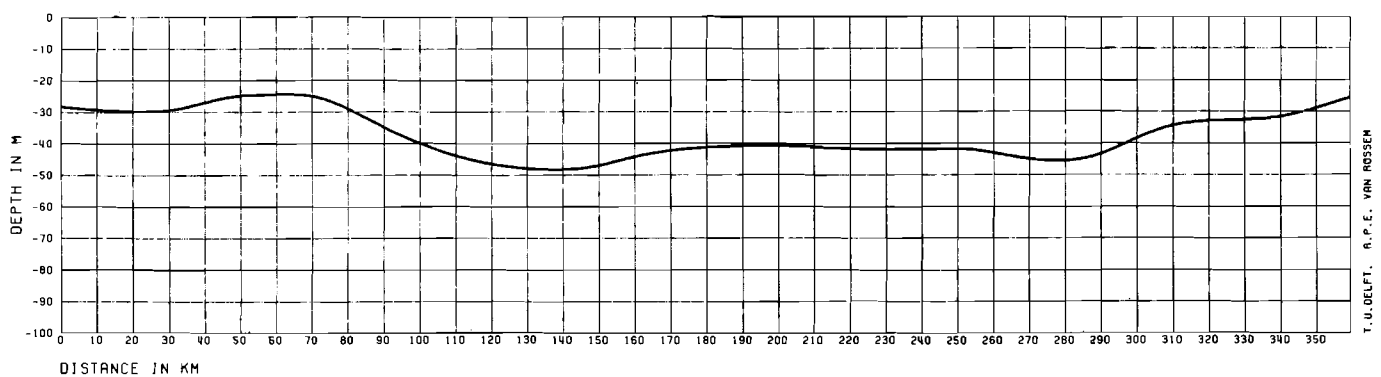

NØRTH SEA: GRAVITY ANØMALY L5513

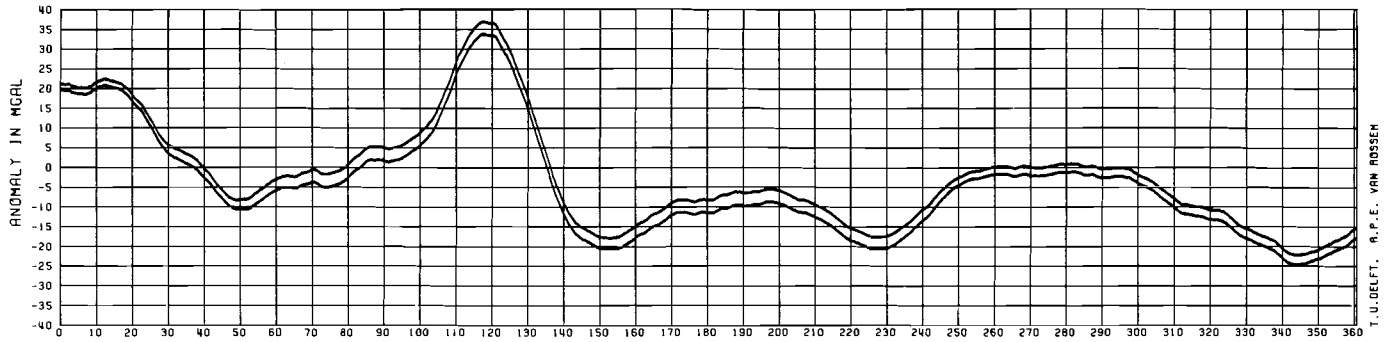

DISTANCE IN KM

FULL LINE: FREE AIR ANØMALY
ØPEN LINE: BØUGUER ANØMALY

LINE: L5513
DATE: MAY 8 1986

		START	FINISH
TIME	H.M.S.:	15 4 45	6 29 45
U.T.M. CØØRDINATES	X:	788444	427775
	Y:	6128730	6119785
GEØGRAPHICAL CØØRDINATES	PHI:	55.219	55.218
	LAMBDA:	7.535	1.865

NØRTH SEA: DEPTH L5513

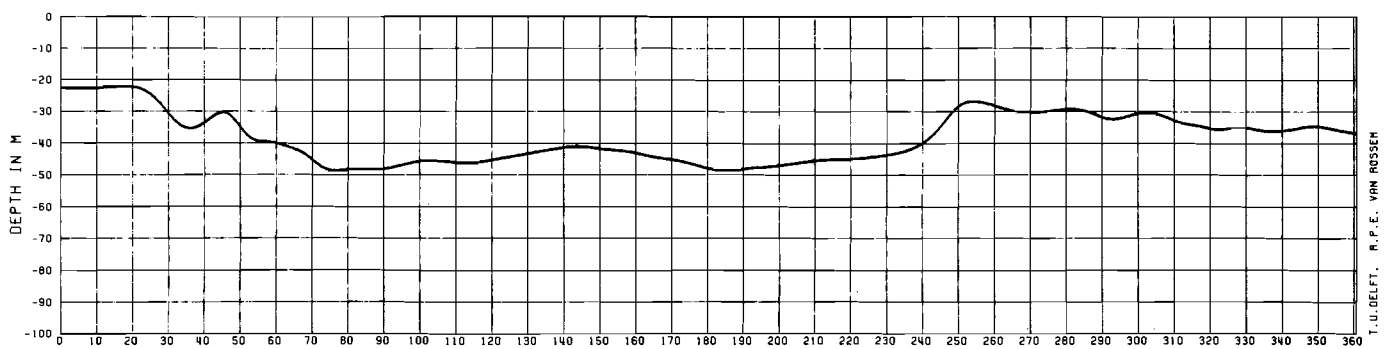

DISTANCE IN KM

NORTH SEA: GRAVITY ANOMALY L5510

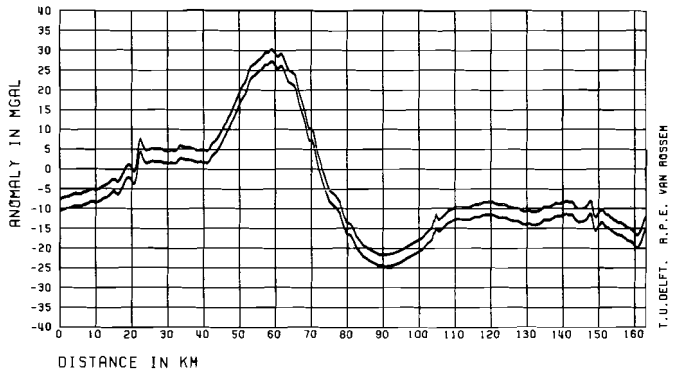

DISTANCE IN KM

FULL LINE: FREE AIR ANOMALY
OPEN LINE: BOUGUER ANOMALY

LINE: L5510
DATE: APRIL 28 1986

		START	FINISH
TIME	H.M.S.:	10 34 52	17 29 57
U.T.M. COORDINATES	X:	725417	562329
	Y:	6119261	6113945
GEOGRAPHICAL COORDINATES	PHI:	55.167	55.167
	LAMBDA:	6.539	3.978

NORTH SEA: DEPTH L5510

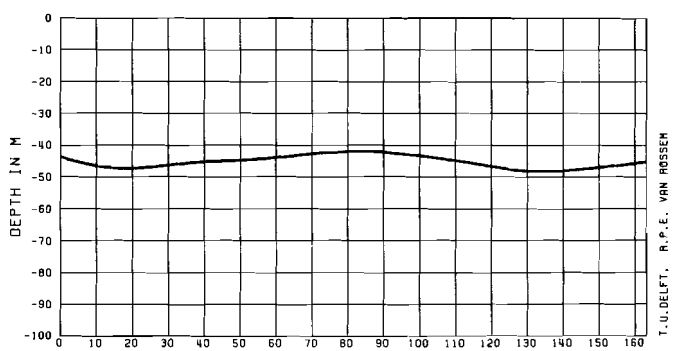

DISTANCE IN KM

NORTH SEA: GRAVITY ANOMALY L5530

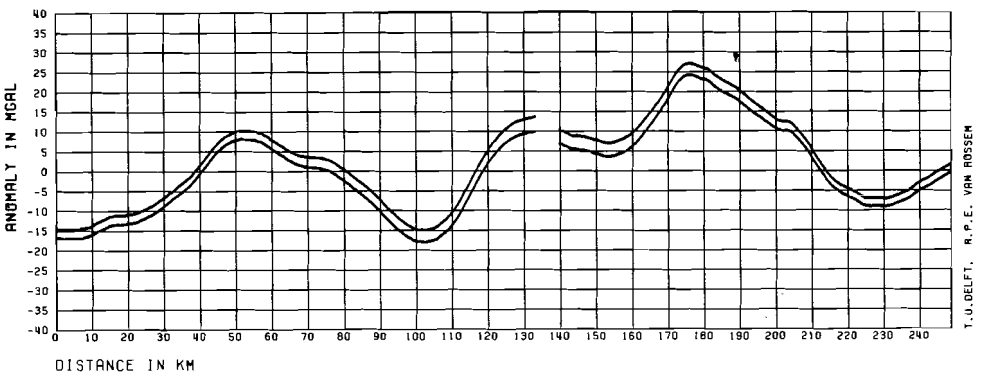

DISTANCE IN KM

FULL LINE: FREE AIR ANOMALY
OPEN LINE: BOUGUER ANOMALY

LINE: L5530
DATE: MAY 8 1986

		START	FINISH
TIME	H.M.S.:	2 59 45	13 14 52
U.T.M. COORDINATES	X:	535390	783974
	Y:	6150805	6159858
GEOGRAPHICAL COORDINATES	PHI:	55.501	55.501
	LAMBDA:	3.560	7.497

NORTH SEA: DEPTH L5530

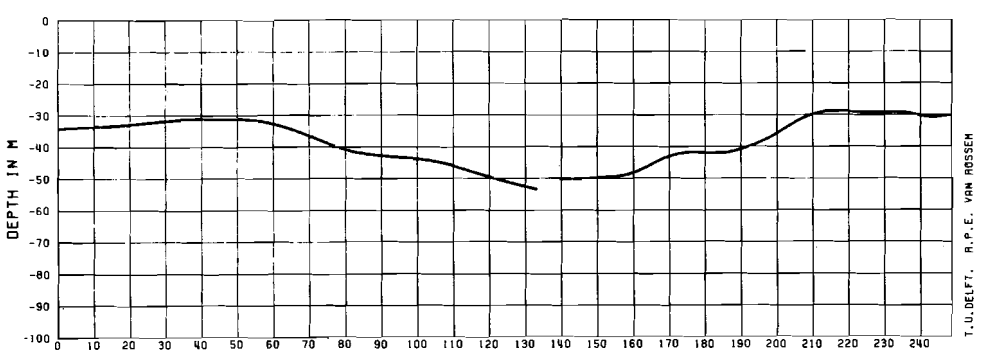

DISTANCE IN KM

NORTH SEA: GRAVITY ANOMALY L5545

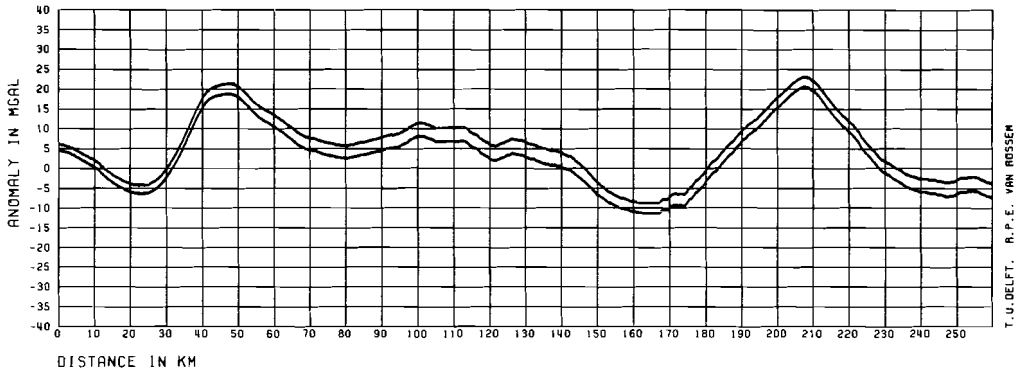

DISTANCE IN KM

FULL LINE: FREE AIR ANOMALY
OPEN LINE: BOUGUER ANOMALY

LINE: L5545
DATE: MAY 7 1986

		START	FINISH
TIME	H.M.S.:	13 59 42	1 9 41
U.T.M. COORDINATES	X:	781319	521672
	Y:	6187781	6176582
GEOGRAPHICAL COORDINATES	PHI:	55.753	55.733
	LAMBDA:	7.484	3.345

NORTH SEA: DEPTH L5545

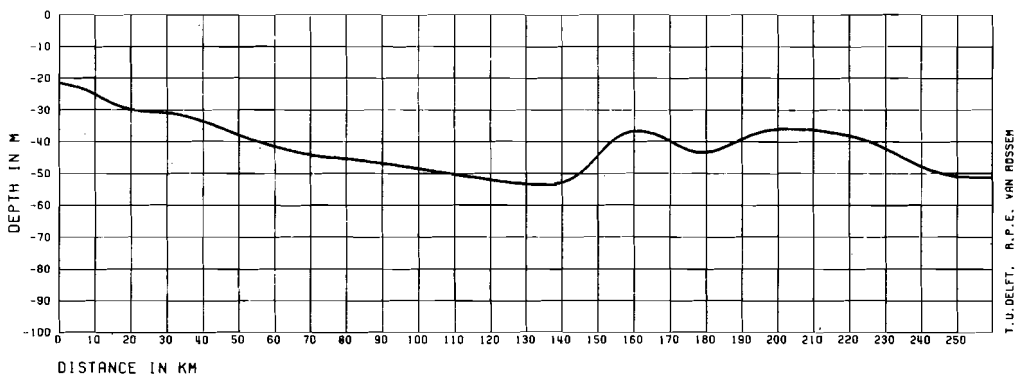

DISTANCE IN KM

NORTH SEA: GRAVITY ANOMALY L5600

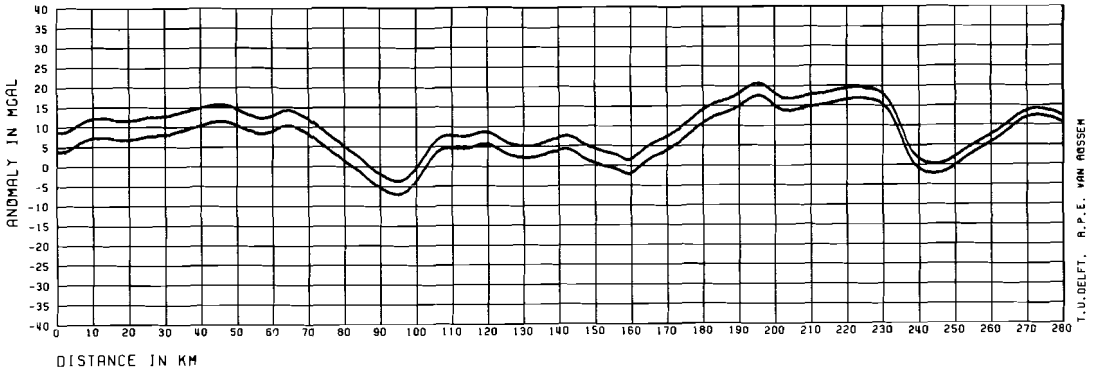

FULL LINE: FREE AIR ANOMALY
OPEN LINE: BOUGUER ANOMALY

LINE: L5600
DATE: MAY 7 1986

		START	FINISH
TIME	H.M.S.:	0 9 45	12 14 40
U.T.M. COORDINATES	X:	504950	785230
	Y:	6206219	6215665
GEOGRAPHICAL COORDINATES	PHI:	56.000	56.000
	LAMBDA:	3.079	7.575

NORTH SEA: DEPTH L5600

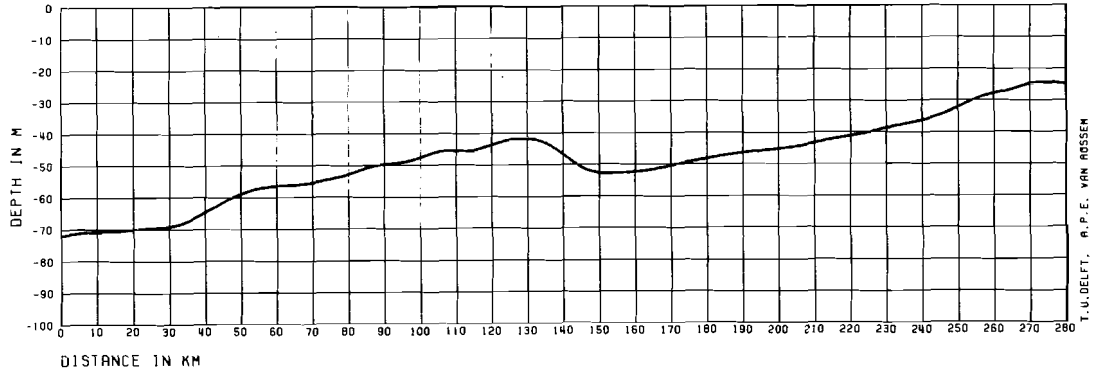

NORTH SEA: GRAVITY ANOMALY

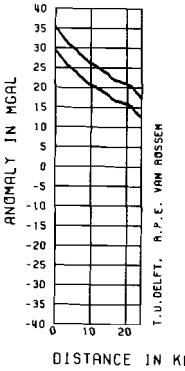

LINE: L5625
DATE: MAY 12 1986

		START	FINISH
TIME	H.M.S.:	6 49 50	7 49 52
U.T.M. COORDINATES	X:	445048	469111
	Y:	6254934	6252735
GEOGRAPHICAL COORDINATES	PHI:	56.434	56.417
	LAMBDA:	2.109	2.499

NORTH SEA: DEPTH L5625